Universität für Bodenkultur Wien
University of Natural Resources
and Life Sciences, Vienna

Department of Forest and Soil Sciences

Institute of Silviculture

Univ.Prof. Dipl.-Ing. Dr.nat.techn. Hubert Hasenauer: Inst. Head and Supervisor

A CONCEPTUAL FRAMEWORK FOR SUSTAINABLE FOREST MANAGEMENT IN THE AMHARA REGION, NORTHWESTERN ETHIOPIA

Dissertation
to obtain the doctoral degree (*Dr.nat.techn.*)
at the University of Natural Resources and Life Sciences
(BOKU), Vienna, Austria

Kibruyesfa Sisay

Vienna, Austria, June 2017

“If you just focus on the smallest details, you never get the bigger picture right.”

Leroy Hood

“When it rains, most birds head for shelter; the Eagle is the only bird that, in order to avoid the rain, starts flying above the clouds.”

Unknown

Preface

We carried out this study within the framework of the project “Carbon Storage and Soil Biodiversity in Forest Landscapes in Ethiopia: Knowledge Base and Participatory Management” with funding from the Austrian Federal Ministry of Agriculture, Forestry, Environment and Water Management.

This is a cumulative dissertation comprising of two peer-reviewed scientific papers which can be found in the Appendix of this work (section 9.1 to 9.2). The first part (section 1 to 8) is a synthesis and extended summary of the papers, which, for the first time, demonstrates the links between the two papers towards the development of the framework for the sustainable forest management in the Amhara region. The second part (Appendix) consists of two first authored papers published in peer reviewed international journals. The formatting of the individual papers varies due to the individual style of the journals.

Citations of this work should refer to: Sisay, K., 2017. Develop a Conceptual Framework for Sustainable Forest Management for the Amhara Region, Northwestern Ethiopia. PhD Dissertation. University of Natural Resources and Life Sciences, Vienna, Austria or by reference of the individual papers.

List of Papers

Paper I

Sisay, K., Thurnher, C., Belay, B., Lindner, G., Hasenauer, H., 2017. Volume and Carbon Estimates for the Forest Area of the Amhara Region in Northwestern Ethiopia. Forests 8, 122. doi:10.3390/f8040122

Paper II

Sisay, K., Thurnher, C., Hasenauer, H., 2016. Daily climate data for the Amhara region in Northwestern Ethiopia. Int. J. Climatol. doi:10.1002/joc.4880

Acknowledgment

This work is part of the project “Carbon Storage and Soil Biodiversity in Forest Landscapes in Ethiopia: Knowledge Base and Participatory Management”. We are grateful for the financial support provided by the Austrian Federal Ministry of Agriculture, Forestry, Environment and Water Management. I would like to thank the Ethiopian Meteorological Agency (EMA), Amhara Region Agricultural Research Institute (ARARI) and Dr Abrham, Dr Dejene Sahlu, Ato Wubneh Belete and Ato Biadgo for the data and logistics you have provided us.

My deepest and most sincere gratitude goes to my supervisor Univ. Prof. Dipl.-Ing. Dr. Hubert Hasenauer. I have been extremely lucky to have a supervisor like you who cared so much about my work and who responded to my questions and queries so promptly. You recreated and redefined my academic perspectives as well as my life as a researcher. Your constant guidance and encouragement, from the early beginning of my research work all the way through to this PhD thesis, has always astonished me. Your special skill in keeping me going when I lose motivation and run out of stamina is extraordinary. I am always overwhelmed with your hard work to teach me the science, make me an independent researcher as well as with your strong enthusiasm to positively impact the forestry research system of Ethiopia. Honestly, I cannot fully express my acknowledgment for your all round and continuous advice and support. You are beyond and above any supervisor I could have wished for to support my PhD studies.

I must express my gratitude to Dr. Christopher Thurnher. Without you, it would have been almost impossible to get the work going and finish my PhD within the given time frame. You always patiently guided me through technical problems of all kinds, and it has always been a privilege for me to work with you. I owe you a tremendous debt of gratitude. I thank you from the bottom of my heart for all the support you have provided me during our stay together during the project.

Special thanks go to my office mates Dr. Charalambos Neophytou and Dr. Marcela Van Loo for the enjoyable company. You have been very supportive in every way. I enjoyed and appreciated sharing different stories and perceptions about the world. The chance and the fun I had while learning German and Greek from Charalambos and teaching him Amharic is unforgettable.

I am also thankful to my fellow colleagues at BOKU, especially Dr Mathias Neumann, Dr. Adam Moreno, Dr Elisabeth Pötzelsberger, Mag Eva Lanz and all the other colleagues at the institute of Silviculture.

I owe a great deal of gratitude to my Ethiopian friends living in Vienna for making my Austrian life so easy.

Ame, Ashu, Bire, Eya, Getch, Mele and Alex (ያያs) deserve great appreciation for going above and beyond being friends by always being part of my life and for ingraining in me a way of logic, self-understanding and soul searching path.

I would also like to thank my beloved family, my mom, Yezina Takele (እናዬ), my dad, Sisay Ejigu (ያያ), and my sisters, Ethehuna (ቲና), Meseret (መሲ) and Lydia (ሊያ) and my brothers, Fekadu (ዋውዬ), Firezegi Teklehaymanot (ፍቅሬ), Naod Firezegi (ናፒሻ - ናፖሊዎን ዘቀዳማዊ) Michael Firezegi (ማኩሻ - ናፖሊዎን ዘዳግማዊ) and Yehun (ይሁንልኝ) who strongly shaped me more than they know to get to this point. You have laid the corner stone for my ever searching and skeptical mind. I hope you are satisfied with my efforts to make the best out of it. I would also like to express my gratitude to my sisters-in-law and brothers-in-law for their constant encouragement.

Finally, special thanks and love go to my wife, Hirut Hailu Alle (እማዬ). I am incredibly lucky to find the virtuous woman with a noble character and prices far above rubies. You uphold me to endure the troubles with patience and composure. My life has been greatly enriched, my mind is stretched beyond limits from this huge learning curve I have been on, and my heart is bursting and beaming with love and pride for all of the wonderful things I have experienced and tasted of the goodness of my beloved wife. You are the one and only person with whom I will always be able to share every idea I have. Besides being a love of my life, you have been an additional advisor to this thesis. You taught me to struggle instead of giving up, to see the possibilities instead of focusing on the problems, to change myself before changing the world, to love unconditionally instead of giving and taking and to make a difference in difficult situations.

Kibruyesfa Sisay Vienna, Austria, June 2017

Abstract

Deforestation and forest degradation, mainly as a result of land use changes, have posed a great danger to the environment as well as the livelihood of many people. About 90% of the people in Amhara region depend on the forest resources. As a consequence of population pressure, the extent of deforestation and forest degradation in the region has been severe during the last century. Forest ecosystem services and goods have diminished at a fast rate. Up until now, no information exists on the current state of forests, nor do any sound forest management schemes in either Ethiopia or the Amhara region. The aim of this study was to (i) estimate the timber volume, the aboveground carbon and the net primary productivities of the forest in the Amhara region and to (ii) downscale the daily climate data for the Amhara region, needed as input data within an ecosystem modeling using the biogeochemical Biome-BGC to assess the forest productivity situations. Height-diameter and form factor functions were calibrated for the most important tree species and forest regions, so that timber volume and carbon could be calculated. Increment core samples were taken for the estimations of annual volume and carbon increment rates and net primary productivities. The terrestrial forest inventory estimations were combined with the land cover map based on agroecological zones and elevation ranges to derive clusters. Extrapolation of terrestrial forest estimates for the whole Amhara region was applied by using the clusters as a reference stand. As a result, forest productivity estimates for the whole Amhara region are provided for the first time. Based on our results, the forest area in the Amhara region is 2% of the total land area with an average volume stock of 65.7 m^3 ha^{-1}; the shrubland covers 27% and a volume stock of 3.7 m^3 ha^{-1}; and the woodland covers 6% with an average volume stock of 27.6 m^3 ha^{-1}. The annual volume increment rates of forests are 3.0 m^3 ha^{-1}; 1.0 m^3 ha^{-1}, for the shrubland; and 1.2 m^3 ha^{-1}, for the woodland. The estimated current total volume stock in the Amhara region is 59 million m^3 or 19.1 million tons of stored carbon. A spatiotemporally consistent grid (1979 – 2010) of daily minimum temperature, maximum temperature and precipitation data with a spatial resolution of 1 km was produced for the whole Amhara region. This had never been available before. The climate data together with the terrestrial forest inventory data are now available for use as input data for running the biogeochemical mechanistic (Biome-BGC) model. Thus, a framework for sustainable forest management will be developed for the Amhara region, for the first time. Finally, we will demonstrate a conceptual, methodological approach to estimate the forest productivities of the whole Amhara region and suggest a sustainable forest management framework.

Kurzfassung

Entwaldung und Walddegradation als Hauptfolgen von Veränderungen bei der Landnutzung stellen eine große Gefahr für die Umwelt sowie für die Existenz des Menschen dar. Etwa 90% der Bevölkerung von Amhara (Äthiopien) sind auf Waldressourcen angewiesen. Ausgelöst durch hohen Bevölkerungsdruck war das Ausmaß der Entwaldung und Walddegradation im letzten Jahrhundert sehr groß in der Region. Waldökosystemdienstleistungen und Güter schwanden in raschem Tempo. Aktuell sind in der Region Amhara sowie in ganz Äthiopien weder Daten zu dem Waldzustand und noch solide Waldbewirtschaftungsstrategien vorhanden. Ziel dieser Studie war (i) das Holzvolumen sowie die oberirdische Kohlenstoff- und Nettoökosystemproduktivität der Wälder in der Region Amhara einzuschätzen und (ii) tägliche Klimadaten für diese Region auf einen kleineren Maßstab zu reduzieren, um sie zur ökologischen Modellierung mithilfe des biogeochemischen Biome-BGC-Modells verwenden und schlussendlich die Waldproduktivität bewerten zu können. Regionale Höhen–Durchmesser und Formzahlfunktionen wurden für die wichtigsten Baumarten abgeleitet, um anschließend das Holzvolumen und die Kohlenstoffmenge zu berechnen. Holzbohrkerne wurden entnommen, um den jährlichen Volumenzuwachs, sowie die jährliche Rate der Kohlenstoffixierung und die Nettoprimärproduktivität einzuschätzen. Schätzwerte aus der terrestrischen Waldinventur wurden mit Landnutzungskarten kombiniert, die auf agroökologischen Zonen sowie Seehöhe basieren, um Cluster abzuleiten. Extrapolation terrestrischer Wald wurde für die ganze Region Amhara mit Verwendung der Cluster als Referenzbestände. Schätzwerte der Waldproduktivität wurden zum ersten Mal für die ganze Region erzeugt. Der berechnete Waldanteil in der Region Amhara beträgt 2% der Gesamtfläche bei einem Holzvorrat von 65,7 m^3 ha^{-1}. Der Anteil und der Holzvorrat des Buschlands liegen jeweils bei 27% und 3,7 m^3 ha^{-1}, während Offenwald 6% der Gesamtfläche bedecken und über ein durchschnittliches Holzvorrat von 27,6 m^3 ha^{-1} verfügen. Die jährliche Zuwachsrate beträgt 3,0 m^3 ha^{-1} im Wald, 1,0 m^3 ha^{-1} im Buschland und 1,2 m^3 ha^{-1} in Offenwald. Der aktuelle geschätzte Holzvorrat in der Region Amhara liegt bei 59 Millionen Festmeter, das 19,1 Millionen Tonnen gespeichertem Kohlenstoff entspricht. Ein quadratisches Rasterpunktnetz von 1 km x 1 km mit täglichen Tiefst- und Höchsttemperaturen sowie Niederschlagswerten (Referenzperiode: 1979 – 2010) wurde zum ersten Mal für die Region Amhara erstellt. Die klimatischen Daten sowie die Daten aus der terrestrischen Waldinventur stehen jetzt zur Verfügung, um das biogeochemisch mechanistische Modell Biome-BGC anzuwenden. Dies ermöglicht die Entwicklung eines Rahmens für die

nachhaltige Waldbewirtschaftung in der Region Amhara zum ersten Mal. Schließlich wird in der vorliegenden Arbeit ein konzeptionell-methodischer Ansatz zur Schätzung der Waldeproduktivität der gesamten Region Amhara dargestellt und Empfehlungen bezüglich eines Rahmens für die nachhaltige Waldbewirtschaftung ausgesprochen.

Contents

1 Introduction

Forests in the world are affected by various environmental and anthropogenic hazards (Köhl et al., 2015). Deforestation and degradation of forests caused by land use change (Morales-Hidalgo et al., 2015); tree harvesting (Ticktin, 2004), fragmentation (Tadesse et al., 2014), as well as climate change (UNFCCC, 2014) pose additional risks to forests worldwide. As a result, large areas of the world's forests have been lost or degraded. Between 1990 and 2015, a net loss of 129 million hectares of forest was observed, the majority in tropical forests (Achard et al., 2014; Köhl et al., 2015). Moreover, forest degradation and deforestation result in additional anthropogenic carbon emissions (Federici et al., 2015). The problem still seems to continue despite the environmental conservation and afforestation efforts (d'Annunzio et al., 2015). Though they are not sufficient to considerably minimize and/or reverse the global trend, reforestation and afforestation, restoration and rehabilitation of degraded forest lands are some of the measures being undertaken (Köhl et al., 2015). As a result, there is a net loss of forest resources and extensive forest degradation across the world and the problem continues to persist. These net losses of forest resources have resulted in a decline in ecosystem services and goods, in global warming, in a loss of biodiversity and in a reduction in human wellbeing (Zeleke and Hurni, 2001).

Ethiopia is no different, if not the best example for the deforestation and forest degradation experiences. Deforestation in Ethiopia is severe and has a long history, especially in the central and northern highlands, the parts where human and animal population pressure has been significant (Wondie et al., 2016). In Ethiopia, farming is subsistence; dependence on the forest resources is extensive and settlements are usually near and/or inside forests which have been changing landscapes for millennia (Lemenih and Kassa, 2014). Consequently, the forest resources have been receding at a fast rate. Most of the remaining moist afromontane forests of the country are found in the southwestern part of the country, which was remote and inaccessible until recently. Ethiopian forest cover was once 40% of the total land mass (Badege Bishaw, 2001) and declined to 3% in 2000s (Sisay et al., 2015). Loss of productivity due to the severe soil and water erosion, loss of biodiversity, decline of benefits from forest resources, etc are the main problems faced due to the deforestation and forest degradation in Ethiopia (Zeleke and Hurni, 2001). Besides these prominent challenges, a number of other factors also justify the need for restoration and forest management in Ethiopia. Biomass is the main energy source for the over 90% of the 100 million people in the country (Federal

Democratic Republic of Ethiopia, 2011). In order to minimize as well as avoid environmental and socioeconomic problems, governments of Ethiopia began taking measures to rehabilitate degraded forests and re-afforest forest lands. Up to the beginning of the 20th century, the people and governments dealt with the scarcity of forest products by moving close to forested areas (Lemenih and Kassa, 2014). However, in the 1890s, an alternative approach involving reforestation and afforestation was introduced by the emperor of Ethiopia, Menilik-II (Melaku Bekele, 2003). This marks one of the first formal forest management attempt in the history of contemporary Ethiopia. Despite the unsuccessful efforts, there is a recently growing awareness that deforestation and forest degradation should be mitigated as soon as possible. Thus, the Ethiopian government, in its December 2011 strategy, identified the forestry sector as one of the pillars of the green economy that the country is planning to build by 2030 (Federal Democratic Republic of Ethiopia, 2011). The government also set targets on afforestation, reforestation and improved management of natural forests and woodlands. However, Ethiopia has not had a standardized and effective, sustainable forest management scheme until now. Sustainable Forest Management (SFM) requires a continuous assessment of forest conditions covering the species distribution, standing tree volume as well as volume increment rates (Hasenauer, 2006). Woody biomass inventory and strategic planning project (WBISPP) 1990 – 2000 have attempted to establish the National Forest Inventory (NFI) for the assessment of forest conditions throughout Ethiopia (Parent, 2000). However, the efforts made by WBISPP could not be further maintained after the phasing out of the project. There have also been recent small scale efforts mainly by Non-Governmental Organizations (NGOs) to curb the mismanagement through the so called participatory forest management (PFM) (Gobeze et al., 2009; Siraj et al., 2016). The historical trend is similar for the Amhara region as well.

The current situation in Ethiopia demands forest management studies which are sufficient for long-term projections and extrapolations to large spatial scales (Moreno et al., 2016). Yet, most of the studies being undertaken are restricted to local level scales, focus on specific species and unfitting to each other to satisfy the large spatiotemporal scale which is currently in demand (Berhe et al., 2013; Negash et al., 2013; Sisay et al., 2015; Wondie et al., 2011). Therefore, conducting a study to ensure a sustainable forest management at a regional level is imperative.

SFM is fundamental to satisfy the diverse interests vested upon forest ecosystems. Modern SFM has, therefore, evolved from basic timber supply to more integrated land use planning with social, economic, and ecological dimensions (Sloan and Sayer, 2015). At the local level, SFM contributes to peoples' livelihoods, income generation and employment (Gobeze et al., 2009). At the environmental level, it contributes through, for example, carbon sequestration, biodiversity protection, water and soil conservation (Liang et al., 2016). Therefore, developing a framework for SFM for the Amhara region is of paramount importance. Empirical studies for the Amhara region alone, which is a large land mass (1.5 million square kilometer) with heterogeneous environmental features, are less efficient for developing a framework for the sustainable forest management. Ethiopia, and particularly the Amhara region, is a mountainous region in which topographic and climatic extreme conditions make the ecosystem vulnerable to changes of climate and land use (Hurni, 1998). Combining forest ecosystem modeling, remote sensing techniques and terrestrial point sampling is essential to bridge the spatiotemporal scaling gap for mitigating the environmental and social threats.

2 Objective and Outline

This PhD work is part of the ongoing larger activity for the assessment of forest productivities and development of sustainable forest management framework for the Amhara region. The project covers two main efforts. The first part is tackled by this PhD work and the second part is being tackled by another PhD work which is in progress (Belay et al., 2017). The mission of this thesis is therefore to assess the current situations of forests and provide the necessary input data for the biogeochemical forest ecosystem model using Biome-BGC. Finally, the conceptual framework for the SFM for the Amhara region will be developed by integrating different conceptual approaches, such as terrestrial forest estimation, land cover classification using remote sensing data and a biogeochemical forest ecosystem modeling. Different forest types were sampled for timber volume, annual volume increment, aboveground carbon stock, annual carbon increment and NPP estimations and extrapolated to the whole region using a land cover map. Due to the lack of data in the Amhara region, we further used the biogeochemical ecosystem model Biome-BGC to fine-tune the regional estimations and assess the state of forests under different environmental and management scenarios. For the modeling work and the development of an SFM framework, additional input data such as daily minimum temperature, maximum temperature and precipitation is needed.

The objectives are:

(i) to estimate the productivity of forests in the Amhara region using terrestrial and remote sensing data (Paper I);
(ii) to provide daily climate data for the Amhara region needed as input data within an ecosystem modeling and productivity assessment scenario (Paper II).

This PhD work is the first part of an ongoing larger activity. The first step of this PhD work was to collate the forest inventory data in different forests in the Amhara region. In the beginning, height-diameter and form factor functions were calibrated for the forests in the Amhara region. The increment cores collected during the forest inventory were used to estimate the forest increment rates. The forest stand data were then used to estimate the current timber volume, carbon stocks, volume and carbon increments and NPP. The results were existing timber volume, volume increments, carbon, carbon increments and NPP. The local terrestrial inventory data is extrapolated to the whole Amhara region using a land cover map. However, because of lack of enough inventory data, a biogeochemical forest ecosystem

modeling is being implemented to further improve the estimations and analyze the different scenarios. This modeling extension is the second part of the ongoing project (Belay et al., 2017). The second and final part of the project, which is the implementation of the modeling and scenario analysis using biogeochemical model Biome-BGC, is in progress by another PhD work, which will enable us develop an SFM framework (see Figure 1).

In order to run the Biome-BGC model, we also needed spatiotemporally consistent input data. Daily climate data, in addition to the terrestrial inventory data for the Amhara region was one of the necessary input data. Therefore, weather data from weather stations in the Amhara region were collected. The collated weather station data was used for calibration and validation of downscaled daily climate data. Global datasets from National Centers for Environmental Predictions (NCEP) and WorldClim are used to produce the daily climate data for the Amhara region. Daily minimum and maximum temperature and precipitation with 1 km spatial resolution from 1979 – 2010 were produced.

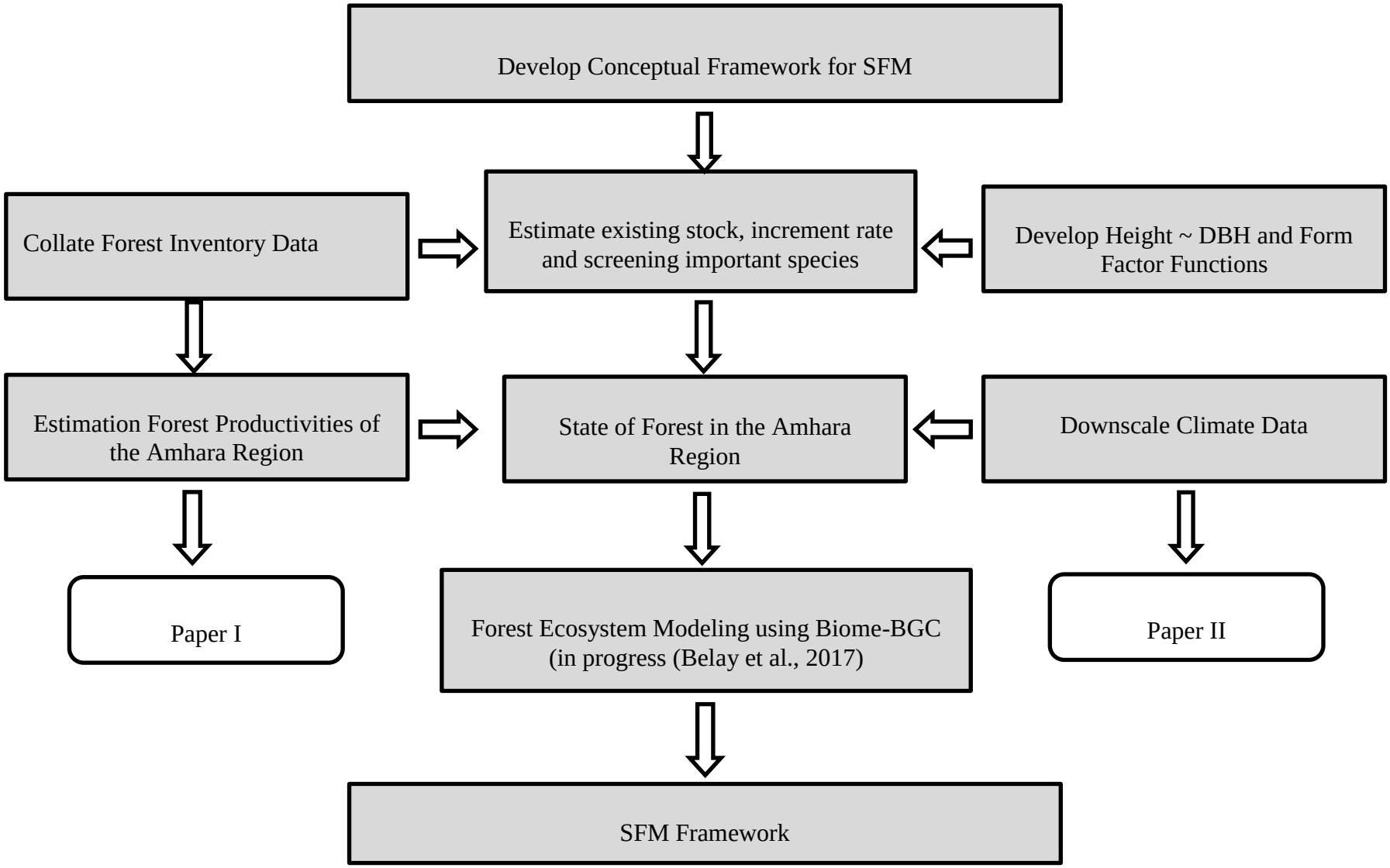

Figure 1. Flowchart of the research. (Paper # refers to the publication where the research is explained in detail)

3 Data

3.1 Description of Ethiopia

Ethiopia is the most populous, mountainous and landlocked country in the world located in the Eastern Horn of Africa. The Great Rift Valley splits the country from West to East. It shares borders with six African countries. To the north and northeast Ethiopia borders Eritrea, with Djibouti and Somalia to the east, Sudan and South Sudan to the west and Kenya to the south. Ethiopia is the oldest, with more than 3000 years written history and one of the independent nations in the world. It has a unique cultural heritage as being the home of the Ethiopian Orthodox Church and the source of the first modern humans (Karbo, 2013; Pagani et al., 2015). The current form of Government in Ethiopia is a Federal Democratic Republic with 9 regional states. The Amhara region is the third largest region and is located in the northwestern part of Ethiopia. Ethiopia covers a total geographical area of 1.1 million square km and a population of more than 100 million (Tegegne et al., 2016).

Ethiopia's landscape varies from barren desert to the green Ethiopian Plateau. It is a land of natural contrasts: vast fertile land from the west; arid and degraded from the east; tropical moist afromontane forests, which are included in the United Nations Biosphere Reserves; numerous rivers and the world's lowest and hottest places of Dallol in the north. Ethiopian highlands are Africa's largest continuous mountain ranges. Ethiopia also suffers recurrent droughts with their concomitant famines. The elevation gradient ranges from the lowest Danakil Depression at 152 meters below sea level to the highest point of Ras Dejen at 4550 meters above sea level. As a result of very wide elevation difference and undulating topography, the country's climate is very diverse. The country can be classified into six major agro-ecological zones based on the agro-climatic conditions determined by altitude and rainfall distribution (Hurni, 1998). The topographical and climatic features of the whole country result in a mosaic of watersheds with a wide array of ecosystems and immense biodiversity, making Ethiopia fulfil the two biodiversity hotspots of global significance: the Eastern afromontane and the Horn of Africa (Myers et al., 2000). Ethiopia is the place of origin of the coffee bean, which originated from a place called Kefa. As the forest covers less than 3% of the country's land surface, the biodiversity resource, including the wild coffee populations are severely in endangered. Ethiopia is home to nine UNESCO World Heritage Sites (Ndoro et al., 2009), the most in Africa.

The Amhara region is located in the Northwestern part of Ethiopia and characterized by its very diverse agroecology, with a highly undulating topography throughout the center and northern highland areas, and flat woodlands covering the western lowlands to the Sudan. The region contains the source of the Nile and the highest point in Ethiopia - Ras Dejen (4550 m). It is also endowed with many endemic species of fauna and flora. There are over 20 million inhabitants in the region of which the majority lives in rural areas where the main livelihood is small-scale agriculture. The average landholding size, mainly in the highland areas where rain-fed agriculture takes place, is roughly one ha of land (Central Statistical Agency, 2008). Given the subsistence farming in the most part of the Amhara region, the dependence on the forest resources is so high it resulted in deforestation and forest degradation (Pistorius et al., 2017; Wondie et al., 2016). The studies which estimated the forest cover of the whole Amhara region reported different numbers and less than 10% (Hailu et al., 2015; Mekonnen et al., 2016).

3.2 Forest Stand Data

The forest data came from five forest regions of the Amhara National Regional State (ANRS). The forest regions represent different forest types at different agroecological zones (Figure 2). Forest stand data consisted of tree species, DBH, total tree height (H), height to live crown base (HLC), azimuth, and horizontal distance from the plot center. Saplings (DBH < 10 cm and height > 1.3 m) and seedlings (50 cm < height < 1.3m) were recorded (Sisay et al., 2017).

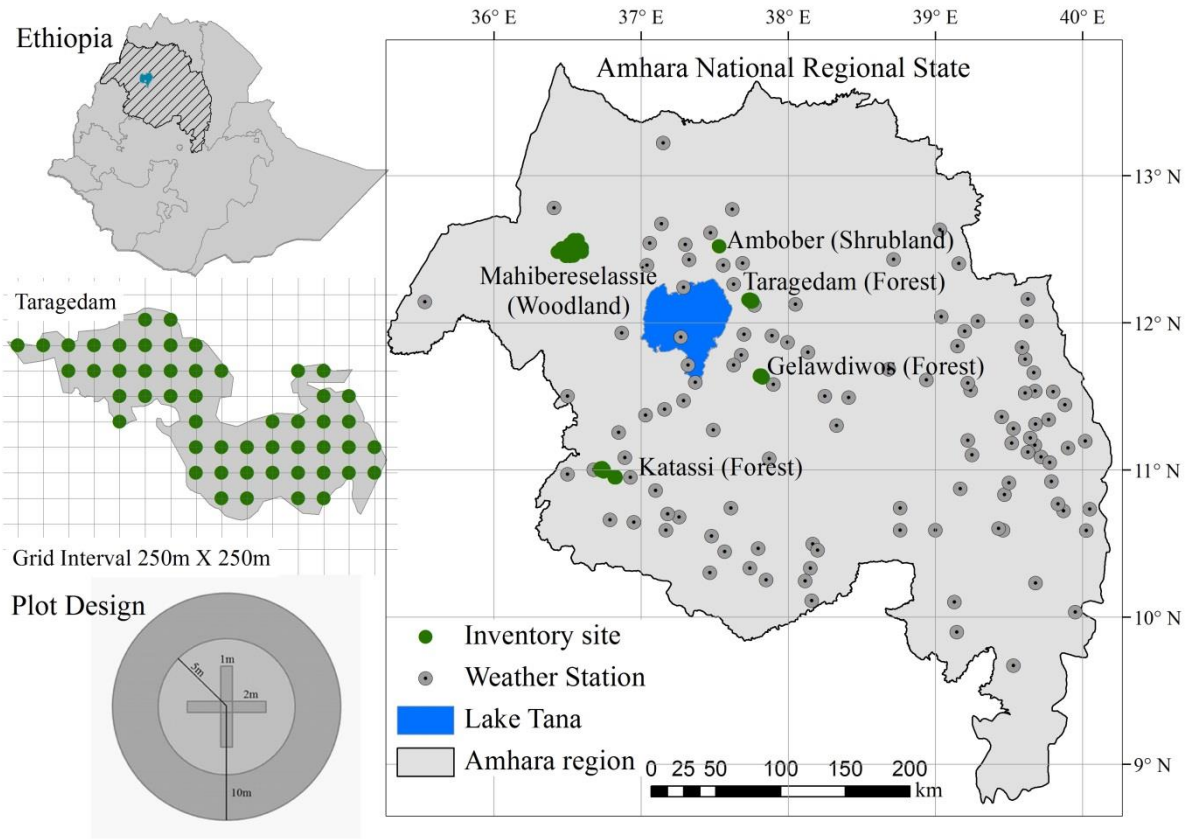

Figure 2. Map of the Amhara region

The terrestrial forest inventory does not address all the forests in the Amhara region. In order to get the full forest conditions of the Amhara region, an extrapolation of the inventory results using land cover map was used.

3.3 Land Cover Data

A land use and land cover map spanning 12 classes with 200 m × 200 m pixel spatial resolution was obtained from the Amhara Bureau of Agriculture. We defined the three simplified forestry relevant land cover classes: (i) forest, (ii) shrubland, and (iii) woodland plus the non-vegetated area. Since elevational gradients are one of the main factors affecting the growing conditions and thus the species distribution of Ethiopian mountains forests, we adopted Hurni's, (1998) elevation classes for agroecological zonation resulting in five elevation classes: (i) low land (500–1500 meters above sea level (m.a.s.l.)), (ii) mid altitude (1500–2300 m.a.s.l.), (iii) high land (2300–3200 m.a.s.l.), (iv) subalpine (3200–3700 m.a.s.l.) and (v) alpine (3700–4530 m.a.s.l.). Then, we assigned the land area derived from Landsat

data to each vegetation type and elevation classes to extrapolate the inventory results over the entire region.

Both the terrestrial inventory and land cover map fell short from the intended target due to the lack of sufficient data. Environmental and management scenario analyses were not possible as well. To circumvent data limitations and run the scenarios, we simulated a biogeochemical ecosystem model Biome-BGC. Among the multiple input data needed for the model to run, spatiotemporally consistent daily climate data is needed. Therefore, daily T_{min}, T_{max} and Prcp data with 1 km spatial resolution is prepared using global and local weather data for the Amhara region.

3.4 Climate Data

3.4.1 Global Weather Data

Daily values of minimum (T_{min}) and maximum (T_{max}) temperature and precipitation (Prcp) are obtained from the Climate Forecast System Reanalysis data set (Saha et al., 2010) produced by the NCEP. The NCEP data consists of various grids of different spatial and temporal resolutions describing the state of the atmosphere, land, ocean and sea ice on a global scale. The data is constructed using the assimilation of observed data and models which take all available observations every 6–12 h over the period being analyzed. Climate variables are available on a T382L64 horizontal resolution (Maraun et al., 2010; Saha et al., 2010) which is about 38 km at the Equator (0.3125 decimal degrees). The weather data needed for our study was extracted from a bounding box for 8.11° – 14.36° N latitude and 34.53° – 40.78° E longitude from the Texas A&M University spatial sciences website (Globalweather, 2012) for the years 1979–2010.

WorldClim (Hijmans et al., 2005) provides global long-term monthly mean, minimum and maximum temperature values as well as precipitation. The resolution is 30 arc seconds, which corresponds to 0.0083 decimal degrees. This resolution is commonly referred to as 1 km spatial resolution. The data set also provides 19 bioclimatic variables derived from the climate, but they are not used in this study. The data is based on climate stations from different sources, such as the Global Historic Climate Network Dataset (Peterson et al., 1998) or the WMO climatological normal (WMO, 1996). The station data were harmonized, which

resulted in a data set of precipitation records from 47 554 locations, mean temperature from 24 542 stations and minimum and maximum temperature from 14 835 stations (Hijmans et al., 2005). The data were interpolated using the thin plate smoothing splines procedure (Hutchinson, 1995). The raster data for T_{min}, T_{max} and Prcp for our study was obtained from the WorldClim website (WorldClim, 2005) for the same bounding box coordinates used for the NCEP data. This resulted in raster files with 750 columns and rows. The raster files were converted into GEOTIFF files, one file per variable with 12 raster bands (one per month).

3.4.2 Weather Station Data

According to the National Meteorology Agency of Ethiopia, meteorological stations in Ethiopia are divided into four classes based on their meteorological observation parameters (http://www.ethiomet.gov.et/stations/regional_information/2). First class stations are established for the purpose of synoptic meteorology. Observations are taken every full hour for 24 h a day. They observe 18 meteorological parameters, amongst them T_{min}, T_{max}, Prcp, relative humidity, wind speed and sunshine duration. Second class stations record meteorological data for climatological purposes. These stations measure more than 13 meteorological variables not relevant for our study. Third class stations only record three meteorological parameters every 24 h; T_{min}, T_{max} and Prcp. Fourth class stations measure only the total amount of precipitation in 24 h. Observations for the fourth class are taken at 0600GMT. For our analysis, we used data only from class 1 and 3 stations because we were interested in daily T_{min}, T_{max} and Prcp. Although the stations are established based on the aforementioned classes, some stations have stopped their operation for different reasons. Some stations were also outdated and replaced by new ones while others were established very recently. This makes acquisition of consistent data for the given time period difficult. In addition, we limited the meteorological station data to the time span between 1979 and 2010 so that they match with the available NCEP data. In the Amhara region, 66 stations fulfilled these criteria. For our analysis, we used 56 stations for calibration (early comparison and bias correction) of the downscaled data. After the downscaling and the associated bias correction were done, we obtained ten additional and independent weather stations from 1979 to 2010 for validation purposes (Sisay et al., 2016).

4 Methods

4.1 Workflow

The papers in this study attempt to estimate the state of forests and the forest estimate in turn used as an input for the modeling of the forest condition under different scenarios for our goal to develop a conceptual framework for SFM in the Amhara region (see Figure 1 and Appendix 9 .1). Paper I describes the analysis of the current state of forest resources and the productivity of the Amhara region through a combination of terrestrial forest inventory and land cover map. As the estimation of the forest conditions with this regional scale is the first attempt, multiple data were lacking to produce a better result. Therefore, a forest ecosystem modeling approach with a biogeochemical Biome-BGC is employed to model the forest condition under different environmental and management scenarios. For the modeling scheme, input data such as terrestrial forest condition and daily climate data are needed. Paper II produces 31 year gridded daily climate data with fine spatial resolution. The modeling effort, which suggests a conceptual framework for SFM is under a manuscript preparation (Belay et al., 2017).

4.2 Collate Forest Inventory Data

Terrestrial forest data was required for our study. Despite the importance of terrestrial forest inventories for the estimation of the state of forest conditions, there are no national or regional forest inventory schemes in Ethiopia. Hence, we designed an inventory plan for our five different forest regions. Total numbers of plots were 198. A consistent plot level data collection method was designed (see Figure 2) (Sisay et al., 2017). The data collected from these forest inventories form the basis of analysis for this study.

4.2.1 Height ~ Diameter Function

Data for the height-diameter function was collected based on the DBH records on a given sampling plot. We selected the so called “central” stem or tree - the 60 percentile of the DBH distribution for each species on a given sampling plot and measured the height of the tree.

However, this needs a height-DBH function to derive the missing tree heights. For our work, we chose the Petterson's (Schmidt, 1956) height-DBH function and estimated the coefficients.

4.2.2 Form Factor Function

As there are no form factor functions for most Ethiopian tree species, we calibrated the F. Evert's Australian Function (Evert, 1968). Data for the form factor function calibration came from the 400 trees belonging to 20 very common species. We selected 20 trees in each 5 most common species in the inventory sites.

4.2.3 Standing Stock and Increment Rates

To develop and implement any forest management activities, it is necessary to first understand the current state and the annual increment of the forests. The inventory is necessary to understand the current timber volume, volume increment, aboveground carbon stocks, carbon increment and NPP (Sisay et al., 2017). As part of this study, the increment rate of important tree species in each site was estimated and their productivities quantified for the first time (see Figure 5, 6, and 7) (Sisay et al., 2017).

4.3 Extrapolation of Terrestrial Estimates to the Whole Amhara Region

To analyze the forests condition throughout the Amhara region, the terrestrial forest inventory estimates are combined with remotely sensed land classification data. The digital land cover classification map was obtained from the Amhara Bureau of Agriculture. The land cover map consists of forests, shrubland, woodland and the non-vegetation classes. The map is further classified by different agroecological zones based on elevation classes (Hurni, 1998). A cluster was created by combining the terrestrial forest inventory estimates and the elevation based land cover map. Therefore, clusters were used as a reference stand approach where the terrestrial inventory information from the forest types are extrapolated into similar land cover types within similar elevational ranges to the whole Amhara region (Sisay et al., 2017).

The result can be further improved by incorporating additional data to develop the SFM framework. Given the severe data scarcity in the Amhara region, a modeling approach using a

biogeochemical Biome-BGC model is implemented to assess the carbon flux within the ecosystems under different scenarios and finally develop the SFM framework.

4.4 Forest Ecosystem Modeling

To analyze and model the forest ecosystems in the Amhara region, input data such as forest characteristic and climate data is required. The required input data should meet the spatial and temporal data requirements. Therefore, calibration of form factor and height-diameter functions as well as terrestrial forest estimation of timber volume, carbon stock and NPP for the forests in the Amhara region were undertaken (Sisay et al., 2017). A daily minimum temperature, maximum temperature and precipitation with 1 km spatial resolution were downscaled from global data (Sisay et al., 2016). The modeling work is still in progress (Belay et al., 2017).

4.5 Downscale Climate Data

There hasn't been spatially and temporally continuous climate data for the Amhara region. We used two global raster data sets (NCEP and WorldClim), both on different spatial and temporal resolutions, to obtain a 1 km daily climate grid consisting of minimum temperature, maximum temperature and precipitation. We obtained the monthly high-resolution (1 km) WorldClim dataset to adjust the daily low-resolution (38 km) NCEP values. We applied the delta downscaling procedure, designed in the study (Sisay et al., 2016). A bias correction factor was additionally applied to further improve the downscaled data. The downscaled datasets include daily precipitation and minimum and maximum temperature all on a 0.0083˚ resolution (approximately 1 km) from 1979-2010. Figure 3 shows the methodological steps of the downscaling process conditions.

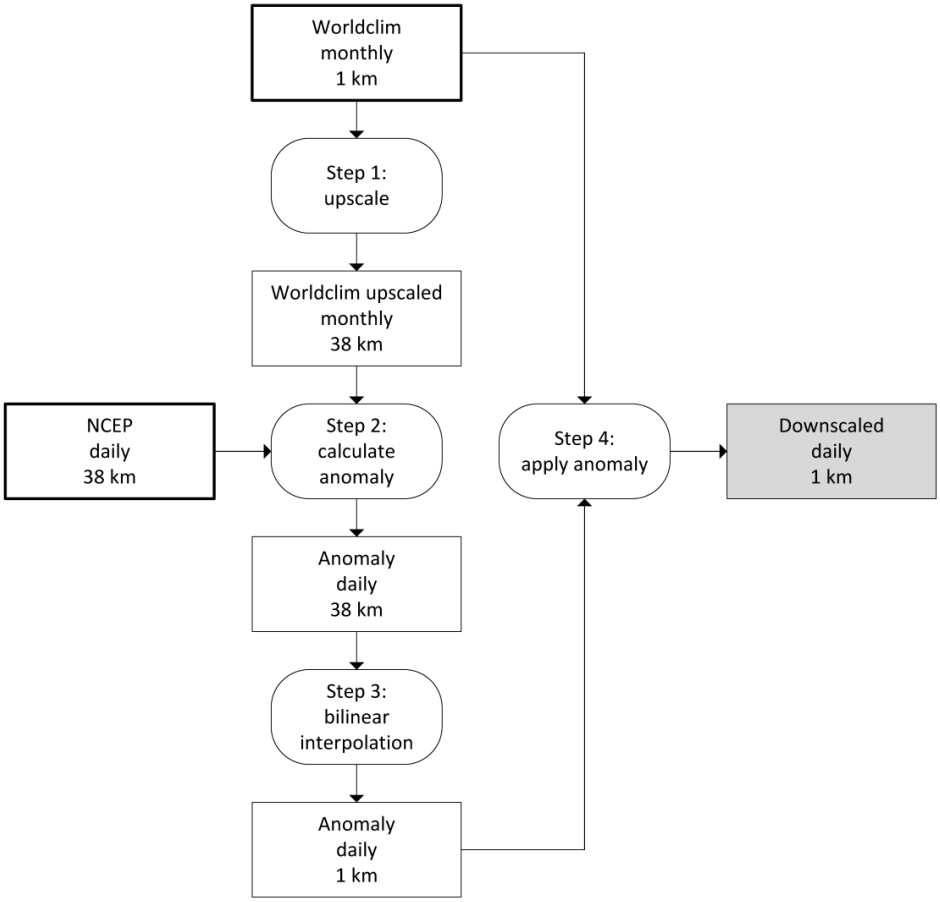

Figure 3. Methodological flow of downscaling

4.6 Developing Sustainable Forest Management Framework

To develop a sustainable forest management framework for the Amhara region, the current condition, their increment rate and projections for different scenarios are required. The type of forest, their spatial coverage under different agroecological zones, the current timber volume and carbon stock, the increment rates and productivities are important forest characteristics for sustainable management. Form factor and height-diameter functions that operate at an individual tree level are crucial models in the estimation of tree growth where there are no such functions in place. Integrating the terrestrial inventory with the remote sensing techniques provides the full picture at the regional scale. The other approach for the development of the SFM is the implementation of a forest ecosystem modeling which is under progress. The modeling approach is very important where the lack of input data is severe. Therefore, forest ecosystem modeling using Biome-BGC is under progress to finally come up with a framework for the sustainable management of forests in the Amhara region (see Figure 4).

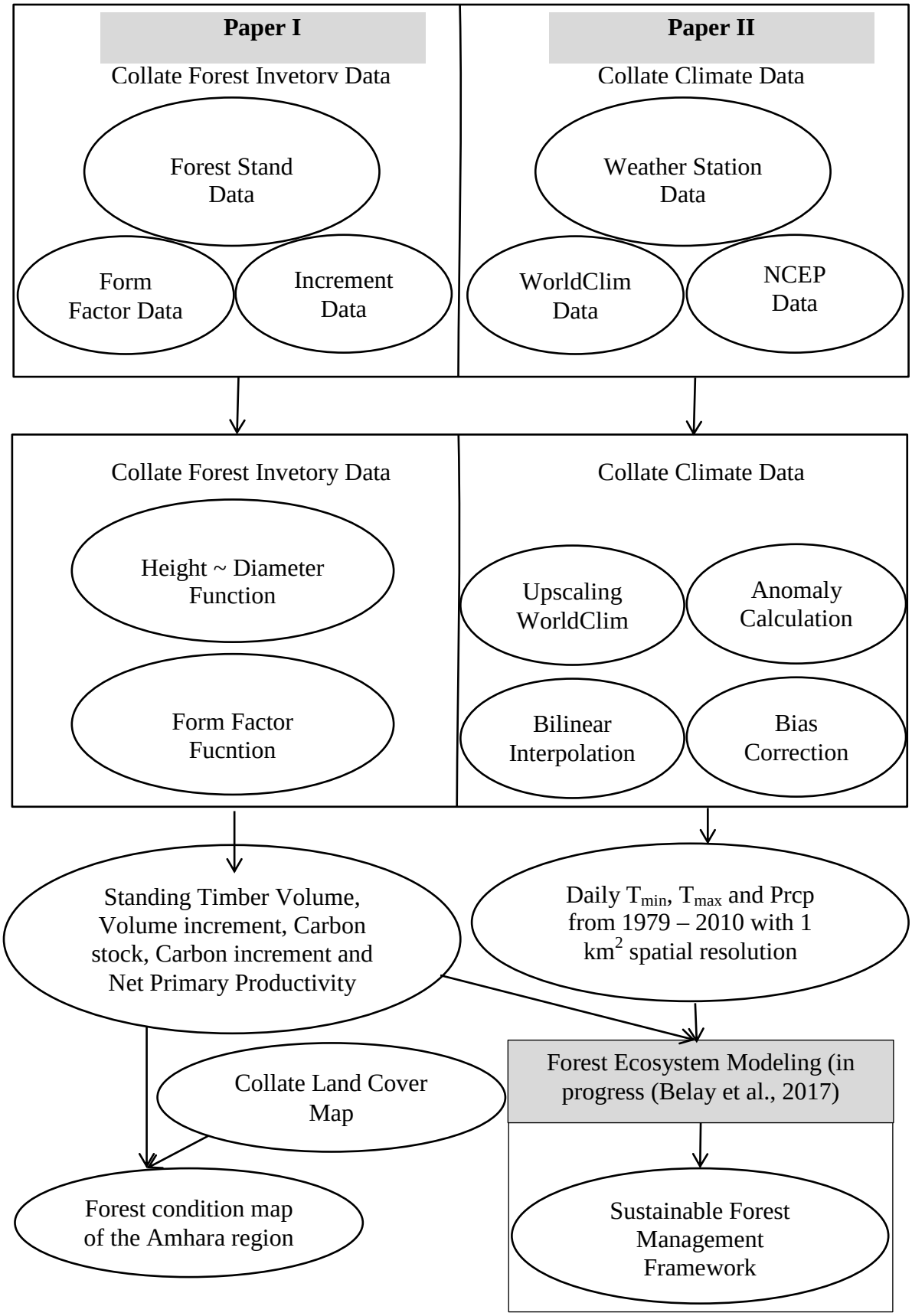

Figure 4. Flowchart showing the different processes involved in developing a sustainable forest management framework. Ovals represent the outputs and rectangles represent the processes. Ovals inside the rectangles indicate data used within the process. The next step of this PhD work, which is Forest Ecosystem Modeling, is in progress.

5 Analysis and Results

In order to develop the conceptual framework of the SFM for the forests in the Amhara region, analyzing the current state of the forests as well as changes under different environmental and social scenarios is essential. Two approaches are implemented in this study. The first approach is assessing the state of the forests in the Amhara region by collecting terrestrial inventory data from five different forest regions and three forest types: forest, shrubland and woodland. Extrapolation of the terrestrial assessments for the whole Amhara region was done by combining with the land cover map of the Amhara region which was obtained from ANRS. The land cover map was reclassified into 3 forest cover types: (i) forests, (ii) shrublands, (iii) woodland and non-woody vegetation and five elevation classes: (i) low land (500–1500 meters above sea level (m.a.s.l.)), (ii) mid-altitude (1500–2300 m.a.s.l.), (iii) high land (2300–3200 m.a.s.l.), (iv) sub-alpine (3200–3700 m.a.s.l.) and (v) alpine (3700–4530 m.a.s.l.). Therefore, a cluster with forest type and elevation range was created. A "reference stand approach" was employed where the regional inventory information is used as a proxy for a given cluster, which enabled the extrapolation of the local inventory results to the whole Amhara region (see Paper I of Appendix 9.1). To further improve the results of the first approach and to assess the forests under different environmental and management scenarios, the second approach, a forest ecosystem modeling, is used. The modeling of the forest ecosystem approach is implemented using the biogeochemical Biome-BGC flux model. Input data from terrestrial point data and gridded climatic data are needed for the Biome-BGC model. Both data in the Amhara region were unavailable. Therefore, various aspects of forest conditions, e.g. forest characteristics, productivity and climate data are produced. A daily Tmin, Tmax and Prcp with 1 km spatial resolution was downscaled for the Amhara region the years from 1979 – 2010.

5.1 Terrestrial Forest Inventory

Terrestrial forest inventory data is needed to spatially analyze forest characteristics of the Amhara region. We selected 5 different forest types spanning wide elevations and agro-ecological zones of the Amhara region. To date, there has never been a dataset that contains plot level information to such an extent. NFI data from 5 forest sites and 198 plots was collated. The height-diameter and form factor functions were calibrated for the most important tree species in the region for the first time. 1154 trees were used to calibrate a

height-diameter function for 24 tree species and 284 trees cover the species groups "other trees" by region. The twenty height-diameter functions are developed for the most important tree species in the four forest sites and the four functions are for the four forest sites. The Petterson's (Schmidt, 1956) height-diameter function was chosen to derive missing tree heights. This dataset is used to calibrate species-specific height-diameter functions, which are then in turn used to derive missing tree heights and calculate timber volume and carbon stock. Combined with the core increment sample data, the annual volume increment, annual carbon increment and NPP were calculated. Next, the plot values for the above parameters are calculated (Sisay et al., 2017).

Gelawdiwos and Katassi exhibited higher mean timber volume, annual volume increment rate, aboveground carbon stock and annual carbon increment rate per plot followed by Taragedam, Mahibereselassie and Ambober (Figure 5 and 6) (see Paper I of Appendix 9.1.).

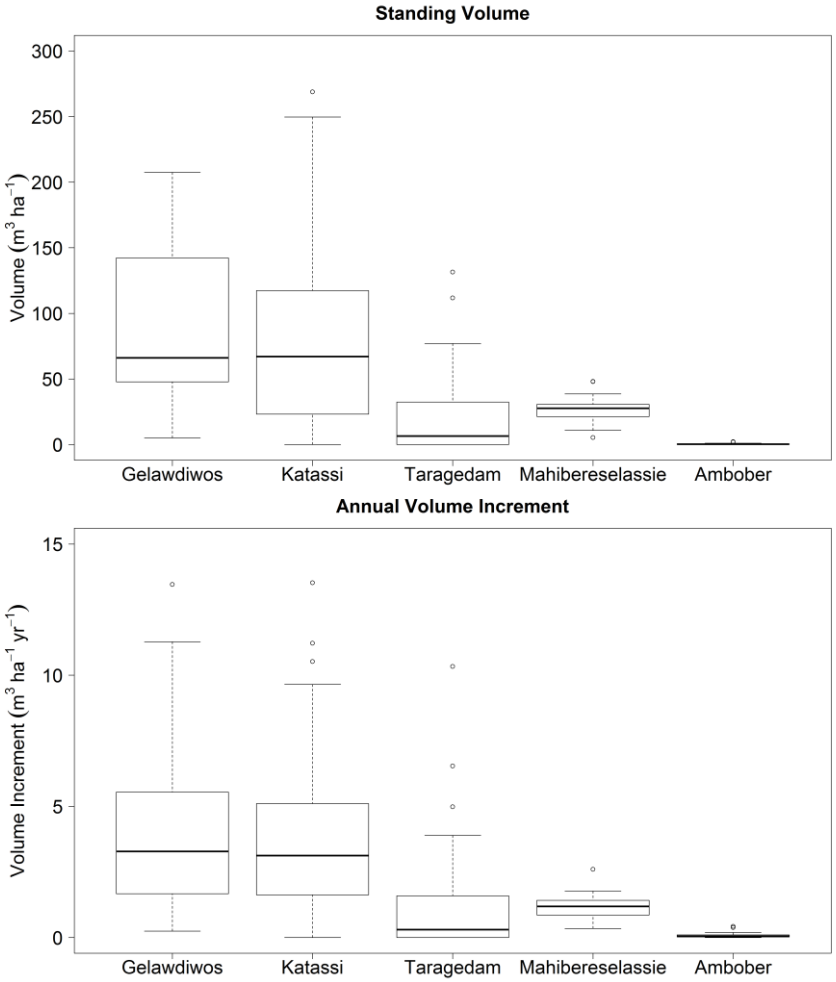

Figure 5. Standing volume (m^3 ha^{-1}) and annual volume increment (m^3 ha^{-1} yr^{-1}) by forest sites

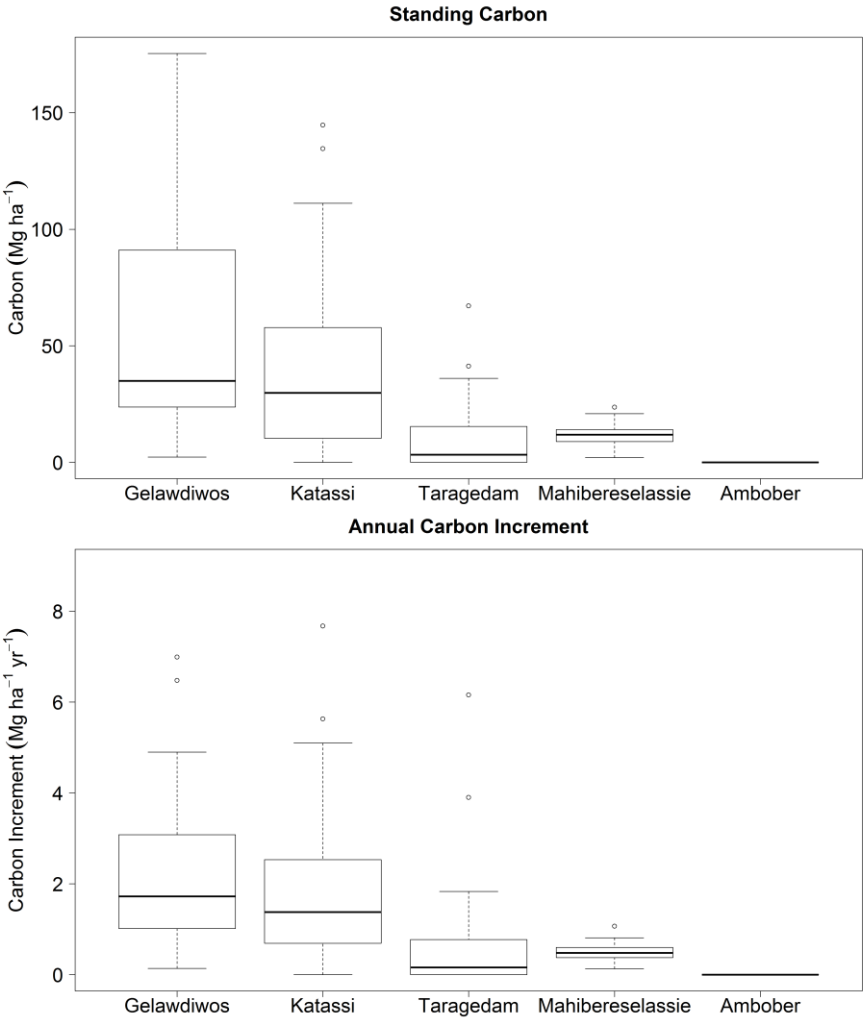

Figure 6. Standing carbon (Mg ha^{-1}) and Annual carbon increment (Mg ha^{-1} yr^{-1}) by forest sites

The NPP, which is the amount of carbon remaining and allocated in the plant parts after autotrophic respiration per growth period, is calculated as the sum of periodic carbon accumulation in the fine root turnover, aboveground woody parts and litter fall (Hasenauer et al., 2012). The NPP of each tree was calculated from 2005 – 2014 by using the core increment data. Next, the tree values were converted into plot and forest site values. Gelawdiwos and Katassi exhibited higher NPP followed by Taragedam, Mahibereselassie and Ambober (Figure 7).

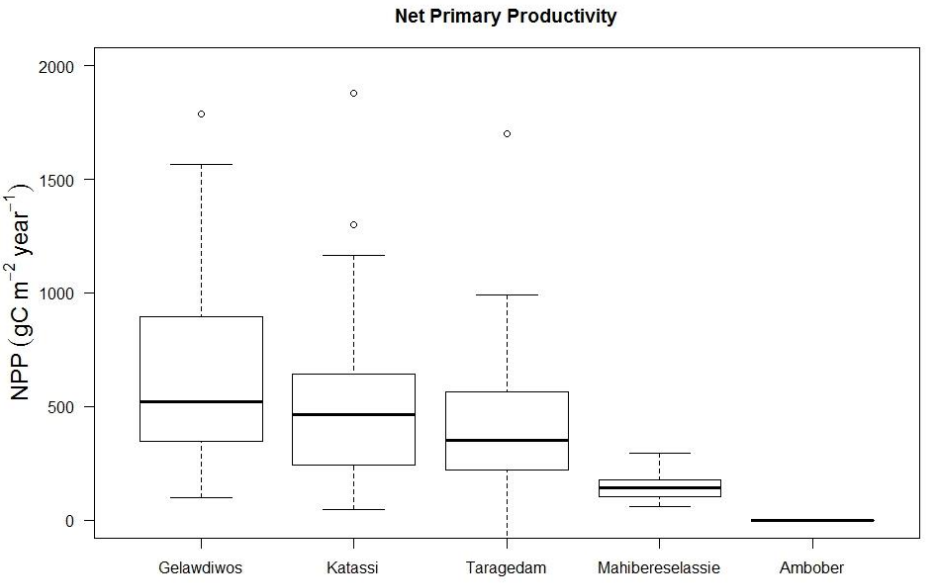

Figure 7. NPP (gC m^{-2} $year^{-1}$) by forest sites

Identification of productive species is essential for a future harvesting plan and reforestation activities. However, tree species identification based on their growth rate and productivity has never been done in the Amhara region which would facilitate the forest management activities. In order to aid the forest management plans and activities, we identified the top 20 tree species, from all the forest inventory regions, based on their NPP value (Figure 8). Therefore, the most important tree species with high productivity are identified (Figure 8). *Schefflera abyssinca* (0.0034 MgC $m^{-2}yr^{-1}$), *Eucalyptus globulus* (0.003 MgC $m^{-2}yr^{-1}$) and *Chionanthus mildbreadii* (0.0019 MgC $m^{-2}yr^{-1}$) have exhibited the largest NPP compared to other tree species in the Amhara region.

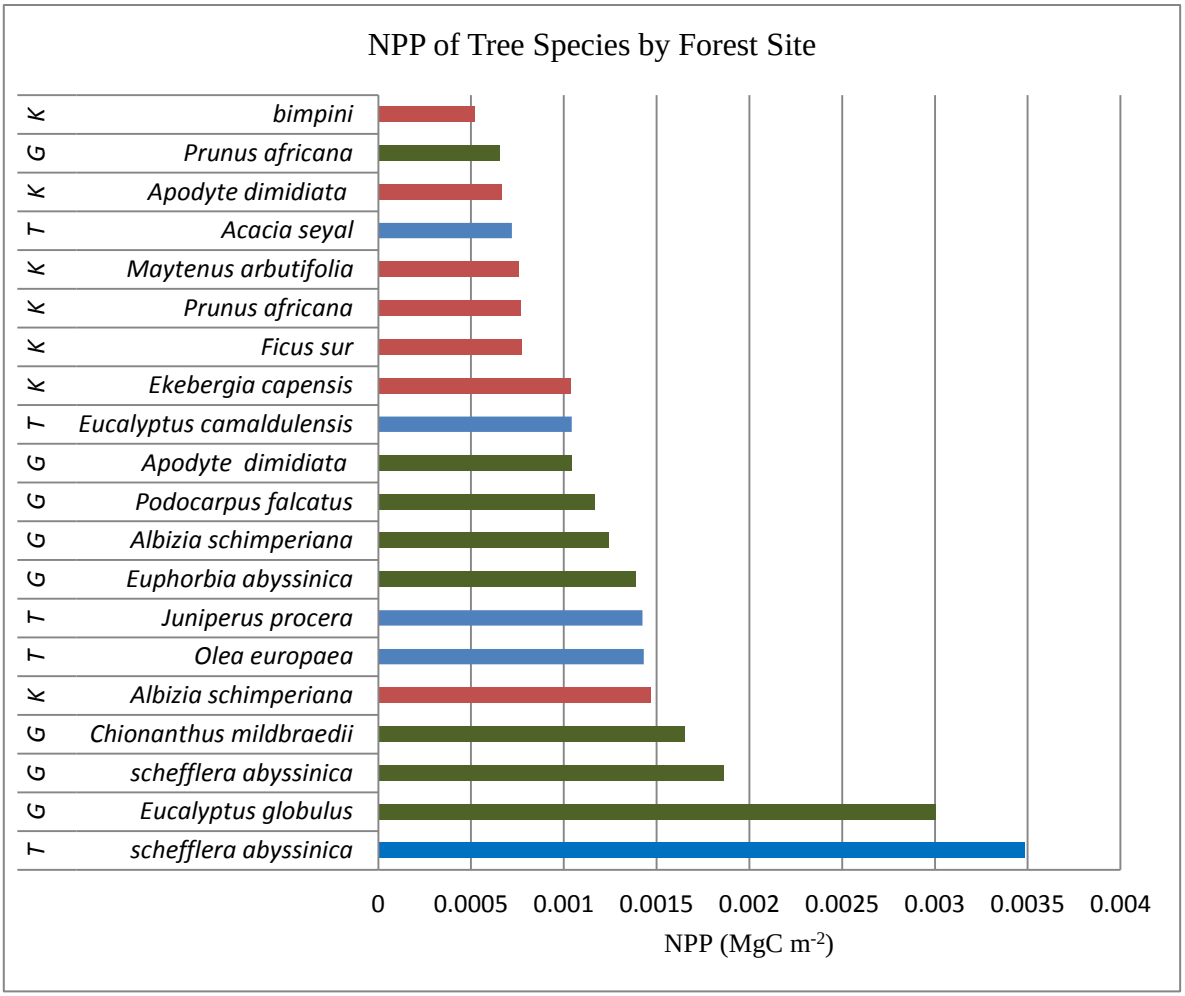

Figure 8. Net Primary Productivity (Mg C m^{-2}) of top 20 tree species by forest Site. K = Katassi, G = Gelawdiwos, T = Taragedam

5.2 Extrapolation of Terrestrial Estimates to the Whole Amhara Region

The land cover map covers 12 classes with 200 m x 200 m pixel spatial resolution based on Landsat satellite images. The 12 land cover classes are afro-alpine, bare land, cultivation, grassland, highland bamboo, natural forest, plantation, shrubland, woodland, urban, wetland and water. We aggregated the 12 land cover classes to six classes based on their vegetation characteristics for fitting our terrestrial inventory as follows: plantation, highland bamboo and natural forest are grouped as forest. Afro-alpine regions and shrubland are aggregated into shrubland. Woodland remained as woodland. Bare land, cultivation, grassland and wetland are grouped as non-woody vegetation. Water and urban classes remained as water and urban, respectively. Our final land cover classes relevant for our analysis are (i) forest, (ii) shrubland, and (iii) woodland. Figure 9 shows the spatial distribution of land cover classes within the Amhara region.

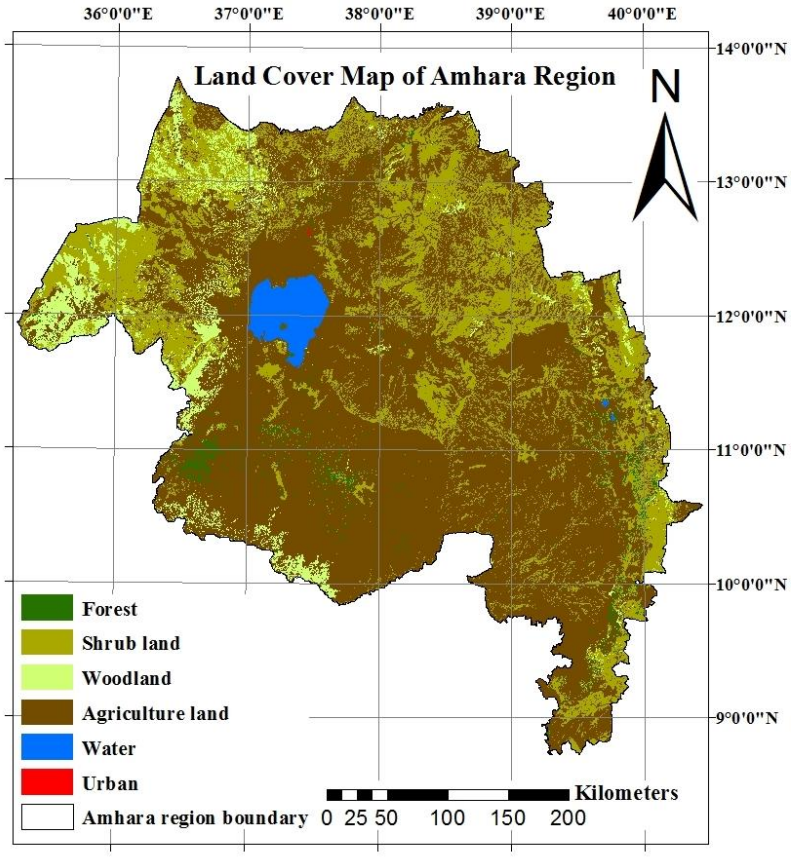

Figure 9. Land cover map of Amhara region after aggregation of the land cover classes

The accuracy of the regrouped land cover map was evaluated by performing stratified sampling. In total, 607 stratified sample points were randomly selected and distributed over the areas of the aggregated classes. The class of each of the 607 pixels was assigned with the help of finer resolution reference data combined with visual interpretation (Morisette et al., 2002). Bing and Google Earth images were used for the independent reference data. As the pixels were often composed of multiple cover types, the main class (a land cover class with largest coverage) of a pixel was assigned as the class of the pixel. The accuracy assessment was applied by using the error matrix according to Olofsson et al.(2013), which compares the known reference data to the corresponding results of automated classification (Liu et al., 2007). Considering the coarse resolution (200 m × 200 m) of the map and the high land fragmentation within the Amhara region, the accuracy of the land cover classification was good.

Since elevational gradients are one of the main factors affecting the growing conditions and thus the species distribution of Ethiopian mountains forests (Berhanu et al., 2016), we adopted

Hurni's (1998) elevation classes for agro-ecological zonation resulting in five elevation classes: (i) low land (500–1500 meters above sea level (m.a.s.l.)), (ii) mid altitude (1500–2300 m.a.s.l.), (iii) high land (2300–3200 m.a.s.l.), (iv) sub-alpine (3200–3700 m.a.s.l.) and (v) alpine (3700–4530 m.a.s.l.). Then, we further classified the land cover map in to each vegetation type and elevation classes which resulted 15 clusters (3 vegetation types x 5 elevation classes). We assigned each of our forest inventory areas to their corresponding clusters. The idea here was to create a kind of a "reference stand approach", where we assumed that regional forest inventory information could be used as a proxy for a given cluster and thus allow us to extrapolate local inventory results (our regional sites) to the whole Amhara region. Based on the reference stand approach, the timber volume, annual volume increment, aboveground carbon stock, annual carbon increment and NPP for the whole Amhara region was calculated (Table 1). The details can be found in Paper I of Appendix 9.1.

Table 1.Total timber volume, volume increment, total carbon stock, carbon increment and Net Primary Production (NPP) of inventory regions and the whole Amhara region. Where x is mean and sd is standard deviation.

Variable	Forest (x ± sd)	Shrubland (x ± sd)	Woodland (x ± sd)
Volume (m^3 ha^{-1})	65.7 ± 61.6	3.7 ± 3.4	27.6 ± 10.7
Volume increment (m^3 ha^{-1} yr^{-1})	1.2 ± 0.5	0.9 ± 0.9	1.2 ± 0.5
Carbon (Mg ha^{-1})	35.4 ± 36.3	1.11 ± 0.92	11.9 ± 5.2
Carbon increment (Mg ha^{-1} yr^{-1})	2.7 ± 1.7	0.22 ± 0.18	0.5 ± 0.2
Total timber volume in the Amhara region (million m^3)	17.6	15.9	25.7
Total timber volume increment in the Amhara region (million m^3 yr^{-1})	0.71	3.9	1.12
Total carbon in the Amhara region (million m^3)	7.78	4.76	11.07
Carbon increment in the Amhara region (million m^3 yr^{-1})	0.34	0.95	0.47
NPP (g C m^{-2} yr^{-1})	463.1 ± 343.2	55.4 ± 46.0	150.4 ± 62.9
NPP of the Amhara region (g C m^{-2} yr^{-1})	484.3	55.4	150.4

5.3 Daily Climate Data

Climate data and terrestrial forest inventory estimates are key input data needed for running the Biome-BGC model. In the Amhara region, meteorological stations record different weather parameters such as minimum temperature, maximum temperature, precipitation, etc. They form networks that are often irregularly spaced and do not provide a systematic grid of parameters across larger areas. Meteorological station data frequently have problems with data quality, inconsistencies and missing data values. Places which are far away from meteorological stations would be left unobserved and often result in less accurate values if estimated from surrounding stations. Because of these irregularities and inconsistencies of climate data coverage, climate grids have been developed to fill the spatiotemporal gaps of meteorological stations. Spatiotemporally consistent climate data is downscaled from global datasets (WorldClim and NCEP) for the Amhara region, for the first time. The downscaled climate data are daily T_{min}, T_{max} and Prcp, with a spatial resolution of 1 km from 1979 – 2010. The downscaled climate data has ensured availability of weather data for places where weather stations do not exist. This has also provided the ability to use the data in the Biome-BGC model as an input data (Figure 10).

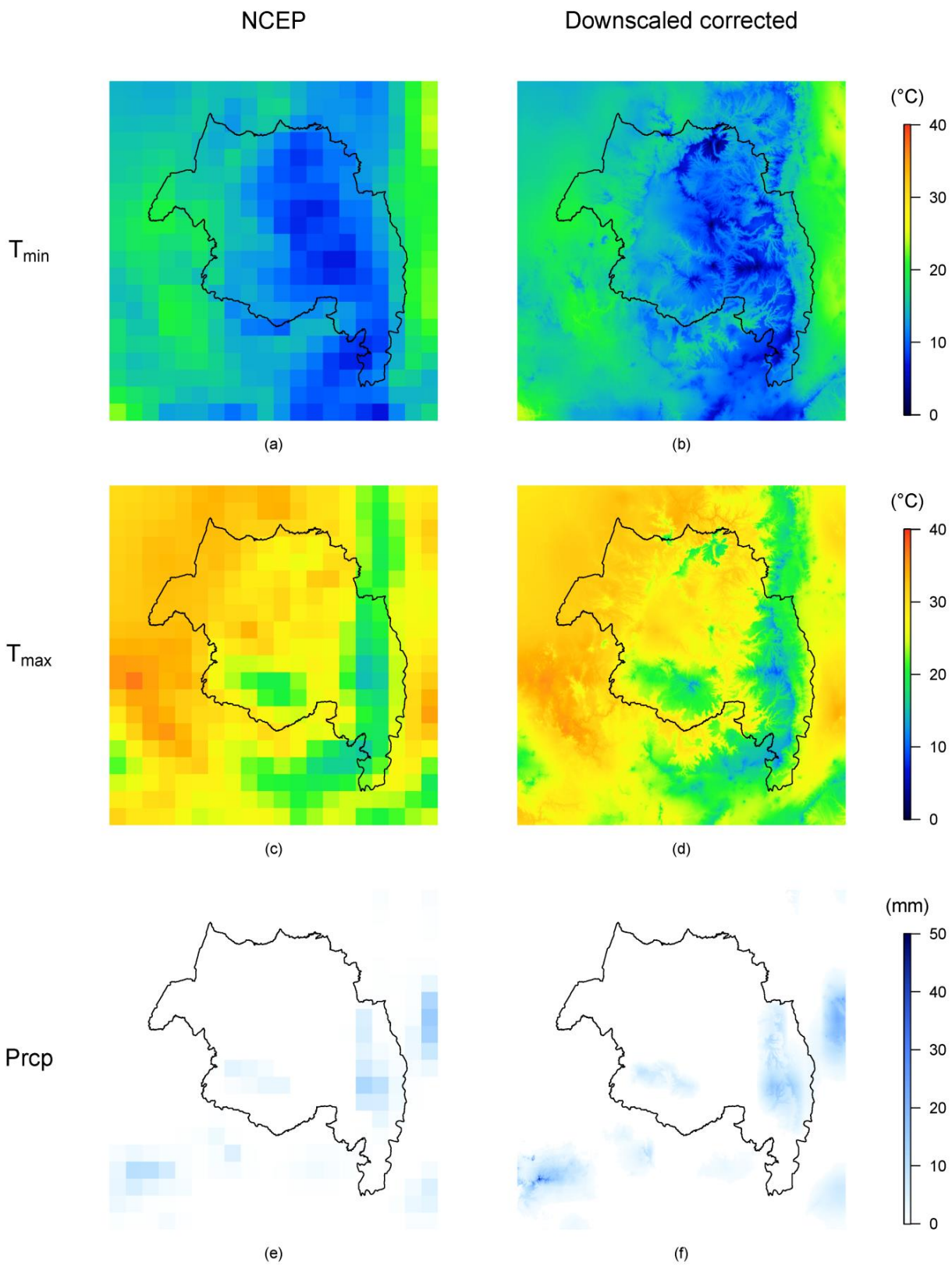

Figure 10. Daily weather data for the Amhara region (a) NCEP Tmin, (b) downscaled corrected Tmin,(c) NCEP Tmax, (d) downscaled corrected Tmax, (e) NCEP Prcp and (f) downscaled corrected Prcp.

After downscaling, the global-scale distribution of precipitation and temperature values come closer to the weather station values. However, the improved downscaled dataset was subjected to biases. A delta change bias correction method is used to minimize the bias. Validation parameters such as bias, mean absolute error (MAE) and root mean squared error (RMSE) decrease for all the corrected variables when compared to the downscaled values. Generally, temperature was improved better than precipitation (Figure 11). Better improvement is seen in temperature because the major benefit of the downscaling incorporates elevation into the data set, which has a larger impact on temperature than on precipitation.

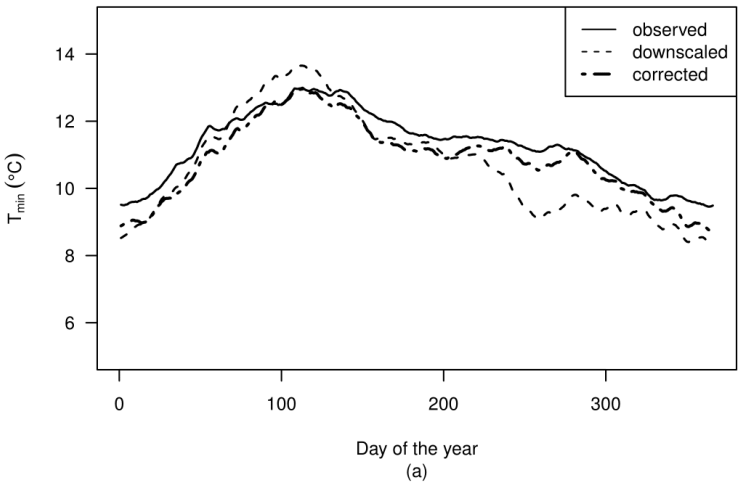

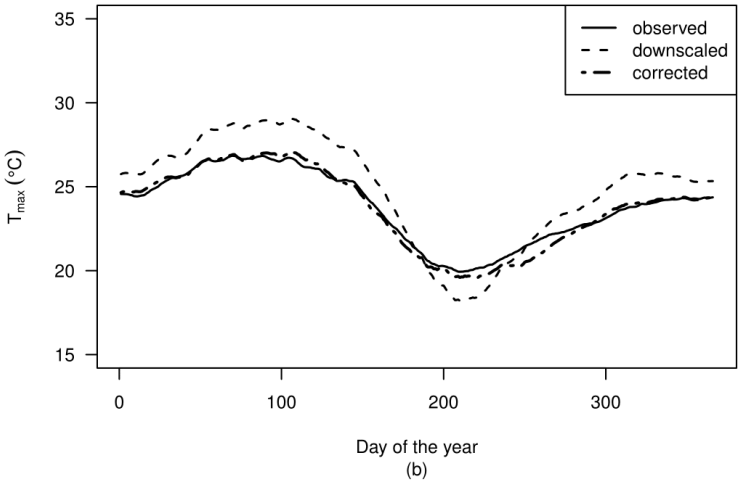

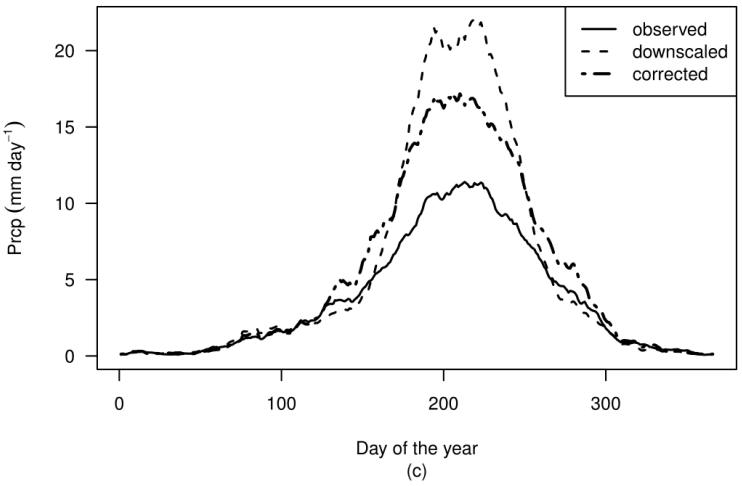

Figure 11. Downscaled climate data

The downscaled, corrected and the terrestrial inventory data were used as input data in the Biome-BGC model. However, the error propagation associated with the precipitation data considerably influenced the estimation of forest productivities in the Amhara region, which demanded further improvement of the precipitation data. The reason for the error was that a single bias correction factor was applied for the whole Amhara region regardless of the wide environmental variability amongst sub-regions. This was done due to the lack of weather station data. Therefore, a new scheme was developed to improve the precipitation data. A mean annual precipitation map from the downscaled climate data is produced to look at the precipitation pattern with in the Amhara region (Figure 12).

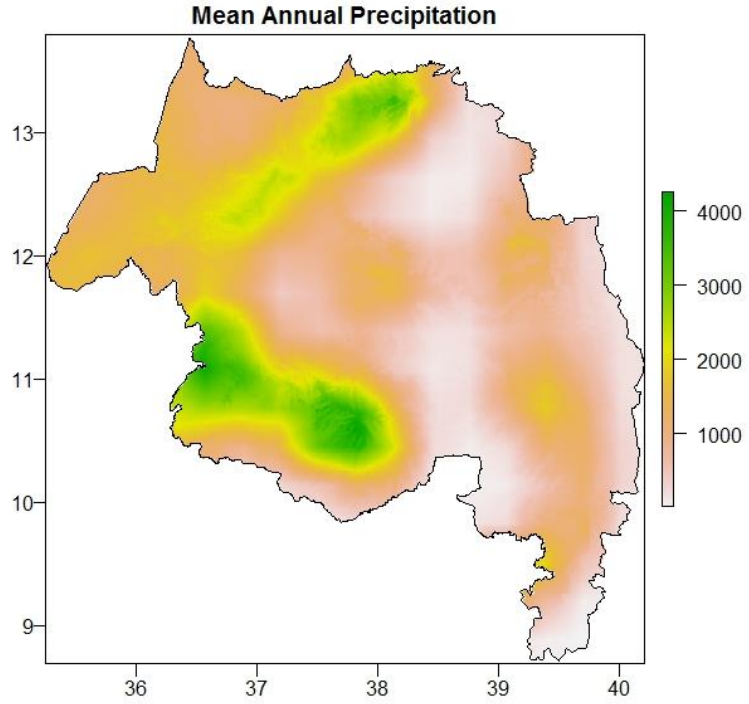

Figure 12. Mean annual precipitation (mm yr^{-1}) of the Amhara region

Besides the mean annual precipitation map, a daily precipitation difference between the downscaled and weather station data was also calculated to facilitate the sub regionalization of the Amhara region. Based on the pattern of the mean annual precipitation map and the precipitation differences, the Amhara region is further classified into four homogenous sub-regions (Figure 13).

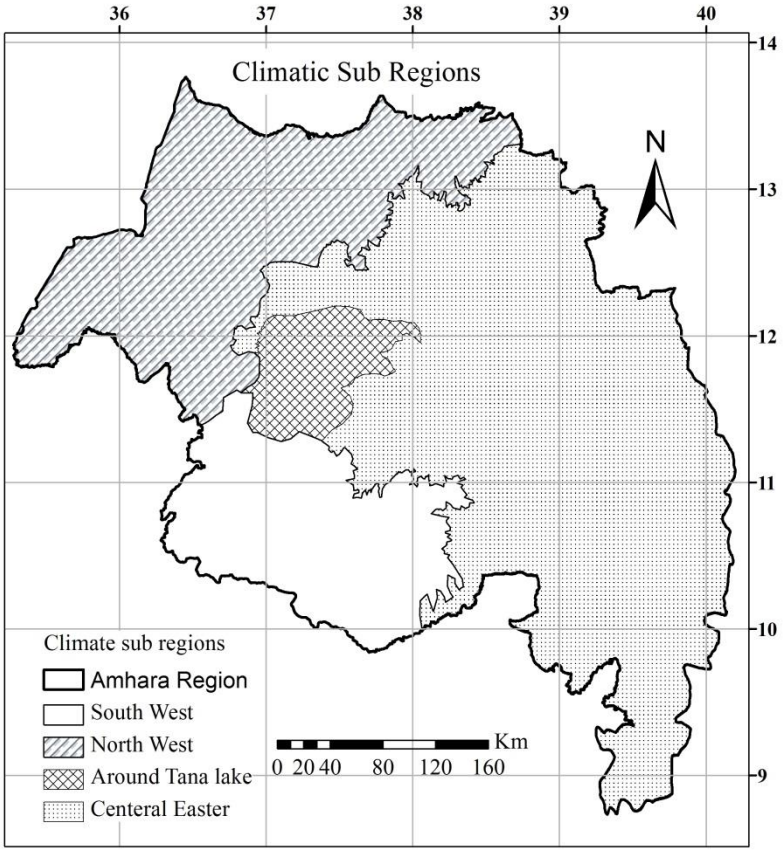

Figure 13. Climatic sub-regions of the Amhara region

The mean precipitation difference between downscaled and weather station data was calculated for each sub-region. Next, a linear regression analysis was applied based on elevation and mean precipitation difference within the sub-regions to produce the correction factors. The correction factors are produced on the 10 day basis for each pixel based on the elevation of the pixel and mean precipitation difference of the sub-region. Based on the 10 days groupings, a year would have 37 groups. A sample linear regression graph of the south west region on the 3rd tenth date is presented in Figure 14.

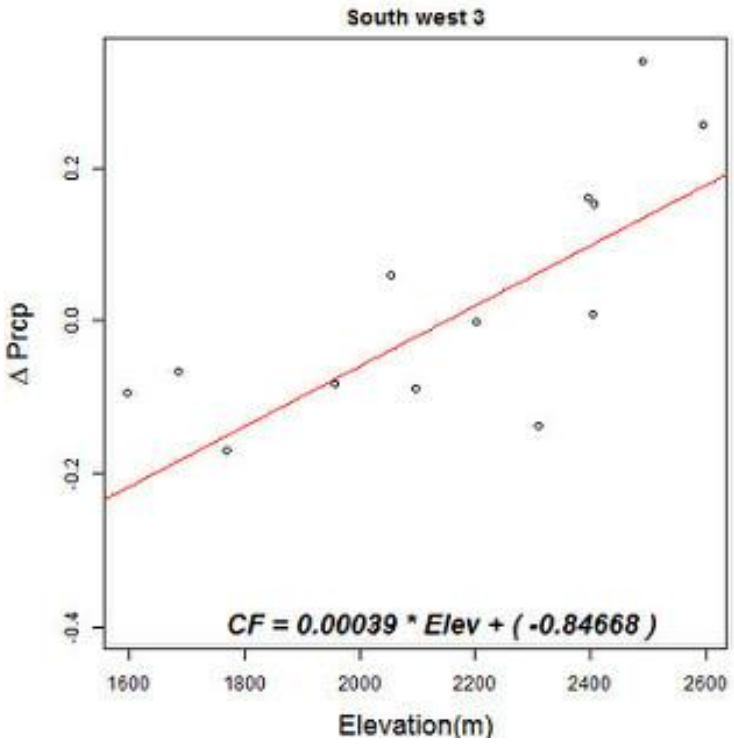

Figure 14. A correction sample for regression analysis of the 3rd tenth dates in the south west region. CF is a correction factor of a pixel based on the precipitation difference and elevation; ΔPrcp is a difference between downscaled and observed precipitation; and Elev is elevation of a pixel in meters

The correction factors calculated for each pixel and all dates will be applied to the daily downscaled data. The details of the application of the daily correction factors on the downscaled data can be found in Appendix 9.2. Producing the improved downscaled data and running the Biome-BGC model is in progress in another PhD work of the same project (Belay et al., 2017).

6 Discussion

6.1 Terrestrial inventory

The results from the forest inventory allows for the assessment of standing forest volume, carbon stocks and NPP. Felling of trees in the Amhara region was not possible due to the legal prohibition. As a result, DBH was used to derive tree heights and core increments were used for the analysis of increment rates. The approach enabled us to calibrate the form factor function and height-diameter function for the tree species in the Amhara region. This establishes a new methodology for forest inventory in the Amhara region. It is now possible to estimate the existing forest state, as well as the growth increment of trees where destructive measurement is impossible (Figure 5, 6, and 7). Additionally, we could also be able to identify growth rate and form factor functions of most important tree species. For example, it is evident that *Schefflera abyssinca*, *Eucalyptus globulus* and *Chionanthus mildbreadii* showed higher productivities compared with other tree species (Figure 8). This helps to easily identify productive tree species for future plantation schemes and the management of forests in the region.

The result shows that the estimations of timber volume, annual volume increments, carbon stock, annual carbon increments and NPPs of the forest sites in the Amhara region are fairly low (Sisay et al., 2017). Besides the climatic and topographical features, population pressure considerably impacted the productivities of the forests (Lemenih and Kassa, 2014; Wondie et al., 2016). The production increment and rapid rehabilitation witnessed in the Ambober confirmed that minimizing and avoiding of human and animal activities is crucial in the forest areas. Thus, the results showed that dry afromontane forests have lower timber volume, carbon stock and NPP than moist afromontane forests (Mokria et al., 2015).

Based on the outcomes from this study, the current condition of the forests and their increment rates in the Amhara region can now be provided for the first time (Sisay et al., 2017). The general method presented, form factor and height-diameter functions developed in this study are the first achievements and can be used as a prototype for the SFM schemes in the Amhara region. Our methods and findings directly influence the process of developing SFM frameworks in Ethiopia as well as the Amhara region, as there are no such schemes in place (Sisay et al., 2017). Besides, the methods and findings can be converted in to simple

management guidelines and support SFM in the Amhara region. Moreover, the conceptual methodological approach and finidngs presented will also fill the existing knowledge gap on SFM in Ethiopia as well as in the Amhara region. Owing to the level of deforestation and forest degradation in Ethiopia as well as in the Amhara region, a pragmatic forest management scheme is imperative. Forest ecosystem modeling is very important where there is a severe lack of data in the region. Therefore, our approach and information can be used as an input for the ongoing modeling efforts in the region.

The United Nations Framework Convention on Climate Change's Reducing Emissions from Deforestation and Forest Degradation (REDD+) need reliable estimations of carbon stocks and productivities of forests, especially in countries like Ethiopia where data is scarce, while the impact of global changes are huge (UNFCCC, 2014). Thus, this work would be of paramount importance to fill the methodological and information gap for the implementation of REDD+ in the Amhara region. The forest ecosystem modeling efforts to develop a reliable SFM framework will also be benefitted by getting the input data. Our findings, together with the climate data, would be used for the ongoing forest ecosystem modeling efforts in the Amhara region (Belay et al., 2017).

6.2 Daily Climate Data

Ethiopia and the Amhara region are characterized by the various climatic conditions, heterogeneous topographic features and wide altitudinal ranges. Because of such features, the Amhara region is endowed with distinctively diverse vegetation types. Therefore, regional scale forest management requires consistent regional scale input data. Climate data is one of the most important features needed for the assessment of the climate's effect on forest structure and management. This requires gridded climate data along with the terrestrial forest inventory data. Forests in the Amhara region are under different levels of pressure and degradation. Quantifying the current condition, growth potentials and future reforestation and afforestation efforts, the effects of climate on the forests should be studied. Therefore, through climate, forest management as affected by climate can be quantified. This can then show how a changing climate could affect forest management options in the future and the limit of forest management has to change forest structure under different climate regimes. Forest ecosystem modeling is the best approach in order to examine the forest ecosystem scenarios with regard to climate and other affecting factors at larger scale and divers situations. Therefore, for our

ongoing modeling works on development of an SFM framework, climate data is downscaled for the Amhara region. A daily T_{min}, T_{max} and Prcp with 1 km spatial resolution is downscaled from the global data sources (Figure 10) (Sisay et al., 2016). Producing a spatiotemporally consistent climate data with fine resolution at the regional scale is the first of its kind in Ethiopia as well as in the Amhara region. This approach would also help to guide the conceptual perspective of forest management as well as the modeling efforts undergoing in the region. Our output would make modeling climate change and its effects on the forest conditions possible. Additionally, the climate data can be used in the REDD+ endeavors.

7 Conclusions and Outlook

The forest ecosystems in the Amhara region have been under tremendous pressure. Implementing sustainable forest management is imperative to stop the downward spiral of deforestation and forest degradation as well as to ensure a sustainable supply of the ecosystem services. However, given the marked environmental heterogeneity and rich biodiversity, providing sustainable forest management frameworks for the whole Amhara region is a major challenge. The new datasets derived and methodological approaches presented through this study allow for analyses of the state of forest resources across the Amhara region that have in the past been limited to local and watershed level assessments. This study attempts to assess the state of different forest types in the Amhara region by integrating terrestrial inventory data, remote sensing data and a biogeochemical Biome-BGC forest ecosystem modeling. This conceptual approach is the first of its kind in the Amhara region and provides a prototype to develop a framework for the sustainable forest management in the region.

This work provides a calibrated height-diameter and form factor functions for the most important species and different forest regions, which are essential for further forest resources assessments and sustainable forest resource harvesting. The framework and methodology documented here can be used to expand the height-diameter, form factor functions to other important tree species and forest regions in the Amhara region as well as Ethiopia. The "reference stand approach" enables inferring estimations for forest regions where there is no data. The results of the empirical assessment can also be improved if more local forest inventory data are available and/or by implementing the modeling approach.

This thesis is part of a larger activity. Thus, it fits into the next part of the forest ecosystem modeling with Biome-BGC (Belay et al., 2017) to provide a full regional forest productivity under different environmental and management scenarios in the Amhara region. Further, this study allows for the preparation of gridded daily climate data at a regional scale with fine spatiotemporal resolution, which will serve as input data for the ongoing forest ecosystem modeling effort. The climate data is now on a resolution that allows the assessment of differences in altitudinal ranges, forest types and land uses. These datasets allow for the large scale studies of forests, forest productivity and how they relate to climate change and management scenarios all throughout the Amhara region.

8 References

Achard, F., Beuchle, R., Mayaux, P., Stibig, H.-J., Bodart, C., Brink, A., Carboni, S., Desclée, B., Donnay, F., Eva, H.D., Lupi, A., Raši, R., Seliger, R., Simonetti, D., 2014. Determination of tropical deforestation rates and related carbon losses from 1990 to 2010. Glob. Chang. Biol. 20, 2540–2554. doi:10.1111/gcb.12605

Badege Bishaw, 2001. Deforestation and Land Degradation in the Ethiopian Highlands : A Strategy for Physical Recovery. Northeast Afr. Stud. 8, 7–25.

Belay, B., Pötzelsberger, E., Thurnher, C., Sisay, K., Assefa, D., Hasenauer, H., 2017. Modelling Carbon and Net Primary Productivity Dynamics of Managed Dry Tropical Afromontane Forest Ecosystem in Ethiopia. *Under Progress*

Berhanu, A., Woldu, Z., Demissew, S., 2016. Elevation patterns of woody taxa richness in the evergreen Afromontane vegetation of Ethiopia. J. For. Res. doi:10.1007/s11676-016-0350-y

Berhe, L., Assefa, G., Teklay, T., 2013. Models for estimation of carbon sequestered by Cupressus lusitanica plantation stands at Wondo Genet, Ethiopia. South. For. a J. For. Sci. 75, 113–122. doi:10.2989/20702620.2013.805511

Central Statistical Agency, 2008. Agricultural Sample Survey: 2007/08; Government of Ethiopia. Addis Ababa, Ethiopia. Pages 1- 44

d'Annunzio, R., Sandker, M., Finegold, Y., Min, Z., 2015. Projecting global forest area towards 2030. For. Ecol. Manage. 352, 124–133. doi:10.1016/j.foreco.2015.03.014

Evert, F., 1968. Form height and volume per square foot of basal area. J. For. 66.

Federal Democratic Republic of Ethiopia, 2011. Ethiopia's Climate Resilient Green Economy .:. Sustainable Development Knowledge Platform.Pages 1 - 200.

Federici, S., Tubiello, F.N., Salvatore, M., Jacobs, H., Schmidhuber, J., 2015. New estimates of CO2 forest emissions and removals: 1990–2015. For. Ecol. Manage. 352, 89–98. doi:10.1016/j.foreco.2015.04.022

Globalweather, 2012. Global Weather Data for SWAT, https://globalweather.tamu.edu/ (accessed 16March 2015).

Gobeze, T., Bekele, M., Lemenih, M., Kassa, H., 2009. Participatory forest management and its impacts on livelihoods and forest status: the case of Bonga forest in Ethiopia. Int. For. Rev. 11, 346–358. doi:10.1505/ifor.11.3.346

Hailu, B.T., Maeda, E.E., Heiskanen, J., Pellikka, P., 2015. Reconstructing pre-agricultural expansion vegetation cover of Ethiopia. Appl. Geogr. 62, 357–365. doi:10.1016/j.apgeog.2015.05.013

Hasenauer, H., 2006. Sustainable Forest Management. Springer Berlin Heidelberg, Berlin, Heidelberg. doi:10.1007/3-540-31304-4

Hasenauer, H., Petritsch, R., Zhao, M., Boisvenue, C., Running, S.W., 2012. Reconciling satellite with ground data to estimate forest productivity at national scales. For. Ecol. Manage. 276, 196–208. doi:10.1016/j.foreco.2012.03.022

Hurni, H., 1998. Agroecologial belts of Ethiopia: Explanatory notes on three maps at a scale of 1:1,000,000. Res. Report, Soil Conserv. Res. program, Addis Ababa 43.

Karbo, T., 2013. Religion and social cohesion in Ethiopia. Int. J. Peace Dev. Stud. 4, 43–52. doi:10.5897/IJPDS2013.0164

Köhl, M., Lasco, R., Cifuentes, M., Jonsson, Ö., Korhonen, K.T., Mundhenk, P., de Jesus Navar, J., Stinson, G., 2015. Changes in forest production, biomass and carbon: Results from the 2015 UN FAO Global Forest Resource Assessment. For. Ecol. Manage. 352, 21–34. doi:10.1016/j.foreco.2015.05.036

Lemenih, M., Kassa, H., 2014. Re-greening Ethiopia: History, challenges and lessons. Forests 5, 1896–1909. doi:10.3390/f5081896

Liang, J., Crowther, T.W., Picard, N., Wiser, S., Zhou, M., Alberti, G., Schulze, E.-D., McGuire, D., Bozzato, F., Pretzsch, H., De-Miguel, S., Paquette, A., Hérault, B., Scherer-Lorenzen, M., Barrett, C.B., Glick, H.B., Hengeveld, G.M., Nabuurs, G.-J., Pfautsch, S., Viana, H., Vibrans, A.C., Ammer, C., Schall, P., Verbyla, D., Tchebakova, N., Fischer, M., Watson, J. V., Chen, H.Y.H., Lei, X., Schelhaas, M.-J., Lu, H., Gianelle, D., Parfenova, E.I., Salas, C., Lee, E., Lee, B., Kim, H.S., Bruelheide, H., Coomes, D.A., Piotto, D., Sunderland, T., Schmid, B., Gourlet-Fleury, S., Sonké, B., Tavani, R., Zhu, J., Brandl, S., Vayreda, J., Kitahara, F., Searle, E.B., Neldner, V.J., Ngugi, M.R., Baraloto, C., Frizzera, L., Bałazy, R., Oleksyn, J., Zawiła-Niedźwiecki, T., Bouriaud, O., Bussotti, F., Finér, L., Jaroszewicz, B., Jucker, T., Valladares, F., Jagodzinski, A.M., Peri, P.L., Gonmadje, C., Marthy, W., O'Brien, T., Martin, E.H., Marshall, A., Rovero, F., Bitariho, R., Niklaus, P.A., Alvarez-Loayza, P., Chamuya, N., Valencia, R., Mortier, F., Wortel, V., Engone-Obiang, N.L., Ferreira, L. V., Odeke, D.E., Vasquez, R.M., Reich, P.B., 2016. Positive biodiversity–productivity relationship predominant in global forests. Science (80-.). 354, 196. doi:10.1126/science.aaf8957

Liu, C., Frazier, P., Kumar, L., 2007. Comparative assessment of the measures of thematic classification accuracy. Remote Sens. Environ. 107, 606–616. doi:10.1016/j.rse.2006.10.010

Maraun, D., Wetterhall, F., Ireson, A.M., Chandler, R.E., J, K.E., Widmann, M., Brienen, S., Rust, H.W., Sauter, T., Themeßl, M., Venema, V.K.C., Chun, K.P., 2010. Precipitation Downscaling Under Climate Change : Recent Developments To Bridge the Gap Between Dynamical Models and the End User 1–34. doi:10.1029/2009RG000314

Mekonnen, M., Sewunet, T., Gebeyehu, M., Azene, B., Melesse, A.M., 2016. GIS and Remote Sensing-Based Forest Resource Assessment, Quantification, and Mapping in Amhara Region, Ethiopia, Landscape Dynamics, Soils and Hydrological Processes in Varied Climates, Springer Geography. Springer International Publishing, Cham. doi:10.1007/978-3-319-18787-7

Melaku Bekele, 2003. Forest Property Rights, the Role of the State, and Institutional Exigency: The Ethiopian Experience. PhD Dissertation. Swedish University of

Agricultural Sciences.

Mokria, M., Gebrekirstos, A., Aynekulu, E., Bräuning, A., 2015. Tree dieback affects climate change mitigation potential of a dry afromontane forest in northern Ethiopia. For. Ecol. Manage. 344, 73–83. doi:10.1016/j.foreco.2015.02.008

Morales-Hidalgo, D., Oswalt, S.N., Somanathan, E., 2015. Status and trends in global primary forest, protected areas, and areas designated for conservation of biodiversity from the Global Forest Resources Assessment 2015. For. Ecol. Manage. 352, 68–77. doi:10.1016/j.foreco.2015.06.011

Moreno, A., Neumann, M., Hasenauer, H., 2016. Optimal resolution for linking remotely sensed and forest inventory data in Europe. Remote Sens. Environ. 183, 109–119. doi:10.1016/j.rse.2016.05.021

Morisette, J.T., Privette, J.L., Justice, C.O., 2002. A framework for the validation of MODIS Land products. Remote Sens. Environ. 83, 77–96. doi:10.1016/S0034-4257(02)00088-3

Myers, N., Mittermeier, R.A., Mittermeier, C.G., da Fonseca, G.A.B., Kent, J., 2000. Biodiversity hotspots for conservation priorities. Nature 403, 853–858. doi:10.1038/35002501

Ndoro, W., Mumma, A., Abungu, G., 2009. Cultural Heritage and the Law Protecting Immovable Heritage in English-Speaking Countries of Sub-Saharan Africa, Cultural Heritage and the Law. Protecting Immovable heritage in English-Speaking Countries of Sub-Saharan Africa.

Negash, M., Starr, M., Kanninen, M., 2013. Allometric equations for biomass estimation of Enset (Ensete ventricosum) grown in indigenous agroforestry systems in the Rift Valley escarpment of southern-eastern Ethiopia. Agrofor. Syst. 87, 571–581. doi:10.1007/s10457-012-9577-6

Olofsson, P., Foody, G.M., Stehman, S. V., Woodcock, C.E., 2013. Making better use of accuracy data in land change studies: Estimating accuracy and area and quantifying uncertainty using stratified estimation. Remote Sens. Environ. 129, 122–131. doi:10.1016/j.rse.2012.10.031

Pagani, L., Schiffels, S., Gurdasani, D., Danecek, P., Scally, A., Chen, Y., Xue, Y., Haber, M., Ekong, R., Oljira, T., Mekonnen, E., Luiselli, D., Bradman, N., Bekele, E., Zalloua, P., Durbin, R., Kivisild, T., Tyler-Smith, C., 2015. Tracing the Route of Modern Humans out of Africa by Using 225 Human Genome Sequences from Ethiopians and Egyptians. Am. J. Hum. Genet. 96, 986–991. doi:10.1016/j.ajhg.2015.04.019

Parent, G., 2000. Manual for woody biomass inventory. Woody Biomass Inventory and Strategic Planning Project, Ministry of Agriculture, Addis Ababa, Ethiopia.

Pistorius, T., Carodenuto, S., Wathum, G., 2017. Implementing Forest Landscape Restorationin Ethiopia. Forests 8, 61. doi:10.3390/f8030061

Saha, S., Moorthi, S., Pan, H.-L., Wu, X., Wang, J., Nadiga, S., Tripp, P., Kistler, R., Woollen, J., Behringer, D., Liu, H., Stokes, D., Grumbine, R., Gayno, G., Wang, J., Hou,

Y.-T., Chuang, H.-Y., Juang, H.-M.H., Sela, J., Iredell, M., Treadon, R., Kleist, D., Van Delst, P., Keyser, D., Derber, J., Ek, M., Meng, J., Wei, H., Yang, R., Lord, S., Van Den Dool, H., Kumar, A., Wang, W., Long, C., Chelliah, M., Xue, Y., Huang, B., Schemm, J.-K., Ebisuzaki, W., Lin, R., Xie, P., Chen, M., Zhou, S., Higgins, W., Zou, C.-Z., Liu, Q., Chen, Y., Han, Y., Cucurull, L., Reynolds, R.W., Rutledge, G., Goldberg, M., 2010. The NCEP Climate Forecast System Reanalysis. Bull. Am. Meteorol. Soc. 91, 1015–1057. doi:10.1175/2010BAMS3001.1

Schmidt, A., 1956. Der rechnerische Ausgleich von Bestandeshöhenkurven. Forstwirtschaftl. Cent. 86, 370–386.

Siraj, M., Zhang, K., Xiao, W., Bilal, A., Gemechu, S., Geda, K., Yonas, T., Xiaodan, L., 2016. Does Participatory Forest Management Save the Remnant Forest in Ethiopia? Proc. Natl. Acad. Sci. India Sect. B Biol. Sci. doi:10.1007/s40011-016-0712-4

Sisay, K., Thurnher, C., Belay, B., Lindner, G., Hasenauer, H., 2017. Volume and Carbon Estimates for the Forest Area of the Amhara Region in Northwestern Ethiopia. Forests 8, 122. doi:10.3390/f8040122

Sisay, K., Thurnher, C., Hasenauer, H., 2016. Daily climate data for the Amhara region in Northwestern Ethiopia. Int. J. Climatol. doi:10.1002/joc.4880

Sisay, K., Yitaferu, B., Garedew, E., Ziadat, F., 2015. Assessment of forest cover change and its environmental impacts using multi-temporal and multi-spectral satellite images, in: Ziadat, F., Bayu, W. (Eds.), Mitigating Land Degradation and Improving Livelihoods. Routledge, New York, pp. 85–98. doi:10.4324/9781315754444

Sloan, S., Sayer, J.A., 2015. Forest Resources Assessment of 2015 shows positive global trends but forest loss and degradation persist in poor tropical countries. For. Ecol. Manage. 352, 134–145. doi:10.1016/j.foreco.2015.06.013

Tadesse, G., Zavaleta, E., Shennan, C., 2014. Effects of land-use changes on woody species distribution and above-ground carbon storage of forest-coffee systems. Agric. Ecosyst. Environ. 197, 21–30. doi:10.1016/j.agee.2014.07.008

Tegegne, A.D., Penker, M., Wurzinger, M., 2016. Participatory Demographic Scenarios Addressing Uncertainty and Transformative Change in Ethiopia. Syst. Pract. Action Res. 29, 277–296. doi:10.1007/s11213-015-9365-0

Ticktin, T., 2004. The ecological implications of harvesting non-timber forest products. J. Appl. Ecol. 41, 11–21. doi:10.1111/j.1365-2664.2004.00859.x

UNFCCC, 2014. Key decisions relevant for reducing emissions from deforestation and forest degradation in developing countries (REDD+). Framew. Conv. Clim. Chang. 44.

Wondie, M., Schneider, W., Katzensteiner, K., Mansberger, R., Teketay, D., 2016. Modelling the dynamics of landscape transformations and population growth in the highlands of Ethiopia using remote-sensing data. Int. J. Remote Sens. 37, 5647–5667. doi:10.1080/01431161.2016.1246773

Wondie, M., Schneider, W., Melesse, A.M., Teketay, D., 2011. Spatial and Temporal Land

Cover Changes in the Simen Mountains National Park, a World Heritage Site in Northwestern Ethiopia. Remote Sens. 3, 752–766. doi:10.3390/rs3040752

Zeleke, G., Hurni, H., 2001. Implications of Land Use and Land Cover Dynamics for Mountain Resource Degradation in the Northwestern Ethiopian Highlands. Mt. Res. Dev. 21, 184–191. doi:10.1659/0276-4741(2001)021[0184:IOLUAL]2.0.CO;2

9 Appendix

9.1 Paper 1

Sisay, K., Thurnher, C., Belay, B., Lindner, G., Hasenauer, H., 2017. Volume and Carbon Estimates for the Forest Area of the Amhara Region in Northwestern Ethiopia. Forests 8, 122. doi:10.3390/f8040122

forests

MDPI

Article

Volume and Carbon Estimates for the Forest Area of the Amhara Region in Northwestern Ethiopia

Kibruyesfa Sisay *, Christopher Thurnher, Beyene Belay, Gerald Lindner and Hubert Hasenauer

Institute of Silviculture, Department of Forest and Soil Sciences, University of Natural Resources and LifeSciences, Vienna 1190, Austria; christopher.thurnher@boku.ac.at (C.T.); beyene.belay@students.boku.ac.at (B.B.); gerald.lindner@boku.ac.at (G.L.); hubert.hasenauer@boku.ac.at (H.H.)

* Correspondence: kibruyesfa.ejigu@students.boku.ac.at; Tel.: +43-1-47654-91336

Academic Editor: Philip J. Polglase

Received: 20 February 2017; Accepted: 11 April 2017; Published: 15 April 2017

Abstract: Sustainable forest management requires a continuous assessment of the forest conditions covering the species distribution, standing tree volume as well as volume increment rates. Forest inventories are designed to record this information. They, in combination with ecosystem models, are the conceptual framework for sustainable forest management. While such management systems are common in many countries, no forest inventory system and/or modeling tools for deriving forest growth information are available in Ethiopia. This study assesses, for the first time, timber volume, carbon, and Net Primary Production (NPP) of forested areas in the Amhara region of northwestern Ethiopia by combining (i) terrestrial inventory data, and (ii) land cover classification information. The inventory data were collected from five sites across the Amhara region (Ambober, Gelawdiwos, Katassi, Mahiberesilasse and Taragedam) covering three forest types: (i) forests, (ii) shrublands (exclosures) and (ii) woodlands. The data were recorded on 198 sample plots and cover diameter at breast height, tree height, and increment information. In order to extrapolate the local terrestrial inventory data to the whole Amhara region, a digital land cover map from the Amhara's Bureau of Agriculture was simplified into (i) forest, (ii) shrubland, and (iii) woodland. In addition, the forest area is further stratified in five elevation classes. Our results suggest that the forest area in the Amhara region covers 2% of the total land area with an average volume stock of 65.7 $m^3 \cdot ha^{-1}$; the shrubland covers 27% and a volume stock of 3.7 $m^3 \cdot ha^{-1}$; and the woodland covers 6% and an average volume stock of 27.6 $m^3 \cdot ha^{-1}$. The corresponding annual volume increment rates are 3.0 $m^3 \cdot ha^{-1}$, for the forest area; 1.0 $m^3 \cdot ha^{-1}$, for the shrubland; and 1.2 $m^3 \cdot ha^{-1}$, for the woodland. The estimated current total volume stock in the Amhara region is 59 million m^3.

Keywords: volume; volume increment; carbon; Net Primary Production (NPP); forest inventory; Ethiopia

1. Introduction

Forest ecosystems provide goods and services [1] and have a higher carbon sequestration potential versus any other terrestrial ecosystems [2]. Deforestation leads to a loss of provided goods and services, induces soil degradation effects and contributes to anthropogenic carbon emissions [3]. Global warming, due to the release of greenhouse gases, is causing unprecedented environmental and social changes. Therefore, the idea of Reducing Emissions from Deforestation and forest Degradation (REDD) was conceived by United Nations Framework Convention on Climate Change (UNFCCC) as the main carbon emission reduction mechanism for developing countries such as Ethiopia [4]. REDD was extended to REDD+ in 2014 by adding the carbon sink potential as well as conservation and sustainable forest management issues [5]. Forest management plays an important role in mitigating impacts of climate change and in sustaining the supply of ecosystem goods and

services [6]. Thus, forest inventory data are essential to assess the available forest resources including their productivity potential. They serve as the basic input data for implementing the REDD+ objectives [5].

Forest inventories collect data about forest conditions by estimating the volume, biomass, carbon and net primary production (NPP) [7]. Based on a certain grid design, sampling plots are established to record the forest data. Another option for deriving forest productivity estimates can be obtained from remote sensing information in combination with ecosystem modeling theories. As a result, several studies [8] combine both methods to assess the forest area, species distribution, volume, carbon and NPP [7–12].

Sustainable forest management requires forest inventories. In combination with modeling tools, forest growth information can be derived and sustainable harvesting or cutting plans are developed [13]. While such systems are common in many parts of the world [9], Ethiopia has no standardized forest inventory system in place and no information about the growing stock and increment rates of the limited remaining forest areas available. This lack of information makes sustainable forest management and harvesting difficult or even impossible. A few studies have analyzed the extent of different forest areas and their changes as a result of land use changes [14–20]. These studies are restricted to local forest areas and/or watersheds and provide no information on the forest conditions (e.g., volume or biomass) and/or its change over time (increment rates). In addition, some studies have estimated aboveground biomass and carbon stocks of specific savannah woodland, forest and agroforestry areas [21,22]. However, up until this study, no information is available about the stocking volume, volume increment rates, carbon stocks and NPP for the forest areas in northwestern Ethiopia.

The purpose of this study is to provide a consistent methodology to derive such productivity estimates of different vegetation types in the Amhara region in northwestern Ethiopia. We establish local forest inventories covering different agro-ecological zones and extrapolate these inventory results to the whole Amhara region by obtaining a remotely sensed land cover classification scheme to provide total numbers for the stocking timber volume, volume increment, aboveground carbon, and NPP estimates.

2. Materials and Methods

2.1. Forest Inventrory

2.1.1. Study Area

The Amhara region, in northwestern Ethiopia, has a land area of 15.7 Mha, of which one-third is covered with woody vegetation. For our analysis, we selected study areas covering different agro-ecological zones with typical vegetation types: (i) forests, (ii) shrubland/exclosure, and (iii) woodland.

The selected study areas and vegetation types are Ambober (shrubland), Gelawdiwos (forest), Katassi (forest), Mahibereselassie (woodland), and Taragedam (forest) (Figure 1).

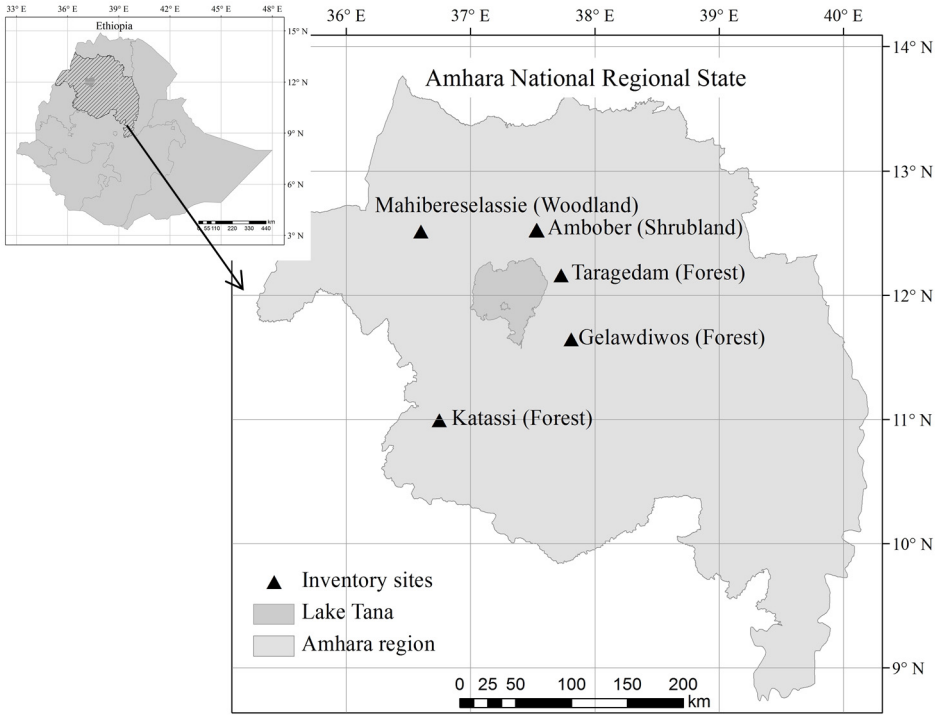

Figure 1. Location of study areas.

Even though the regional and/or local governments declared these forests as protected, human activities and cattle grazing are still active and common. The Mahibereselassie woodland has the highest cattle population and agricultural activities. The Ambober exclosure is guarded and protected since its establishment in 2009. Human and animal activities are minor at the Gelawdiwos and Katassi sites. The Taragedam forest has a minor anthropogenic disturbance history [18]. The most common types of human activities occurring within these forest areas are cutting and harvesting trees for energy, production of different household and farm implements and clearing for agriculture and grazing activities [23].

2.1.2. Sampling Technique

Our five study regions (see Figure 1) cover the main ecological zones of the area and differ in size: the largest area is the Mahibereselassie woodland with 19,162 ha followed by the forest areas in Katassi (553 ha), Taragedam (324 ha) and Gelawdiwos (68 ha). The Ambober shrubland/exclosure covers 6 ha.

The decision on the grid size, and thus the number of sample plots was derived based on statistical principles by achieving a minimum number of inventory plots. After a number of pilot studies in the different forest inventory areas and test calculations, we defined the following grid size by study region: for the Mahibereselassie woodland area, a 3 km by 3 km grid size with 21 sampling plots was established. For the forest areas in Katassi, a 300 m by 300 m with 63 sampling plots; Taragedam 250 m by 250 m with 52 sampling plots; and for Gelawdiwos, 250 m by 250 m with 34 sampling plots were established. For the Ambober shrubland/exclosure, a 50 m by 50 m sampling design with 28 sampling plots was established. This resulted in a total number of 198 sampling plots. A typical example (Taragedam) is given in Figure 2. The data collection was carried out during the summer 2014 (July to September).

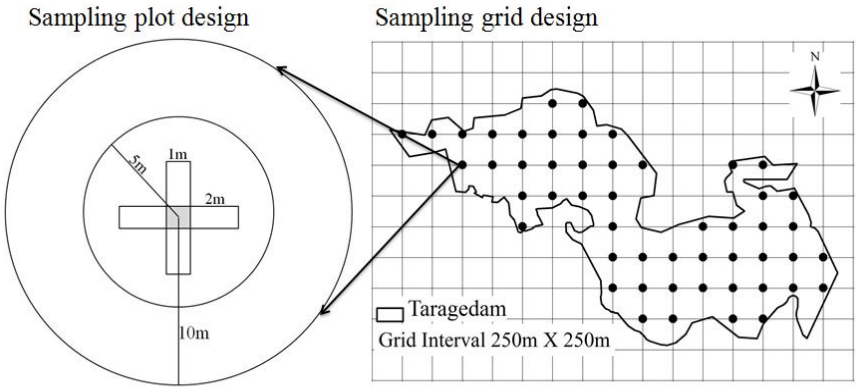

Figure 2. Sampling plot design and sample grid design (Taragedam site). A 10-m radius plot was used in Ambober, Gelawdiwos and Taragedam. A 15-m radius plot was used in Katassi and Mahibereselassie.

Each sample plot consists of two concentric circles and four rectangular plots (1 m × 2 m) (see Figure 2). The plot area was corrected as a function of the slope angle [4]. The radius of the larger circle records all trees with a DBH ≥ 10 cm and exhibits a radius of 10 m for the study areas in Gelawdiwos, Taragedam, and Ambober and 15 m for Katassi and Mahibereselassie. For each tree found within the specified radial range, we recorded the tree species, diameter at breast height (DBH) in cm, and the tree position on the plot.

One of the important goals of the study is to derive annual growth information. Since we have no repeated tree records, increment cores are taken according to the following procedure: Based on the DBH records on a given sampling plot, we selected the so-called "central" stem or tree—this is the 60 percentile of the DBH distribution—on a given sampling plot. We follow here a procedure suggested by [24], which showed in their studies that the "central" stem represents the "mean" tree (= quadratic mean DBH) on a given plot, and cuts the basal area in two equal halves. The "mean" tree dimension is derived from the per hectare values e.g., the tree represents the quadratic mean DBH (basal area divided by the stem number/ha) and consequently approximately the average volume (volume/ha divided by the stem number/ha). Thus, the growth rates of the "central" stem (60 percentile of the DBH distribution on a given plot) are proportional to the growth rates of the per hectare values assuming that the stem number remains equal for the growth period.

One important precondition of this approach is that each tree ring represents one year. According to Worbes [25] and Zhang et al. [26], distinct tree rings are formed in response to annual precipitation pattern. Sisay et al. [27] confirmed this pattern by showing that the rainy season in the Amhara region is between June and August.

Based on the DBH distribution on a given inventory plot, for each tree species a "central" stem according to the DBH distribution was selected. For this tree, the tree height (h (m)), the height to the live crown base (HLC (m)), and an increment core was taken to derive the ten-year increment rate. Although obtaining full cross-sectional discs may minimize the effect of false and/or missing tree rings [28], destructive sampling (e.g., cutting trees and taking discs to the lab) is forbidden in the area. Moreover, it is neither a requirement nor is it carried out within the scope of routine inventory data collection [29].

For each central plot and species-specific "central" stem, an increment core sample was taken towards the plot center at the DBH to address potential slope effects in the tree form (e.g., ellipse). All sample cores were checked for potentially missing tree rings by comparing the increment core with a so-called "standard" [30], which compares single increment rates of a given core versus so-called "signal" years of the "standard" (>90% of the increment rates increase or decrease versus the previous year). In total, 424 increment cores are available for our study (see Table 1).

Table 1. Summary of the stand characteristics by region, where x is mean, Sd is standard deviation, min is minimum, max is maximum and show the range of the data, and DBH is diameter at breast height.

Variable	Forest			Woodland	Shrubland
	Gelawdiwos x ± Sd (min–max)	Katassi x ± Sd (min–max)	Taragedam x ± Sd (min–max)	Mahibereselassie x ± Sd (min–max)	Ambober x ± Sd (min–max)
Number of sample plots	34	63	52	21	28
Number of increment cores	106	196	58	84	-
Number of trees (ha^{-1})	314.5 ± 197.6 (63.7–859.4)	207.1 ± 119.8 (14.1–509.3)	175.1 ± 131.0 (31.8–541.1)	191.4 ± 89.5 (70.7–410.3)	NA
Number of sapling (ha^{-1})	4231.7 ± 3195.8 (0.0–11586.5)	1954.3 ± 1988.6 (0.0–9294.7)	3447.7 ± 3893.1 (0.0–16297.5)	660.9 ± 878.1 (0.0–3310.4)	3676.5 ± 2679.7 (127.3–16170.1)
Quadratic mean DBH (cm)	29.3 ± 12.8 (13.7–73.7)	28.6 ± 14.4 (14.4–111.9)	25.1 ± 13.4 (11.5–69.9)	22.5 ± 4.1 (13.6–31.8)	3.4 ± 0.9 (1.9–6.9)
Tree height (m)	10.2 ± 3.6 (5.1–27.5)	11.0 ± 4.9 (3.5–29.1)	10.5 ± 2.9 (4.2–23.5)	7.7 ± 1.6 (5.0–12.1)	1.9 ± 0.5 (1.7–4.8)

Trees with a tree height >1.3 m and a DBH of <10 cm are considered as saplings and were recorded on the smaller circle with a radius of 5 m. The 5-m radius was applied to all our study areas for recording saplings. Due to the large number of trees, we simplified the design by creating DBH classes ranging from ≤4 cm, 4–6 cm and 7–9.9 cm. We counted all individuals by species and assigned the numbers according to the DBH classes. We selected one representative tree by species and DBH class and recorded the tree height.

All trees with a tree height of ≤1.3 m are seedlings and are recorded on the four 1 m by 2 m rectangular (total 8 m²) (see Figure 2). Again, the seedlings were grouped in two classes according to tree height: Group 1 (≤50 cm) and Group 2 (50 cm to 1.3 m). The numbers were recorded by species and height class (Table 1).

We recorded the DBH for each tree on a given plot but only the tree height from the central trees. This is a common procedure within routine inventory designs to enhance data collection activities especially in difficult terrain [13,31,32]. However, this approach requires DBH–height functions to derive missing tree heights [31,33]. We also defined the five most frequent tree species within each study area plus a species group "others" and collected at least 20 trees per species, within the study areas (not limited to the plots) covering the full DBH and height range. The only exception was Ambober, where no DBH–tree height data were recorded because the area was covered with shrubs and thus the trees were too small. The Petterson's [34] height–diameter function was chosen to derive missing tree heights:

$$h = \frac{1}{\left(a_0 + {a_1}/{DBH}\right)^2} + 1.3 \quad (1)$$

where h is the tree height (m) and DBH is the diameter at breast height (cm), a_0 and a_1 are the resulting parameter estimates. We used R standard software package [35] to run non-linear regressions. The results are given in Table 2.

Table 2. Estimated coefficients of Petterson [34] height-diameter function, where N is the number of inventory plots, and R^2 is coefficient of determination.

Species	N	DBH (cm) x ± Sd (min–max)	Height (m) x ± Sd (min–max)	Coefficients a_0	Coefficients a_1	R^2
Acacia abyssinica	50	27.8 ± 10.0 (10.0–55.0)	9.8 ± 3.1 (2.9–20.0)	0.2000	3.8238	0.60
Ameja	28	17.2 ± 4.2 (11.0–29.0)	7.4 ± 1.8 (3.8–10.5)	0.2343	2.8516	0.45
Boswellia papyrifera	33	23.5 ± 4.8 (17.1–37.0)	8.8 ± 1.3 (6.4–12.0)	−0.3113	−1.2048	0.09
Combretum hartmannianum	27	18.5 ± 3.9 (10.0–27.6)	8.9 ± 1.7 (5.2–11.6)	0.2162	2.6838	0.54
Croton macrostachyus	94	18.7 ± 7.9 (10.0–56.0)	10.3 ± 4.4 (4.3–28.3)	0.1818	2.6777	0.43
Eucalyptus camaldulensis	72	24.0 ± 12.8 (10.0–60.0)	16.4 ± 7.8 (4.0–36.3)	0.1589	2.0771	0.60
Juniperus procera	52	27.0 ± 7.3 (11.0–39.0)	12.5 ± 2.8 (4.3–18.5)	0.2473	1.3106	0.19
Lannea fruticose	30	18.3 ± 3.8 (12.0–30.0)	7.6 ± 1.8 (4.7–11.8)	−0.3196	−1.4110	0.08
Olea europaea	27	34.0 ± 21.9 (10.2–103.0)	9.7 ± 4.6 (2.5–28.5)	0.1937	4.6001	0.61
Sterculia setigera	28	28.7 ± 5.7 (16.0–43.0)	8.2 ± 1.0 (6.2–10.3)	−0.3274	−1.4856	0.17
Albizia schimperiana	116	23.1 ± 13.2 (10.0–86.0)	13.0 ± 6.2 (5.3–30.7)	0.1633	2.7559	0.53
Allophylus abyssinicus	35	29.2 ± 12.2 (13.0–54.5)	13.4 ± 4.7 (6.0–23.1)	0.2110	2.0123	0.33
Bugtsi	27	20.6 ± 6.0 (11.0–37.0)	10.8 ± 2.7 (5.7–17.4)	0.2351	1.7723	0.28
Chionanthus mildbraedii	38	49.3 ± 15.8 (11.9–95.0)	14.2 ± 3.9 (4.0–24.2)	−0.2123	−3.0405	0.29
Gimblitini	37	22.0 ± 8.3 (11.0–38.0)	9.2 ± 2.5 (4.6–13.0)	0.2531	2.0776	0.47
Kanabal	37	15.7 ± 4.7 (10.0–28.5)	7.9 ± 2.1 (3.4–11.3)	0.2746	1.7087	0.26
Nuxia congesta	48	15.6 ± 4.1 (10.0–29.0)	8.8 ± 3.2 (3.1–23.1)	0.3273	0.5572	0.01
Podocarpus falcatus	24	20.8 ± 4.9 (12.0–27.0)	13.1 ± 1.7 (9.9–16.2)	−0.2244	−1.3208	0.67
Prunus Africana	42	39.5 ± 20.8 (13.0–132.0)	18.1 ± 6.2 (6.6–34.7)	0.1781	2.2629	0.47
Teclea nobilis	25	21.3 ± 10.5 (10.0–44.0)	9.3 ± 1.7 (7.0–14.4)	−0.3169	−0.6551	0.17
Other Species Gelawdiwos	121	26.0 ± 22.7 (10.0–108.0)	10.4 ± 5.3 (3.5–29.9)	0.2170	2.2612	0.17
Other species Katassi	58	24.1 ± 16.7 (10.0–102.0)	11.1 ± 7.6 (3.8–33.8)	0.1772	3.0084	0.46
Other species Taragedam	33	21.5 ± 17.8 (11.0–114.0)	10.7 ± 4.9 (4.4–28.8)	0.1894	2.6257	0.39
Other species Mahibereselassie	72	21.4 ± 9.5 (10.0–50.0)	8.0 ± 2.7 (3.5–15.9)	0.2514	2.6596	0.33

This dataset is used for calibrating species-specific diameter–height functions for deriving missing tree heights. In total, we recorded more than 1154 trees, of which 870 trees cover the 20 tree species, and 284 trees cover the species groups "other trees" by region.

Timber Volume

Based on the results of Table 2, we calculated the missing tree heights and the corresponding standing timber volume on a given inventory plot. The general formula for deriving standing timber volume for each tree (V) (m^3) can be expressed as [24]:

$$V = \frac{DBH^2 \times \pi}{4} \times h \times f \quad (2)$$

where f is the form factor addressing the shape of the tree, and all other parameters are as previously defined. Since no form factor functions for the tree species in the region exist, we decided to follow the suggestions by [36–38] and use a form factor of 0.5.

Volume Increment

Within sustainable forest management, the assessment of annual volume increment rates is important to ensure sustainable harvesting [13,39]. Up until this point, no such information exists for the forest areas in the Amhara region of northwestern Ethiopia. For our work, we have systematically collected increment cores for all our study regions. As outlined in the sampling technique section, these increment cores were taken from the "central" stem (the mean tree which is approximately the 60 percentile of the DBH distribution) by species on a given plot [24].

After determining the 10-year increment rates (2005 to 2014) with a 0.01 mm precision using the Velmex TA measuring system (Velmex Inc. Bloomfield, New York, NY, USA), the DBH of the "central" stem and inventory plot can be calculated for the year 2005. Applying the DBH–height function (Equation (1)) using the species parameter estimates of Table 2, and inserting in the volume function (Equation (2)), the corresponding volume in 2005 was calculated.

With this information, the volume ratios by plot and tree species can be calculated as:

$$inc_i = \frac{V2005_i}{V2014_i} \quad (3)$$

where inc_i refers to the individual tree volume increment ratio, $V2005_i$ and $V2014_i$ are the timber volume derived from the "central stem" in 2005 and 2014, respectively. Since this tree volume increment ratio is equal to the total volume increment ratio of a given plot, we can multiply the total plot volume V_{2014} with inc_i to derive the plot volume in 2005. With these numbers, we can calculate the 10-year periodic mean annual volume increments *(IV)* ($m^3\ h^{-1}\ year^{-1}$) by inventory plot:

$$IV = \frac{(V_{2014} - V_{2005})}{10} \quad (4)$$

where V_{2014} and V_{2005} are the tree volumes (m^3) in 2014 and 2005, respectively; 10 is the 10-year increment interval. Dead trees due to mortality are included if recorded.

Aboveground Carbon and Carbon Increment

The aboveground carbon estimations through destructive sampling is the most recommended and accurate method [40–42]. Given the small amount of forest resources, the high species diversity and the current forest conservation policy by the state, it is nearly impossible to undertake destructive sampling for the development of allometric functions in Ethiopia as well as for the Amhara region. Thus, we considered existing allometric functions developed for commercial tree species in Ethiopia [43–46]. Since Sileshi [47] has shown that these functions introduce a potential source of uncertainty, especially if applied in a very diverse structured of natural forests, we decided to use the mixed species allometric biomass function developed for tropical forests by Chave et al. [48], which has the following form:

$$ln(AGB) = -2.922 + 0.99 \times ln(DBH^2 \times h \times \rho), \quad (5)$$

where $ln(AGB)$ is the natural logarithm of the aboveground biomass (kg) and ρ is wood density (ton·m^{-3}).

A wood density of ρ = 0.614 ton m^{-3} developed for Africa is used [49,50]. A total of 50% of the resulting aboveground biomass (AGB) of Equation (5) provides the final carbon estimates [51,52].

Similar to the volume calculation, we calculated the aboveground biomass and carbon estimates for each tree then at the plot level and finally for each study area. Similar to the periodic mean annual volume increment rates, the periodic mean annual carbon increment rates for the period 2005 to 2014 can be derived. Again, we use here the approach of the "central" tree with the corresponding tree dimensions as outlined in the previous section.

Net Primary Production (NPP)

NPP is the amount of carbon remaining and allocated in the plant parts after autotrophic respiration (cellular and maintenance respiration) per growth period [12,53,54]. The growth period is determined depending on the interval between the repeated measurements which usually vary from 5 to 10 years [12,55]. We calculated NPP (gC·m^{-2}·year^{-1}) as the sum of periodic (2005–2014) carbon accumulation in the fine root turnover, aboveground woody parts and litter fall (Equation (6)) [55,56].

$$NPP = C_{woody} + C_{fineroot} + C_{litter} \quad (6)$$

where C_{woody} (gC·m^{-2}·year^{-1}) is the dry carbon increment of the woody biomass resulting from repeated plot observations between time$_2$ and time$_1$. $C_{fineroots}$ and C_{litter} (gC·m^{-2}·year^{-1}) are the carbon flow in to fine roots and litter, respectively.

The annual aboveground dry carbon in the woody part of the tree (C_{woody}) is calculated as follows:

$$C_{woody} = \left\{ \frac{\left(\frac{g_{2014} - g_{2005}}{10} \right)}{g_{2014}} \right\} \times C_{2014}, \quad (7)$$

where g_{2014} and g_{2005} are the tree basal area (m^2 ha^{-1}) in 2014 and 2005, respectively, 10 is the 10-year increment interval. C_{2014} (gC·m^{-2}) is the aboveground woody dry carbon content in 2014.

For Ethiopia, a reliable model for estimating the proportion of fine root turnover and litter fall does not exist. Malhi [57] and Raich and Nadelhoffer [58] found that for a given time period, the proportion of dry carbon turnover through fine roots and litter fall comprises 60% of the total dry carbon accumulation and that the carbon uptake by fine roots and litter is equal. The proportion of the increment of aboveground dry carbon in the woody part of the tree also comprises 40% of the total dry carbon increment. With this information, we assume that the dry carbon increment in the fine roots and foliage turnovers can be calculated from the dry carbon increment of the aboveground woody biomass. For all trees (DBH ≥ 10 cm) and saplings (DBH < 10 cm), the procedure was applied.

2.2. Land Cover Data

The Amhara region in northwestern Ethiopia covers a land area of 15.7 Mha, of which approximately 35% are either forests, shrublands or woodlands. The area is characterized by highly fragmented land use forms and a large variety of growing conditions due to the elevational gradients and the different agro-ecological zones. Mekonnen [17] and Gizachew et al. [59] carried out a land cover classification of the entire Amhara region, however, they failed to provide their methodology and digital data. Therefore, their study could not be verified. Other studies on land use and land cover classification of the Amhara region are limited to small scale areas within the region [14,60–62]. Finally, we obtained the land use and land cover map produced by the office of Amhara National Regional State (ANRS) covering 12 classes with 200 m × 200 m pixel spatial resolution, based on Landsat satellite images (Figure 3). The 12 land cover classes are afro-alpine, bare land, cultivation, grassland, highland bamboo, natural forest, plantation, shrubland, woodland, urban, wetland and water.

We aggregated the 12 land cover classes to six classes based on their vegetation characteristics for fitting our terrestrial inventory land cover types as follows: plantation, highland bamboo and natural forest are grouped as forest. Afro-alpine and shrubland are aggregated into shrubland. Woodland remained as woodland. Bare land, cultivation, grassland and wetland are grouped as non-vegetation. Water and urban classes remained as water and urban, respectively. Our final land cover classes relevant for our analysis are (i) forest, (ii) shrubland, and (iii) woodland. The remaining land cover classes are (iv) non-vegetation areas, (v) water and (vi) urban areas, which are not relevant for our analysis. Figure 3 shows the spatial distribution of land cover classes within the Amhara region.

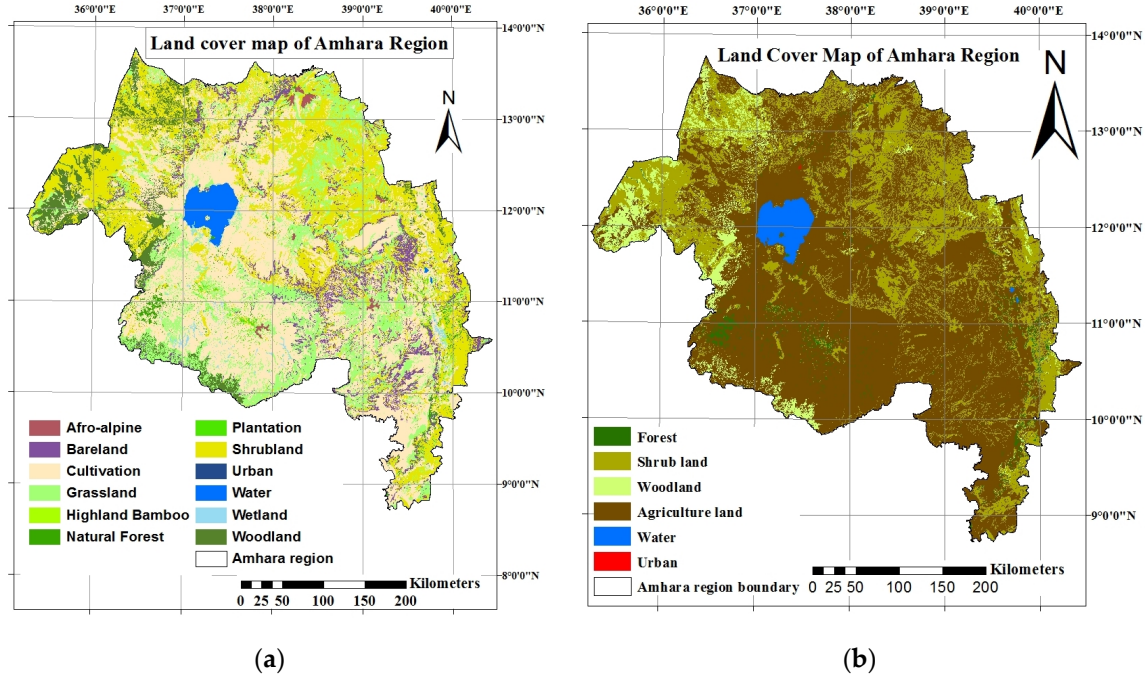

(**a**) (**b**)

Figure 1. Land cover map of Amhara region (**a**) before land cover aggregation and (**b**) after aggregation of the land cover classes.

The accuracy of our regrouped classified map was evaluated by performing stratified sampling. For land cover classifications, the calculation of the appropriate sample size was computed using the multinomial distribution [63]. With an expected accuracy of 90% and an error probability of 5%, the numbers of samples were determined. In total, 607 stratified sample points were randomly selected and distributed over the areas of the aggregated classes. The class of each of the 607 pixels was assigned with the help of finer resolution reference data combined with visual interpretation [64]. Bing and Google Earth images were used for the independent reference data. Due to the low spatial resolution (200 m × 200 m) of the land cover map and the high land fragmentation in the Amhara region, single pixels are often composed of multiple land cover types. Therefore, we assigned the main (largest areas) class of a pixel as the class (land cover type) of the pixel. Table 3 provides a detailed description of the characterizations of the land cover classes.

Table 3. Land cover classes and characterization features.

Land Cover Class	Characterization Features
Forest	More than or equal to half of the pixel should be first covered with vegetation. The vegetation part was checked for its relative density, color and consistency. If the vegetation is relatively dense and consistently became greater than or equal 1 ha, the class of the pixel is assigned as a forest cover.
Shrubland	Scattered shrubs, bushes: If the half or larger part of the pixel is vegetation with scattered, light green and inconsistent pattern, the class of the pixel is assigned as a shrubland.
Woodland	Woodlands are mainly situated in the northwestern low land parts of Amhara region. The agricultural fields and grass lands in the lowland parts are clearly and easily detectable due to their distinct color and pattern. Woodlands have green and grey color. Unlike to woodlands, shrubs lands have bright color.
Non-Vegetation (Cultivation, Grassland, bare land)	Cultivation: Agricultural fields can be identified with their patterns, proximity to rural resident areas and dark to grey color.
	Grassland: Grasslands appear from bright grey to white areas. It is often between vegetation and agriculture fields.
	Bare land: Similar to grassland but remain grey to white during even the rainy season unlike grasslands.
Urban	Built ups, main roads, bright reflectance.
Water	Lake Tana consists of more than 95% of the water bodies in the Amhara region. The lake is easily detectable. Pond-like structures. Rivers are not included as a water body as they often cover small parts of the 4-ha pixel.

We defined the three simplified forestry relevant land cover classes (see Table 3): (i) forest, (ii) shrubland, and (iii) woodland plus the non-vegetated area. Since elevational gradients are one of the main factors affecting the growing conditions and thus the species distribution of Ethiopian mountains forests [65,66], we adopted Hurni's [67] elevation classes for agro-ecological zonation resulting in five elevation classes: (i) low land (500–1500 meters above sea level (m.a.s.l.)), (ii) mid altitude (1500–2300 m.a.s.l.), (iii) high land (2300–3200 m.a.s.l.), (iv) sub-alpine (3200–3700 m.a.s.l.) and (v) alpine (3700–4530 m.a.s.l.). Then, we assigned the land area derived from Landsat data to each vegetation type and elevation classes.

3. Results

3.1. Terrestrial Inventory

Timber Volume, Aboveground Carbon and NPP

We began our analysis by estimating the height diameter coefficients of the Petterson [34] function using the available tree data (DBH and height measurements) (see Table 1). The results by tree species are presented in Table 2. Next, the plot values for timber volume, aboveground carbon and NPP are calculated and the mean values per hectare plus the corresponding standard deviation by study region are calculated. The mean timber volume ranges from 3.7 $m^3 \cdot ha^{-1}$ (Ambober) to 92.4 $m^3 \cdot ha^{-1}$ (Gelawdiwos). The corresponding mean aboveground carbon values are between 1.11 $Mg \cdot ha^{-1}$ (Ambober) and 54.6 $Mg \cdot ha^{-1}$ (Gelawdiwos). Table 4 provides the results of the stand situation in 2014, the year of the data recording.

Table 4. Results of the stand situation in 2014.

Region	*N*	Volume ($m^3 \cdot ha^{-1}$) x ± sd (min–max)	Carbon ($Mg \cdot ha^{-1}$) x ± sd (min–max)
Gelawdiwos	34	92.4 ± 68.1 (6.0–317.4)	54.6 ± 43.6 (2.3–175.4)
Katassi	63	75.9 ± 60.2 (2.5–270.1)	37.7 ± 32.6 (0.0–144.7)
Taragedam	52	28.9 ± 56.5 (0.0–352.8)	13.8 ± 32.7 (0.0–210.4)
Ambober	28	3.7 ± 3.4 (0.3–18.2)	1.11 ± 0.92 (0.1–4.6)
Mahibereselassie	21	27.6 ± 10.7 (7.1–48.5)	11.9 ± 5.2 (2.1–23.7)

The volume increment rates are 3.5 $m^3 \cdot ha^{-1}$ (Gelawdiwos), 3.6 $m^3 \cdot ha^{-1}$ (Katassi) and 1.0 $m^3 \cdot ha^{-1}$ (Taragedam). The mean annual aboveground carbon increments of inventory regions are between 0.22 $Mg \cdot ha^{-1}$ year (Ambober) and 1.9 $Mg \cdot ha^{-1}$ year (Gelawdiwos).

The mean NPP of Gelawdiwos forest is 597.2 $gC \cdot m^{-2} \cdot year^{-1}$ followed by Kattassi (486.8 $gC \cdot m^{-2} \cdot year^{-1}$) and Taragedam (305.4 $gC \cdot m^{-2} \cdot year^{-1}$). The NPP at the Ambober shrubland is very low with 55.4 $gC \cdot m^{-2} \cdot year^{-1}$ while the Mahibereselassie woodland NPP exhibited 150.4 $gC \cdot m^{-2} \cdot year^{-1}$. The values for the annual volume and carbon increments and NPP are presented in Table 5.

Table 5. Annual volume increment, carbon increments and Net Primary Production (NPP) of inventory plots by region.

Region	*N*	Volume Increment ($m^3 \cdot ha^{-1} \cdot year^{-1}$) x ± sd (min–max)	Carbon Increment ($Mg \cdot ha^{-1} \cdot year^{-1}$) x ± sd (min–max)	NPP ($gC \cdot m^{-2} \cdot year^{-1}$) x ± sd (min–max)
Forest				
Gelawdiwos	34	3.5 ± 2.7 (0.2–11.3)	1.9 ± 1.5 (0.1–6.5)	597.2 ± 393.8 (101.4–1705.5)
Katassi	63	3.6 ± 2.6 (0.0–11.2)	1.7 ± 1.3 (0.0–5.6)	486.8 ± 322.7 (46.5–1306.5)
Taragedam	52	1.0 ± 1.4 (0.0–6.2)	0.5 ± 0.7 (0.0–3.7)	305.4 ± 313.2 (0.0–1506.8)
Shrubland				
Ambober	28	0.9 ± 0.9 (0.0–4.6)	0.22 ± 0.18 (0.02–0.93)	55.4 ± 46.0 (4.8–231.2)
Woodland				
Mahibereselassie	21	1.2 ± 0.5 (0.3–2.6)	0.5 ± 0.2 (0.1–1.1)	150.4 ± 62.9 (61.4–296.2)

3.2. Land Cover Classification

After we have assigned the land cover classes of the 607 pixels, based on the independent reference images, we assessed the accuracy of the map by comparing the land cover map produced by ANRS (Amhara National Regional State) with our independent reference data. The accuracy assessment was applied by using error matrix, according to Olofsson et al. [68], which compares the known reference data with the corresponding results of automated classification [68,69]. Considering the coarse resolution (200 m × 200 m) of the map and the highly land fragmentation within the Amhara region [18], the accuracy of the land cover classification was good (Table 6).

Table 6. Land cover classification accuracy assessment.

Automated Result	Independent Data						Total
	Forest	Shrubland	Woodland	Non-Vegetation	Water	Urban	
Forest	23	1	11	8	1	1	45
Shrubland	19	45	29	28	-	-	121
Woodland	1	20	33	3	-	-	57
Non-vegetation	56	72	27	123	-	-	278
Water	1	-	-	-	99	-	100
Urban	-	-	-	-	-	6	6
Total	100	138	100	162	100	7	607

3.3. The Forest Conditions of the Amhara Region

Fifteen forestry relevant clusters (five elevational classes and three vegetation types) are created. The summary of the results is shown in Table 7.

Table 7. Land cover classes and their respective area by agroecological zones of Amhara region.

Agroecological Zones	Elevation (m.a.s.l.)	Forest (ha)	Shrubland (ha)	Woodland (ha)	Non-Vegetation (ha)	Inventory Sites
Low Land (Kolla)	500–1500	25,098	1,855,284	780,448	1,752,212	Mahibereselassie
Mid Altitude (Weyna Dega)	1500–2300	115,838	1,845,350	131,030	4,643,435	Ambober, Katassi and Taragedam
High Land (Dega)	2300–3200	100,692	473,927	13,621	3,169,069	Gelawdiwos
Sub-Alpine (Wurch)	3200–3700	9354	52,847	5192	355,661	-
Alpine (High Wurch)	3700–4530	104	60,111	93	10,088	-
Total		251,088	4,287,519	930,384	9,930,464	
Grand Total				15,399,456		

We assigned each of our forest inventory areas to the corresponding clusters. The idea here is that we created a kind of a "reference stand approach", where we assumed that regional forest inventory information can be used as a proxy for a given cluster and thus allows us to extrapolate local inventories results (our regional sites) to the whole Amhara region. Considering our regional sites, Mahibereselassie is located in the low land—woodland (500–1500 m.a.s.l.) cluster, Ambober belongs to the mid altitude—shrubland area (1500–2300 m.a.s.l.), Katassi and Taragedam to the mid altitude—forest (1500–2300 m.a.s.l.) and Gelawdiwos to the high land—forest area (2300–3200 m.a.s.l.). Most of the woodland is located in the low land and most of the shrubs are in the elevation class low land and mid altitude. Thus, for the total woodland, we decided to use the results of the forest inventory in Mahibereselassie and for the total shrubland, we decided to use the results of the inventory in Ambober as reference stand information. Most of the forest area is located in the mid altitude and the high land area where our forest inventories in Katassi and Taragedam as well as Gelawdiwos are located. Thus, we decided to create reference productivity values according to the following procedure. We averaged the forest inventory productivity estimates of Katassi and Taragedam. We used these numbers for the low land and the mid altitude clusters. For the remaining elevational classes (high land, sub-alpine and alpine), we used the inventory results of Gelawdiwos as reference numbers. Obtaining the number presented in Tables 5 and 6 and multiplying these numbers with the corresponding land area by vegetation type and elevation class, provides the total productivity estimates for the forested area of the Amhara region (see Table 8).

Table 8. Total volume stock, annual increment, carbon stock, annual increment, and NPP for the Amhara region. The results are obtained through: Total Volume/Carbon = the size of forest areas in elevation classes (Table 7) × corresponding to the mean terrestrial forest inventory volume/carbon estimates (Table 5). We used the mean volume/carbon estimates of Mahibereselassie woodland and Ambober shrubland to extrapolate to the total volume/carbon estimates of woodland and shrubland, respectively found in all elevation classes of the Amhara region.

Land Cover	Volume (million m^3)	Volume Increment (million $m^3 \cdot year^{-1}$)	Carbon (Tg)	Carbon Increment ($Tg \cdot year^{-1}$)	NPP ($gC \cdot m^{-2} \cdot year^{-1}$)
Forest	17.56	0.71	7.78	0.34	484.32
Shrubland	15.86	3.86	4.76	0.95	55.4
Woodland	25.68	1.12	11.07	0.47	150.40

4. Discussion

The Amhara region in northwestern Ethiopia consists of a forested area of about 251,000 ha or 2% of the total land area (15.7 Mha); 4,287,000 ha or 27% of shrubland; and 930,000 ha or 6% of woodland. The total stocking tree volume is 59 million m^3 or 19.1 Tg stored carbon (Tables 7 and 8). Gibbs et al. [70] estimated a total aboveground carbon stock for Ethiopia within a range of 153 to 867 Tg. Note that the total land mass of Ethiopia is about seven times the size of the Amhara region and most of the forest areas are located in the southwestern part of Ethiopia [23].

In our analysis, we estimated, for the forested area (251,000 ha), a stocking timber volume of approximately 17.6 million m^3 and a total carbon of 7.8 Tg with annual volume and carbon increment rates of 0.7 million m^3 and 0.34 Tg, respectively (Table 8). These numbers show that the stocking timber volume and annual productivity rates are fairly low: For example, the volumes of our investigated forests range from 28.9 ± 56.5 $m^3 \cdot ha^{-1}$ in Taragedam to 92.4 ± 68.1 $m^3 \cdot ha^{-1}$ in Gelawdiwos and 75.9 ± 60.2 $m^3 \cdot ha^{-1}$ in Katassi (Table 5). Mokria et al. [40] reported much lower carbon stocks for similar dry afro-montane forests in northern Ethiopia. Compared to other moist afro-montane forests in Southwest Ethiopia [71,72] and Mozambique woodlands [73], our numbers are low. Since the forest sites are highly sensitive, any removal of forest plants leads to erosion problems [18,74], which suggests that careful planning of any harvesting operation is essential to ensure sustainability.

The shrubland area of the Amhara region covers 27% or 4,287,000 ha of the land area in the Amhara region. The estimated total stocking volume is 15.9 million m^3 with an average annual volume increment of 3.86 $m^3 \cdot ha^{-1}$. The total carbon stock stored in the shrublands is 4.8 Tg with 0.95 Tg annual increment (Table 8). The shrubland may be seen as a result of deforestation and cattle grazing activities. In our assessment, the Ambober site provided the reference area for the shrubland assessment. Although the forest inventory covered a rather small area, it may be seen as a typical shrubland in northwestern Ethiopia with an estimated volume stock of 3.7 ± 3.4 $m^3 \cdot ha^{-1}$ and a mean annual volume increment rates of 0.9 m^3 ± 0.9 $m^3 \cdot ha^{-1}$ (Tables 5 and 6).

The Amhara woodland area covers 6% (930,000 ha) of the land area with an estimated total volume and carbon stock of 25.68 million m^3 and 11.1 Tg, respectively. The shrublands exhibited annual volume and carbon increments of 3.86 million m^3 and 0.21 Tg. The inventory in Mahibereselassie served as the reference with a volume stock of 27.6 ± 10.7 $m^3 \cdot ha^{-1}$ and a mean annual volume increment rate of 1.2 ± 0.5 $m^3 \cdot ha^{-1}$ (Tables 5 and 6). Comparing the woodland inventory in Mahibereselassie with the forest inventories in Gelawdiwos, Katassi, and Taragedam (Table 5), one can see that the forest area in Taragedam exhibits a similar stoking volume as the woodland area in Mahibereselassie. This suggests that the historic and current forest management impacts in Taragedam must be high. Wondie et al. [18] showed a strong relationship between population growth and deforestation in the Taragedam area since 1957.

The mean NPP of forests in the Amhara region is 484.3 $gC \cdot m^{-2} \cdot year^{-1}$. The NPP of the shrubland is estimated with 55.4 $gC \cdot m^{-2} \cdot year^{-1}$, while the woodland NPP estimates are with 150.4 $gC \cdot m^{-2} \cdot year^{-1}$ (Table 8).

A literature search revealed that studies in Ethiopia related to biomass and carbon stock are concentrated in the southwestern part of the country where most of the country's larger undisturbed moist montane forests are growing [1,21,45,75]. In contrast, the vegetation types in the Amhara region are fragmented dry-afromontane evergreen forests [40,76–78]. The forest carbon stock decreases from moist to dry vegetation types [70]. Climate, topography and human and animal activity are the main factors for our low productivity estimated numbers versus the moist afro-montane forests [79]. For example, Muluken et al. [65] and Mokria et al. [35] reported carbon stocks above 278.03 $MgC \cdot ha^{-1}$ and 19.3 ± 3.9 $MgC \cdot ha^{-1}$ in southwestern moist-montane community forests and northern dry-afromontane forests in Ethiopia, respectively.

Our aboveground carbon estimations are consistent with estimates provided by Mekuria et al. [80]. The protection of shrublands (= exclosures) from livestock appears to have an important potential to improve vegetation cover and aboveground productivity [23,81,82].

One important result of our study is the development of height–DBH (Diameter at Breast Height) functions for more than 20 tree species in the area for deriving missing tree heights (Table 2) and thus resulting in an easy estimation of tree volume. This substantially improves the data collection in the future, however, we suggest that our calibrated height–DBH functions should be used only within the area where we obtained data for calibration (the Amhara region, Figure 3).

5. Conclusions

For the first time, this study provides forest growth information for the Amhara region as it is essential for sustainable forest management decisions. We developed diameter–height functions for all major tree species in the region. The regional forest inventory data also exhibited tree volume and carbon stocks in combination with the volume and carbon increment data. Prior to this study, no forest productivity information was available and the data collection in the area is extremely difficult. Hence, we selected only five local forest inventories and based our approach on a "reference stand" concept. This assumes that our five established forest inventories cover the key regions and are representative of the remotely sensed vegetation classes (Table 7). With this procedure, we are able to combine regional forest inventory information and remote sensing techniques to provide estimates of the forest productivity in the Amhara region. The methodology is simple and can be easily improved if more local forest inventory data are available. Therefore, this study is critical in pioneering a full forest inventory system in the Amhara region.

Acknowledgments: This work is part of the project "Carbon storage and soil biodiversity in forest landscapes in Ethiopia: Knowledge base and participatory management". We are grateful for the financial support provided by the Austrian Federal Ministry of Agriculture, Forestry, Environment and Water Management. We thank Hadera Abraha, Khlot Gebrehana, Sibhatu Abera and Tesfaye Teklehaymanot for the success of data collection and compilation. We would like to thank Hirut Hailu Alle for all her indispensable help. Special thanks to Abrham Abiyu for providing us 2009 Ambober data. The comments made by Elisabeth Pötzelsberger and the two anonymous reviewers greatly improved the manuscript. We thank Brady Mattsson for English language corrections.

Author Contributions: Kibruyesfa Sisay designed the study, coordinated data collection, analyzed the data and wrote the manuscript, Christopher Thurnher designed and coordinated the R-scripts and helped the data analysis, Beyene Belay helped on the data collection, data analysis and interpretation, Gerald Lindner coordinated and managed the land cover classification analysis and Hubert Hasenauer designed, coordinated and supervised the methods, analysis, interpretation and the manuscript writing.

Conflicts of Interest: The authors declare no conflict of interest.

References

1. Hailemariam, S.N.; Soromessa, T.; Teketay, D. Non-carbon benefits for effective implementation of REDD+: The case of Bale Mountains Eco-Region, Southeastern Ethiopia. *Afr. J. Environ. Sci. Technol.* **2015**, *910*, 747–764.
2. Lal, R. Forest soils and carbon sequestration. *For. Ecol. Manag.* **2005**, *220*, 242–258.
3. Groom, B.; Palmer, C. REDD+ and rural livelihoods. *Biol. Conserv.* **2012**, *154*, 42–52.
4. Vanderhaegen, K.; Verbist, B.; Hundera, K.; Muys, B. REALU vs. REDD+: Carbon and biodiversity in the Afromontane landscapes of SW Ethiopia. *For. Ecol. Manag.* **2015**, *343*, 22–33.
5. United Nations Framework Convention on Climate Change (UNFCCC). Key decisions relevant for reducing emissions from deforestation and forest degradation in developing countries (REDD+); United Nations Framework Convention on Climate Change (UNFCCC): Bonn, Germany, 2014.
6. Spittlehouse, D.L. Integrating climate change adaptation into forest management. *For. Chron.* **2005**, *81*, 691–695.
7. van Tuyl, S.; Law, B.E.; Turner, D.P.; Gitelman, A.I. Variability in net primary production and carbon storage in biomass across Oregon forests—An assessment integrating data from forest inventories, intensive sites, and remote sensing. *For. Ecol. Manag.* **2005**, *209*, 273–291.
8. Moreno, A.; Neumann, M.; Hasenauer, H. Optimal resolution for linking remotely sensed and forest inventory data in Europe. *Remote Sens. Environ.* **2016**, *183*, 109–119.
9. Neumann, M.; Moreno, A.; Mues, V.; Härkönen, S.; Mura, M.; Bouriaud, O.; Lang, M.; Achten, W.M.J.; Thivolle-Cazat, A.; Bronisz, K.; et al. Comparison of carbon estimation methods for European forests. *For. Ecol. Manag.* **2016**, *361*, 397–420.
10. Magcale-Macando, D.; Delgado, M.E.; Ty, E.; Villarin, J. A GIS-based model to improve estimation of aboveground biomass of secondary forests in the Philippines. *J. Trop. For. Sci.* **2006**, *18*, 8–21.
11. Muukkonen, P.; Heiskanen, J. Biomass estimation over a large area based on standwise forest inventory data and ASTER and MODIS satellite data: A possibility to verify carbon inventories. *Remote Sens. Environ.*

2007, *107*, 617–624.
12. Hasenauer, H.; Petritsch, R.; Zhao, M.; Boisvenue, C.; Running, S.W. Reconciling satellite with ground data to estimate forest productivity at national scales. *For. Ecol. Manag.* **2012**, *276*, 196–208.
13. Thurnher, C.; Klopf, M.; Hasenauer, H. Forests in transition: A harvesting model for uneven-aged mixed species forests in Austria. *Forestry* **2011**, *84*, 517–526.
14. Wondie, M.; Schneider, W.; Melesse, A.M.; Teketay, D. Spatial and Temporal Land Cover Changes in the Simen Mountains National Park, a World Heritage Site in Northwestern Ethiopia. *Remote Sens.* **2011**, *3*, 752–766.
15. Gebrehiwot, S.G.; Bewket, W.; Gärdenäs, A.I.; Bishop, K. Forest cover change over four decades in the Blue Nile Basin, Ethiopia: Comparison of three watersheds. *Reg. Environ. Change* **2014**, *14*, 253–266.
16. Dessie, G.; Kleman, J. Pattern and Magnitude of Deforestation in the South Central Rift Valley Region of Ethiopia. *Mt. Res. Dev.* **2007**, *27*, 162–168.
17. Mekonnen, M.; Sewunet, T.; Gebeyehu, M.; Azene, B.; Melesse, A.M. *GIS and Remote Sensing-Based Forest Resource Assessment, Quantification, and Mapping in Amhara Region, Ethiopia*; Melesse, A.M., Abtew, W., Eds.; Springer: Cham, Switzerland, 2016.
18. Wondie, M.; Schneider, W.; Katzensteiner, K.; Mansberger, R.; Teketay, D. Modelling the dynamics of landscape transformations and population growth in the highlands of Ethiopia using remote-sensing data. *Int. J. Remote Sens.* **2016**, *37*, 5647–5667.
19. Hailemariam, S.; Soromessa, T.; Teketay, D. Land Use and Land Cover Change in the Bale Mountain Eco-Region of Ethiopia during 1985 to 2015. *Land* **2016**, *5*, 41.
20. Sisay, K.; Yitaferu, B.; Garedew, E.; Ziadat, F. Assessment of forest cover change and its environmental impacts using multi-temporal and multi-spectral satellite images. In *Mitigating Land Degradation and Improving Livelihoods*; Ziadat, F., Bayu, W., Eds.; Routledge: New York, NY, USA, 2015; pp. 85–98.
21. Negash, M.; Starr, M. Biomass and soil carbon stocks of indigenous agroforestry systems on the south-eastern Rift Valley escarpment, Ethiopia. *Plant Soil* **2015**, *393*, 95–107.
22. Feyisa, K.; Beyene, S.; Megersa, B.; Said, M.Y.; de Leeuw, J.; Angassa, A. Allometric equations for predicting above-ground biomass of selected woody species to estimate carbon in East African rangelands. *Agrofor. Syst.* **2016**, doi:10.1007/s10457-016-9997-9.
23. Lemenih, M.; Kassa, H. Re-greening Ethiopia: History, challenges and lessons. *Forests* **2014**, *5*, 1896–1909.
24. Assmann, E. *The Principles of Forest Yield Study: Studies in the Organic Production, Structure, Increment and Yield of Forest Stands*; Davis, P.W., Ed.; Pergamon Press: Oxford, UK, 1970. (In German)
25. Worbes, M. One hundred years of tree-ring research in the tropics—A brief history and an outlook to future challenges. *Dendrochronologia* **2002**, *20*, 217–231.
26. Zhang, X.; Friedl, M.A.; Schaaf, C.B.; Strahler, A.H.; Liu, Z. Monitoring the response of vegetation phenology to precipitation in Africa by coupling MODIS and TRMM instruments. *J. Geophys. Res.* **2005**, *110*, 1–14.
27. Sisay, K.; Thurnher, C.; Hasenauer, H. Daily climate data for the Amhara region in Northwestern Ethiopia. *Int. J. Climatol.* **2016**, doi:10.1002/joc.4880.
28. Gebrekirstos, A.; Bräuning, A.; Sass-Klassen, U.; Mbow, C. Opportunities and applications of dendrochronology in Africa. *Curr. Opin. Environ. Sustain.* **2014**, *6*, 48–53.
29. Tomppo, E.; Gschwantner, T.; Lawrence, M.; McRoberts, R.E. *National Forest Inventories*; Tomppo, E., Gschwantner, T., Lawrence, M., McRoberts, R.E., Eds.; Springer: Dordrecht, The Netherlands, 2010.
30. Vins, B. Die Auswertung jahrringchronologischer Untersuchungen in rauchgeschädigten Fichtenwäldern des Erzgebirges. *Wiss. Z. Techn. Univ. Dresden* **1962**, *11*, 579–580.
31. Arcangeli, C.; Klopf, M.; Hale, S.E.; Jenkins, T.A.R.; Hasenauer, H. The uniform height curve method for height-diameter modelling: An application to Sitka spruce in Britain. *Forestry* **2014**, *87*, 177–186.
32. Feldpausch, T.R.; Banin, L.; Phillips, O.L.; Baker, T.R.; Lewis, S.L.; Quesada, C.A. Height-diameter allometry of tropical forest trees. *Biogeosci. Discuss.* **2011**, *8*, 1081–1106.
33. Wonn, H.T.; O'hara, K.L. Height:Diameter Ratios and Stability Relationships for Four Northern Rocky Mountain Tree Species. *West. J. Appl. For.* **2001**, *16*, 87–94.
34. Schmidt, A. Der rechnerische Ausgleich von Bestandeshöhenkurven. *Forstwiss. Centralbl.* **1967**, *86*, 370–386.
35. R Development Core Team. *R: A Language and Environment for Statistical Computing*; The R Foundation for Statistical Computing: Vienna, Austria, 2014.

36. Masota, A.M. Volume Models for Single Trees in Tropical Rainforests in Tanzania. *J. Energy Nat. Resour.* **2014**, *3*, 66.
37. Petrokofsky, G.; Kanamaru, H.; Achard, F.; Goetz, S.J.; Joosten, H.; Holmgren, P.; Lehtonen, A.; Menton, M.C.; Pullin, A.S.; Wattenbach, M. Comparison of methods for measuring and assessing carbon stocks and carbon stock changes in terrestrial carbon pools. How do the accuracy and precision of current methods compare? A systematic review protocol. *Environ. Evid.* **2012**, *1*, 6.
38. Teklehaymanot, T. Development of Form Factor and Height-Diameter Functions for Selected Tree Species in the Amhara Region, Ethiopia. Master's Thesis, University of Natural Resources and Life Sciences, Vienna, Austria, 2015.
39. Ledermann, T. Using Logistic Regression to Model Tree Selection Preferences for Harvesting in Forests in Conversion. In *Continuous Cover Forestry*; Springer Netherlands: Dordrecht, The Netherlands, 2002; pp. 203–216.
40. Mokria, M.; Gebrekirstos, A.; Aynekulu, E.; Bräuning, A. Tree dieback affects climate change mitigation potential of a dry afromontane forest in northern Ethiopia. *For. Ecol. Manag.* **2015**, *344*, 73–83.
41. Hasenauer, H.; Eastaugh, C.S. Assessing Forest Production Using Terrestrial Monitoring Data. *Int. J. For. Res.* **2012**, *2012*, 8.
42. Clark, D.B.; Kellner, J.R. Tropical forest biomass estimation and the fallacy of misplaced concreteness. *J. Veg. Sci.* **2012**, *23*, 1191–1196.
43. Berhe, L.; Assefa, G.; Teklay, T. Models for estimation of carbon sequestered by Cupressus lusitanica plantation stands at Wondo Genet, Ethiopia. *South. For. J. For. Sci.* **2013**, *75*, 113–122.
44. Berhe, L.; Arnoldsson, G. Tree taper models for Cupressus lusitanica plantations in Ethiopia. *South. For. J. For. Sci.* **2008**, *70*, 193–203.
45. Negash, M.; Starr, M.; Kanninen, M.; Berhe, L. Allometric equations for estimating aboveground biomass of *Coffea arabica L.* grown in the Rift Valley escarpment of Ethiopia. *Agrofor. Syst.* **2013**, *87*, 953–966.
46. Hunde, T.; Duguma, D.; Gizachew, B.; Mamushet, D.; Teketay, D. Growth and form of Eucalyptus grandis provenances at Wondo Genet, Southern Ethiopia. *Aust. For.* **2003**, *66*, 170–175.
47. Sileshi, G.W. A critical review of forest biomass estimation models, common mistakes and corrective measures. *For. Ecol. Manag.* **2014**, *329*, 237–254.
48. Chave, J.; Andalo, C.; Brown, S.; Cairns; M.A.; Chambers, J.Q.; Eamus, D.; Fölster, H.; Higuchi, N.; Kira, T; Lescure, J.-P; et al. Tree allometry and improved estimation of carbon stocks and balance in tropical forests. *Oecologia* **2005**, *145*, 87–99.
49. Reyes, G.; Brown, S.; Chapman, J.; Lugo, A.E. Wood densities of Tropical tree species. *Gen. Tech. Rep.* **1992**, *88*, 1–18.
50. Brown, S. Estimating biomass and biomass change of tropical forests: A primer; Food and Agriculture Organization of the United Nations: Rome, Italy, **1997**; Volume 134, p. 55.
51. Brown, S.; Lugo, A.E. The Storage and Production of Organic Matter in Tropical Forests and Their Role in the Global Carbon Cycle. *Biotropica* **1982**, *14*, 161–187.
52. Malhi, Y.; Baker, T.R.; Phillips, O.L.; Almeida, S.; Alvarez, E.; Arroyo, L.; Chave, J.; Czimczik, C.I.; Di Fiore, A.; Higuchi, N.; et al. The above-ground coarse wood productivity of 104 Neotropical forest plots. *Glob. Change Biol.* **2004**, *10*, 563–591.
53. Piao, S.; Luyssaert, S.; Ciais, P.; Janssens, I.A.; Chen, A.; Chao, C.A.O.; Fang, J.; Friedlingstein, P.; Luo, Y.; Wang, S. Forest annual carbon cost: A global-scale analysis of autotrophic respiration. *Ecology* **2010**, *91*, 652–661.
54. Zhao, M.; Heinsch, F.A.; Nemani, R.R.; Running, S.W. Improvements of the MODIS terrestrial gross and net primary production global data set. *Remote Sens. Environ.* **2005**, *95*, 164–176.
55. Neumann, M.; Zhao, M.; Kindermann, G.; Hasenauer, H. Comparing MODIS Net Primary Production Estimates with Terrestrial National Forest Inventory Data in Austria. *Remote Sens.* **2015**, *7*, 3878–3906.
56. He, L.; Chen, J.M.; Pan, Y.; Birdsey, R.; Kattge, J. Relationships between net primary productivity and forest stand age in U.S. forests. *Glob. Biochem. Cycles* **2012**, *26*, 1–19.
57. Malhi, Y. The productivity, metabolism and carbon cycle of tropical forest vegetation. *J. Ecol.* **2012**, *100*, 65–75.
58. Raich, J.W.; Nadelhoffer, K.J. Belowground Carbon Allocation in Forest Ecosystems: Global Trends. *Ecology* **1989**, *70*, 1346–1354.
59. Gizachew, B.; Solberg, S.; Næsset, E.; Gobakken, T.; Bollandsås, O.M.; Breidenbach, J.; Zahabu, E.;

Mauya, E.W. Mapping and estimating the total living biomass and carbon in low-biomass woodlands using Landsat 8 CDR data. *Carbon Balance Manag.* **2016**, *11*, 13.

60. Tesfaye, S.; Guyassa, E.; Raj, A.J.; Birhane, E.; Wondim, G.T. Land Use and Land Cover Change, and Woody Vegetation Diversity in Human Driven Landscape of Gilgel Tekeze Catchment, Northern Ethiopia. *Int. J. For. Res.* **2014**, *2014*, 614249.
61. Garede, N.M.; Minale, A.S. Land Use/Cover Dynamics in Ribb Watershed, North Western Ethiopia. *J. Nat. Sci. Res.* **2014**, *4*, 9–16.
62. Tolessa, T.; Senbeta, F.; Abebe, T. Land use/land cover analysis and ecosystem services valuation in the central highlands of Ethiopia. *For. Trees Livelihoods* **2016**, *26*, 111–123.
63. Congalton, R. *Assessing the Accuracy of Remotely Sensed Data: Principles and Practices*, 2nd ed.; CRC Press: Boca Raton, FL, USA, 2008.
64. Morisette, J.T.; Privette, J.L.; Justice, C.O. A framework for the validation of MODIS Land products. *Remote Sens. Environ.* **2002**, *83*, 77–96.
65. Berhanu, A.; Woldu, Z.; Demissew, S. Elevation patterns of woody taxa richness in the evergreen Afromontane vegetation of Ethiopia. *J. For. Res.* **2016**, doi:10.1007/s11676-016-0350-y.
66. Schmitt, C.B. *Montane Rainforest with Wild Coffea Arabica in the Bonga Region (SW Ethiopia): Plant Diversity, Wild Coffee Management and Implications for Conservation*; Cuvillier Verlag: Göttingen, Germany, 2006.
67. Hurni, H. *Agroecologial belts of Ethiopia: Explanatory notes on three maps at a scale of 1:1,000,000*; Research Report for Soil Conservation Research Program: Addis Ababa, Ethiopia, 1998; p. 43.
68. Olofsson, P.; Foody, G.M.; Stehman, S.V.; Woodcock, C.E. Making better use of accuracy data in land change studies: Estimating accuracy and area and quantifying uncertainty using stratified estimation. *Remote Sens. Environ.* **2013**, *129*, 122–131.
69. Liu, C.; Frazier, P.; Kumar, L. Comparative assessment of the measures of thematic classification accuracy. *Remote Sens. Environ.* **2007**, *107*, 606–616.
70. Gibbs, H.K.; Brown, S.; Niles, J.O.; Foley, J.A. Monitoring and estimating tropical forest carbon stocks: Making REDD a reality. *Environ. Res. Lett.* **2007**, *2*, 45023.
71. Muluken, N.B.; Teshome, S.; Eyale, B. Carbon stock in Adaba-Dodola community forest of Danaba District, West-Arsi zone of Oromia Region, Ethiopia: An implication for climate change mitigation. *J. Ecol. Nat. Environ.* **2015**, *7*, 14–22.
72. Wondrade, N.; Dick, O.B.; Tveite, H. Estimating above Ground Biomass and Carbon Stock in the Lake Hawassa Watershed, Ethiopia by Integrating Remote Sensing and Allometric Equations. *For. Res.* **2015**, *4*, 151.
73. Williams, M.; Ryan, C.M.; Rees, R.M.; Sambane, E.; Fernando, J.; Grace, J. Carbon sequestration and biodiversity of re-growing miombo woodlands in Mozambique. *For. Ecol. Manag.* **2008**, *254*, 145–155.
74. Zeleke, G.; Hurni, H. Implications of Land Use and Land Cover Dynamics for Mountain Resource Degradation in the Northwestern Ethiopian Highlands. *Mt. Res. Dev.* **2001**, *21*, 184–191.
75. De Beenhouwer, M.; Geeraert, L.; Mertens, J.; van Geel, M.; Aerts, R.; Vanderhaegen, K.; Honnay, O. Biodiversity and carbon storage co-benefits of coffee agroforestry across a gradient of increasing management intensity in the SW Ethiopian highlands. *Agric. Ecosyst. Environ.* **2016**, *222*, 193–199.
76. Abiyu, A.; Teketay, D.; Glatzel, G.; Gratzer, G. Tree seed dispersal by African civets in the Afromontane Highlands: Too long a latrine to be effective for tree population dynamics. *Afr. J. Ecol.* **2015**, *53*, 588–591.
77. Wassie, A.; Sterck, F.J.; Bongers, F. Species and structural diversity of church forests in a fragmented Ethiopian Highland landscape. *J. Veg. Sci.* **2010**, *21*, 938–948.
78. Aerts, R.; van Overtveld, K.; November, E.; Wassie, A.; Abiyu, A.; Demissew, S.; Daye, D.D.; Giday, K.; Haile, M.; TewoldeBerhan, S.; et al. Conservation of the Ethiopian church forests: Threats, opportunities and implications for their management. *Sci. Total Environ.* **2016**, *551–552*, 404–414.
79. Clark, D.B.; Clark, D.A. Landscape-scale variation in forest structure and biomass in a tropical rain forest. *For. Ecol. Manag.* **2000**, *137*, 185–198.
80. Mekuria, W.; Langan, S.; Johnston, R.; Belay, B.; Amare, D.; Gashaw, T.; Desta, G.; Noble, A.; Wale, A. Restoring aboveground carbon and biodiversity: A case study from the Nile basin, Ethiopia. *For. Sci. Technol.* **2015**, *11*, 86–96.
81. Neelo, J.; Teketay, D.; Kashe, K.; Masamba, W. Stand Structure , Diversity and Regeneration Status of Woody Species in Open and Exclosed Dry Woodland Sites around Molapo Farming Areas of the Okavango Delta , Northeastern Botswana. *Open J. For.* **2015**, *5*, 313–328.

82. Birhane, E.; Teketay, D.; Barklund, P. Enclosures to Enhance Woody Species Diversity in the Dry Lands of Eastern Tigray. *East Afr. J. Sci.* **2007**, *1*, 136–147.

© 2017 by the authors. Licensee MDPI, Basel, Switzerland. This article is an open access article distributed under the terms and conditions of the Creative Commons Attribution (CC BY) license (http://creativecommons.org/licenses/by/4.0/).

9.2 Paper 2

Sisay, K., Thurnher, C., Hasenauer, H., 2016. Daily climate data for the Amhara region in Northwestern Ethiopia. Int. J. Climatol. doi:10.1002/joc.4880

INTERNATIONAL JOURNAL OF CLIMATOLOGY
Int. J. Climatol. (2016)
Published online in Wiley Online Library
(wileyonlinelibrary.com) DOI: 10.1002/joc.4880

RMetS
Royal Meteorological Society

Daily climate data for the Amhara region in Northwestern Ethiopia

Kibruyesfa Sisay,[a,b]* Christopher Thurnher[a] and Hubert Hasenauer[a]
[a] *Institute of Silviculture, University of Natural Resources and Life Sciences, Vienna, Austria*
[b] *Amhara Region Agricultural Research Institute, Gondar Agriculture Research Center, Ethiopia*

ABSTRACT: Many spatial vegetative physiological and environmental impact studies demand consistent as well as fine resolution daily meteorological data, which is often unavailable. This problem is evident when studies and applications focus at the regional and local scale. Meteorological stations cannot provide the needed data due to their irregular locations and several associated shortcomings such as missing data. Climate data from global sources like the National Centers for Environmental Prediction (NCEP) and WorldClim are provided at a coarse resolution which makes them inappropriate to use directly at regional and local scales. In order to circumvent this problem, we downscaled daily WorldClim and NCEP global climate grids to produce weather data sets using a delta method to $0.008\overline{3}$ (approximately 1×1 km) spatial resolution for the Amhara region of northwestern Ethiopia. The downscaled data set includes daily precipitation, and minimum and maximum temperature from 1979 to 2010. The drizzle effect in the downscaled data set was first eliminated by using a rain threshold that removed values of <1 mm per day. We compared the downscaled values with our calibration data from 56 meteorological stations in the Amhara region. The comparison between the downscaled and the calibrated data from weather stations showed biases in the downscaled values. A delta-change bias correction technique on a 10-day average basis was used to correct the biases associated with the downscaled data. Simple additive and multiplicative bias correction methods were used for temperature and precipitation, respectively. We then validated the corrected downscaled daily weather data using ten independent weather stations from the region. We found that the downscaling and the bias correction methods have improved the NCEP values. The validation exhibited no bias. The full data set can be accessed freely under the following link: ftp://palantir.boku.ac.at/Public/ClimateDataEthiopia/.

KEY WORDS precipitation; temperature; downscaling; Amhara; WorldClim; NCEP

Received 30 November 2015; Revised 22 July 2016; Accepted 1 August 2016

1. Introduction

Daily weather measures the atmospheric conditions at a given location and time, while climate is the measure of average weather conditions at a location for a longer time period. Weather conditions strongly affect vegetative physiological and ecological processes (Lüttge and Scarano, 2004; Longa *et al.*, 2008; Grimm *et al.*, 2013) such as photosynthesis and respiration, as well as the flux dynamics of ecosystems, including carbon, nitrogen, water and energy cycles (Bakkenes *et al.*, 2002; Lüttge and Scarano, 2004; Nekola and Brown, 2007; Longa *et al.*, 2008). The demand of daily weather data for different ecological applications has increased in the past decades since they are used for modelling purposes (Walther *et al.*, 2002; Cavanaugh *et al.*, 2015). Net primary production of forest ecosystems (Running *et al.*, 2004; Zhao and Running, 2010; Hasenauer *et al.*, 2012; Neumann *et al.*, 2015), agricultural productivity (Tesso *et al.*, 2012; Fitsume *et al.*, 2015) and hydrological modelling (Sennikovs and Bethers, 2009; Dile and Srinivasan, 2014; Fuka *et al.*, 2014) are some of the applications which strongly depend on weather data. Therefore, recording daily weather data by installing meteorological stations is crucial to produce accurate outcomes and predictions for ecological and other environmental studies.

Meteorological stations record different weather parameters such as temperature, precipitation, humidity, atmospheric pressure, solar radiation, wind speed, etc. They form networks that are often irregularly spaced and do not provide a systematic grid of parameters across larger areas. Meteorological station data frequently have problems with data quality, inconsistencies and missing data values. Places which are far away from meteorological stations would be left unobserved and often result in less accurate values if estimated from surrounding stations (Haylock *et al.*, 2008; Van Den Besselaar *et al.*, 2011). Simple climate interpolation tools like MT-CLIM (Thornton and Running, 1999) were developed to estimate meteorological variables from the nearest weather station, but the validity of the outcomes decreases with the distance to the station, especially in mountainous areas.

* Correspondence to: K. Sisay, Institute of Silviculture, University of Natural Resources and Life Sciences, Vienna, Peter-Jordan Straße 82, A-1190 Vienna, Austria. E-mail: kibruyesfa.ejigu@students.boku.ac.at

© 2016 Royal Meteorological Society

Climate grids have been developed at different spatial and temporal resolutions to fill the spatial gaps of meteorological stations and are used as a data source for areas without meteorological records. They are often based on interpolation techniques from surrounding stations. Examples are DAYMET (Thornton *et al.*, 1997) and PRISM (Daly *et al.*, 2008) for the USA, or E-OBS (Haylock *et al.*, 2006) for Europe. The interpolation algorithms can be used only in regions with enough climate stations available (e.g. DAYMET for Austria; Petritsch and Hasenauer, 2011).

Global data sets combining observations with a meteorological forecast model to produce gridded data sets of many atmospheric and oceanic variables, with a temporal resolution of a few hours, are commonly referred as reanalysis data. Amongst these data sets, the National Centers for Environmental Prediction (NCEP) Climate Forecast System Reanalysis data (Maraun *et al.*, 2010; Saha *et al.*, 2010) is one of the most commonly used climate data (Winkler *et al.*, 2011; Dile and Srinivasan, 2014; Fuka *et al.*, 2014; Rose and Apt, 2015). NCEP provides multiple data sets with different spatial and temporal resolutions, amongst them, the daily climate data from 1979 to 2010 with a ~38 km (0.3125 decimal degrees) spatial resolution. Another global data set that provides spatial and temporal information is WorldClim (Hijmans *et al.*, 2005). It is solely based on interpolation and provides long-term monthly mean values of precipitation, minimum and maximum temperature at a 1×1 km ($0.008\overline{3}$ decimal degrees) grid.

The coarse resolution of global data sets, either spatial (NCEP) or temporal (WorldClim), is not an ideal solution for regional and local-scale applications. A gridded climate data set with $\leq 1\,\text{km}^2$ spatial resolution is often needed for applications to capture environmental variability (Justice *et al.*, 2002; Hijmans *et al.*, 2005). Additionally, many ecological studies rely on daily climate input variables that may be interpolated from daily weather station data. Often such data sets are not available due to a lack of weather stations. A possible way to circumvent this problem is to downscale available global climate grids to the required spatial and temporal resolution.

Different climate downscaling techniques are commonly used to address the spatiotemporal mismatch between the globally available coarse resolution climate data and the regional and/or local-scale application demands (Schmidli *et al.*, 2006; Fowler and Wilby, 2007; Jakob Themeßl *et al.*, 2011; Abatzoglou, 2013; Hennemuth *et al.*, 2013; Moreno and Hasenauer, 2015). A typical downscaling method is the spatial delta method which addresses the spatiotemporal discrepancies between different climate data sets (Mosier *et al.*, 2014). In this study, we derive daily weather data for the Amhara region of northwestern Ethiopia by applying a spatial delta method with bilinear interpolation and correct regional weather anomalies with observed data from meteorological stations. We produce a 1×1 km daily precipitation, minimum and maximum temperature grid based on the NCEP and WorldClim data sets, similar to the methodology presented by Moreno and Hasenauer (2015) and Mosier *et al.* (2014).

The mountainous Amhara region of Ethiopia covers an area of about $156\,000\,\text{km}^2$. The area is highly productive and consistent daily climate data are important for various impact studies. Existing studies which involve the study of weather and climate suffer from insufficient weather data which restricts them to rather small areas (Bewket and Conway, 2007; Ayalew, 2012; Ayalew *et al.*, 2012; Taye and Zewdu, 2012). For example Taye *et al.* (2011) used data from coarse global and regional climate models for the assessment of effects of climate change on the Lake Tana catchment ($15\,000\,\text{km}^2$). Setegn *et al.* (2008) used weather data from ten sparsely and irregularly situated stations for large catchment ($15\,096\,\text{km}^2$) in the Amhara region and had to use a weather generator for the missing values. In the case of Seleshi and Zanke's (2004) study of changes in rainfall and rainy days for the entire country, they could only use 11 weather stations due to the lack of weather data. Kebede *et al.* (2013) assessed temperature and precipitation change projections.

The aim of this study is to prepare spatially and temporally consistent daily weather data for the whole Amhara region by:

- downscaling available global climate grids to daily 1×1 km climate raster for the whole Amhara region between 1979 and 2010;
- applying regional bias corrections of the climate grid based data using locally available weather stations; and
- validating the downscaled data.

2. Materials and methods

2.1. Data

2.1.1. National Centers for Environmental Prediction (daily 38 km climate data)

Daily values of minimum (T_{min}) and maximum (T_{max}) temperature and precipitation (Prcp) are obtained from the Climate Forecast System Reanalysis data set (Saha *et al.*, 2010) produced by the NCEP. The NCEP data consists of various grids of different spatial and temporal resolutions describing the state of the atmosphere, land, ocean and sea ice on a global scale. The data is constructed using assimilation of observed data and models which take all available observations every 6–12 h over the period being analysed. Climate variables are available on a T382L64 horizontal resolution (Maraun *et al.*, 2010; Saha *et al.*, 2010) which is about 38 km at the Equator (0.3125 decimal degrees). The weather data needed for our study was extracted from a bounding box for 8.11°–14.36°N latitude and 34.53°–40.78°E longitude from the Texas A&M University spatial sciences website (Globalweather, 2012) for the years 1979–2010. They extract the hourly temperature *TMP2M* and precipitation *PWAT* fields from the NCEP grid and provide the daily minimum and maximum temperature and precipitation sum (Dile and Srinivasan, 2014; Fuka *et al.*, 2014). The 400 climate files contained within the bounding box were converted to GEOTIFF raster files with 20 columns and 20 rows each. Based on this data,

© 2016 Royal Meteorological Society

we created one raster file per variable and year containing one raster band per day (365 for normal and 366 for leap years). Although the resolution of the data is not exactly 38 km, for simplicity we will refer to a 38 km resolution throughout the study.

2.1.2. *WorldClim (monthly 1 km climate data)*

WorldClim (Hijmans *et al.*, 2005) provides global long-term monthly mean, minimum and maximum temperature values as well as precipitation. The resolution is 30 arc seconds which corresponds to $0.008\overline{3}$ decimal degrees. This resolution is commonly referred as 1 km spatial resolution. The data set also provides 19 bioclimatic variables derived from the climate but they are not used in this study. The data is based on climate stations from different sources such as the Global Historic Climate Network Dataset (Peterson *et al.*, 1998) or the WMO climatological normal (WMO, 1996). The station data were harmonized which resulted in a data set of precipitation records from 47 554 locations, mean temperature from 24 542 stations and minimum and maximum temperature from 14 835 stations (Hijmans *et al.*, 2005). The data were interpolated using the thin plate smoothing splines procedure (Hutchinson, 1995). The raster data for $T_{\min}$, $T_{\max}$ and Prcp for our study was obtained from the WorldClim website (WorldClim, 2005) for the same bounding box coordinates used for the NCEP data. This resulted in raster files with 750 columns and rows. The raster files were converted into GEOTIFF files, one file per variable with 12 raster bands (one per month).

2.1.3. *Meteorological station data*

According to National Meteorology Agency of Ethiopia, meteorological stations in Ethiopia are divided into four classes based on their meteorological observation parameters (http://www.ethiomet.gov.et/stations/regional_information/2). First class stations are established for the purpose of synoptic meteorology. Observations are taken every full hour for 24 h a day. They observe 18 meteorological parameters, amongst them $T_{\min}$, $T_{\max}$, Prcp, relative humidity, wind speed and sunshine duration. Second class stations record meteorological data for climatological purposes. These stations measure more than 13 meteorological variables not relevant for our study. Third class stations only record three meteorological parameters every 24 h; $T_{\min}$, $T_{\max}$ and Prcp. Fourth class stations measure only the total amount of precipitation in 24 h. Observations for the fourth class are taken at 0600 GMT. For our analysis, we used data only from class 1 and 3 stations because we were interested in daily $T_{\min}$, $T_{\max}$ and Prcp.

Although the stations are established based on the aforementioned classes, some stations have stopped their operation for different reasons. Some stations were also outdated and replaced by new ones while others were established very recently. This makes acquisition of consistent data for the given time period difficult. In addition, we limited the meteorological station data to the time span between 1979 and 2010 so that they match with the available NCEP data. In the Amhara region, 66 stations fulfilled these criteria (Figure 1). For our analysis, we used 56 stations for calibration (early comparison and bias correction) of the downscaled data. After the downscaling and the associated bias correction were done, we obtained ten additional and independent weather stations from 1979 to 2010 for validation purposes.

2.2. Methods

2.2.1. *Downscaling*

We used two global raster data sets (NCEP and WorldClim), both on different spatial and temporal resolutions to obtain a 1 km daily climate grid consisting of $T_{\min}$, $T_{\max}$ and Prcp. We obtained the monthly high-resolution WorldClim data set to adjust the daily low-resolution NCEP values. We applied the delta downscaling procedure, similar to the methods described in Moreno and Hasenauer (2015) and Mosier *et al.* (2014). Figure 2 shows the methodological steps of the downscaling process.

As a first step, we up-scaled the daily 1 km WorldClim data to the 38 km NCEP resolution by averaging all WorldClim pixel values that fall into the respective 38 km cell. In this way, we generated two raster data sets at the same spatial resolution, the daily NCEP and the up-scaled WorldClim raster, with differing temporal scales. In the next step, we calculated the anomalies between the two data sets by calculating the differences of the up-scaled WorldClim data to the NCEP value of the appropriate month for every day in the NCEP data set. We used additive anomalies for temperature and multiplicative anomalies for precipitation. This was done to avoid possible negative precipitation values. The temperature anomaly is defined as the up-scaled WorldClim minus the respective NCEP value, whereas the precipitation anomaly is the ratio of the NCEP to the up-scaled WorldClim value of the appropriate month. This was done for every day included in the NCEP data set. We obtained the anomaly rasters for $T_{\min}$, $T_{\max}$ and Prcp on a 38 km resolution for every day included in the NCEP data.

The downscaling modifies the 1 km WorldClim data set by the daily anomaly values created in the previous step. Using the 38 km anomaly raster would have created strong edge effects in the resulting 1 km raster at the barriers of each 38 km cell since the values of the anomalies change abruptly. Thus, we first downscaled the anomaly raster to the 1 km resolution by interpolating the values before we used them to adjust the WorldClim raster. We applied a bilinear interpolation for that step (step 3 in Figure 2) because it avoids over and undershooting of the calculated values (Mosier *et al.*, 2014) and ensures that all values of the interpolated data set are within the borders of the original data.

This resulted in a 1 km anomaly raster for $T_{\min}$, $T_{\max}$ and Prcp on a daily time step and the same spatial resolution as the WorldClim raster. As mentioned earlier, the final step of the downscaling process was to apply daily anomaly values to the WorldClim data (step 4).

© 2016 Royal Meteorological Society

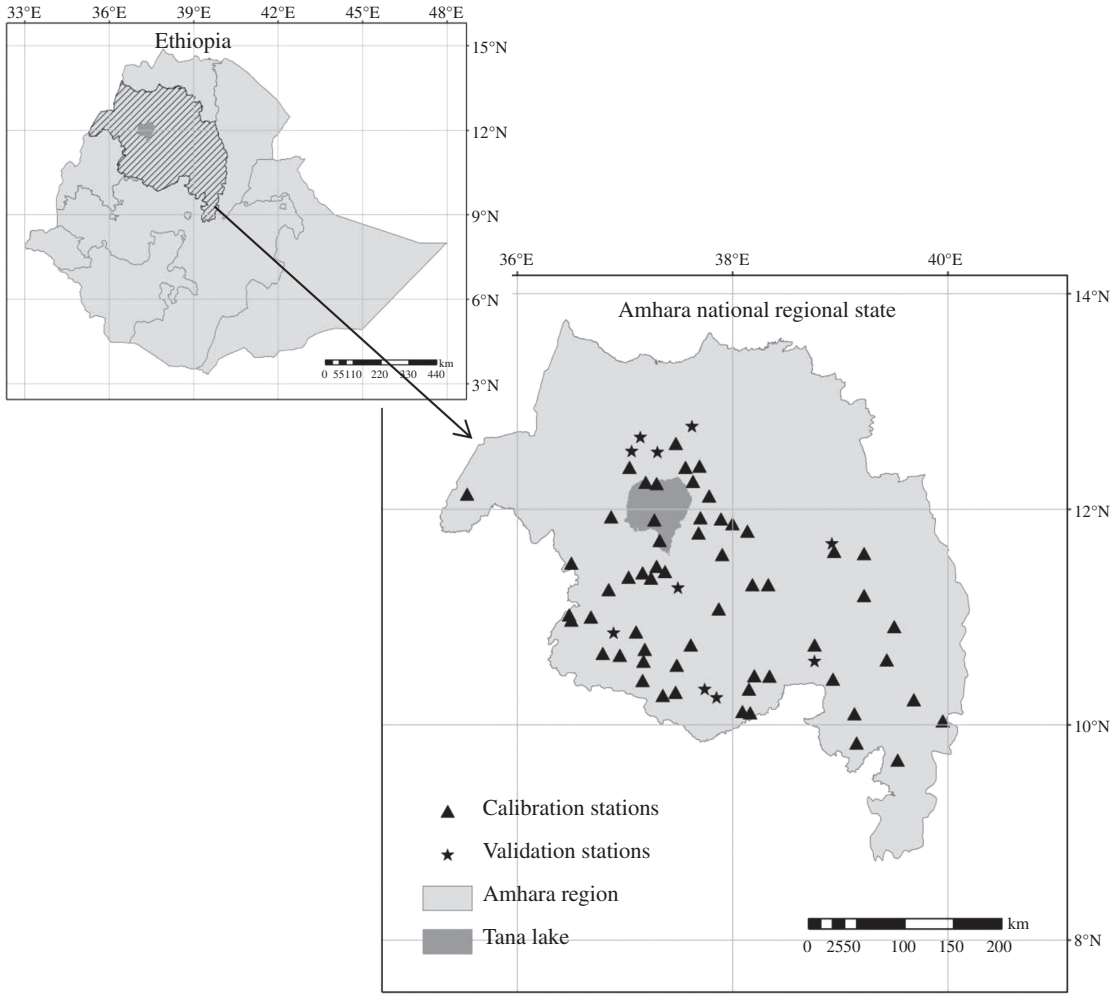

Figure 1. Map showing the meteorological stations in the Amhara region, Ethiopia. Fifty-six weather stations plots are available for calibration and bias correction. Ten additional weather stations are obtained for validation of the results.

We used Python programming language to implement the downscaling algorithm. The Geospatial Data Abstraction Library (GDAL) module for Python was used for processing the raster data sets. The GDAL function *ReprojectImage* was used for the bilinear interpolation.

2.2.2. *Bias correction procedures*

2.2.2.1. Precipitation: The total number of rainy days observed from the calibration weather stations (observations used for correcting the biases created after downscaling) *versus* downscaled data was calculated for each month of the reference period. Several very low precipitation intensities occurred in our downscaled data set leading to an overestimation of rainy days as compared to the calibration weather station data sets. A precipitation rate of <1 mm of rainfall per day is considered low intensity precipitation (Schmidli *et al.*, 2006; Feldmann *et al.*, 2008; Piani *et al.*, 2010; Berg *et al.*, 2012; Chen *et al.*, 2013; Teutschbein and Seibert, 2013). Therefore, rainy days with ≤ 1 mm of rain in the downscaled data set were set equal to 0 mm to suppress the overestimation (New *et al.*, 1999; Manton *et al.*, 2001; Seleshi and Zanke, 2004; Haylock *et al.*, 2006; Ines and Hansen, 2006; Hadgu *et al.*, 2013).

2.2.3. *Delta-change correction*

We calculated arithmetic means of the climate variables for each of the 366 days within the available years. Next, we compared observed data from the calibration weather stations and downscaled values similar to Legates and McCabe (1999). Common systematic model biases were detected during the comparison of observed data from the calibration weather stations with the downscaled data (Charles *et al.*, 2007; Leander *et al.*, 2008; Chen *et al.*, 2013; Teutschbein and Seibert, 2013). There are different bias correction methods that help to adjust the global data on a regional scale (Gellens and Roulin, 1998; Schmidli *et al.*, 2006; Graham *et al.*, 2007b; Lenderink *et al.*, 2007; Block *et al.*, 2009; Berg *et al.*, 2012; Teutschbein and Seibert, 2013). We used the delta-change correction method due to its popularity, simplicity, and its good performance in the field (Lenderink *et al.*, 2007; Johnson and Sharma, 2011; Berg *et al.*, 2012; Teutschbein and Seibert, 2012). We split the 366 days in 37 groups (each group with 10 days except the last or the 37th group). We calculated the arithmetic mean of each group to get the correction factors. The corrections were applied to daily values of the whole Amhara region (Lenderink *et al.*,

© 2016 Royal Meteorological Society

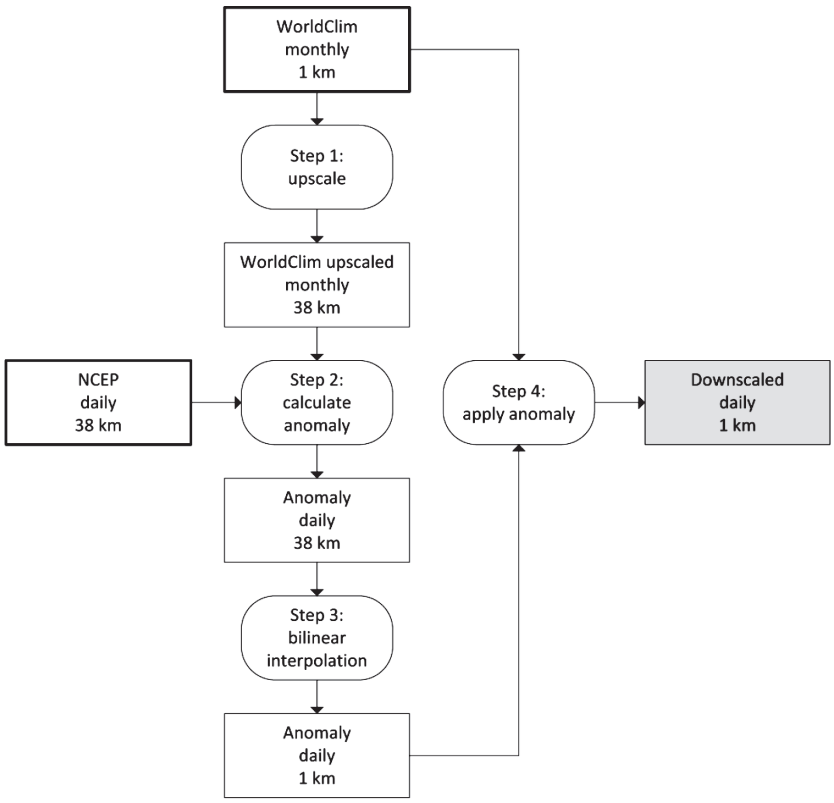

Figure 2. Downscaling algorithm. Squared boxes denote raster data sets, the input data sets are highlighted with thick borders. The resulting downscaled data is the grey shaded box. Intermediate raster data that are created during the downscaling algorithm are represented by white boxes. Each box holds information about the temporal and spatial resolution. The round boxes depict processes that transform the raster data sets during the downscaling algorithm.

2007). Simple additive and multiplicative correction techniques were used for temperature and precipitation, respectively (Equations (1) and (2)).

$$P^i_{\text{corr}} = P^i_{\text{down}} * \left(\overline{P^i_{\text{obs}}}/\overline{P^i_{\text{down}}}\right) \tag{1}$$

$$T^i_{\text{corr}} = T^i_{\text{down}} + \left(\overline{T^i_{\text{obs}}} - \overline{T^i_{\text{down}}}\right) \tag{2}$$

where P^i_{corr} is the corrected daily precipitation of day i, P^i_{down} is the downscaled daily precipitation of day i and $\overline{P^i_{\text{obs}}}$ and $\overline{P^i_{\text{down}}}$ are the 10-day mean values of observed data from the calibration weather stations and downscaled precipitation, respectively. T^i_{corr} is the corrected daily temperature of day i, T^i_{down} is the downscaled daily temperature of day i and $\overline{T^i_{\text{obs}}}$ and $\overline{T^i_{\text{down}}}$ are the 10-day mean values of observed data from the calibration weather stations and downscaled temperature, respectively.

2.2.4. *Validation*

Validation of the corrected downscaled data with independent weather station observations was performed by comparing corrected *versus* observed values of the validation weather stations. Statistics from Hasenauer *et al.* (2003), Hofstra *et al.* (2008, 2009), Moreno and Hasenauer (2015), Pietsch and Hasenauer (2002) and Willmott and Matsuura (2006) were applied for validation of the corrected values. We calculated the mean, minimum and maximum values, the mean absolute error (MAE), the coefficient of determination (R^2), the linear error in probability space (LEPS), the critical success index (CSI), the confidence, prediction and tolerance intervals of the climatic variables. We calculated LEPS to assess the potential error in probability space. It shows the deviation of predicted values from observed values. Its resistance to outliers is an advantage. Normal distribution is a prerequisite to calculate LEPS. Therefore LEPS for Prcp is not calculated. The LEPS is calculated as:

$$\text{LEPS} = \frac{\left|p_v - 0.5\right| - \left|p_f - p_v\right|}{0.25} \tag{3}$$

where p_v is the probability of occurrence of the weather station value in the weather station data's cumulative distribution function (CDF). p_f is the probability of occurrence of the downscaled corrected data value in the weather station data's CDF. This particular LEPS equation gives values from −1 (no skill) to 1 (prefect skill). A 0 value is given if the median value ($p = 0.5$) of the weather station data is given as a derived value on every data point.

We calculated CSI for our Prcp data to check the matching success in capturing rainy days. We also calculated the CSI for all climatic variables for extreme high and extreme low values. Above 95th and below 5th percentile of the weather station CDF are the extreme high and extreme low

© 2016 Royal Meteorological Society

values, respectively. A CSI value of 1 means perfect skill and 0 means no skill. The CSI is calculated as:

$$\mathrm{CSI} = \frac{\text{hits}}{\text{hits} + \text{misses} + \text{false alarms}} \tag{4}$$

where hits represent the number of days when rain was observed in the weather station data and predicted in the downscaled data. Misses are the number of days when rain was observed but not predicted, and false alarms are the number of days when rain was predicted but not observed.

The confidence, prediction and tolerance intervals were calculated to determine the limits and ranges of errors in future predictions of the downscaled data (Reynolds, 1984). The confidence interval (CI) shows the degree of uncertainty around common population estimators such as mean and standard deviation. The D (predicted − observed), can be used to evaluate discrepancies between the expected difference and the estimator $\overline{D}$. The CI is calculated as:

$$\mathrm{CI} = \overline{D} \pm \frac{S_D}{\sqrt{n}} t_{1-\alpha/2(n-1)} \tag{5}$$

The prediction interval (PI) gives the range of the residuals for each observation (D_i) between the predicted and observed values for future observations. The PI is calculated as:

$$\mathrm{PI} = \overline{D} \pm \sqrt{1 + \frac{1}{n}} S_D t_{1-\alpha/2(n-1)} \tag{6}$$

The tolerance interval (TI) provides the limit that contains a specified portion (e.g. 95%) of the distribution of the differences when the model is used repeatedly. The TI is calculated as:

$$\mathrm{TI} = \overline{D} \pm S_D g_{1-\gamma,\, n, 1-\alpha} \tag{7}$$

where D_i is the difference between predicted and observed values of an observation, $\overline{D}$ is the mean of D_i, S_D the standard deviation of the D_i, n is the sample size and t is the $1-\alpha/2$ quantile of the t-distribution with $n-1$ degrees of freedom, $g_{1-\gamma,\, n, 1-\alpha}$ is a tolerance factor for normal distribution inferring for the probability that $(1-\gamma)100\,\%$ of the distribution D is within the probability of $(1-\alpha)$ which can easily be found from statistical tables.

3. Analysis and results

3.1. Downscaling

We downscaled the NCEP and WorldClim global data sets and produced a 1×1 km grid of daily $T_{\min}$, $T_{\max}$ and Prcp from 1979 to 2010 for the Amhara region of Ethiopia. For determining the precipitation threshold, we first compared the rainy days of the downscaled data to the station data and found a large number of rainy days in the downscaled data sets; much higher than in the observations (Figure 3). We then set a 1 mm precipitation threshold and made a comparison between the downscaled number of days, with and without the threshold, and the observed number of rainy days. Changing the days with rainfall intensities of <1 mm to no rainy days (0 mm per day) in the downscaled data showed an improvement in results that became closer to the observed number of rainy days (Figure 3).

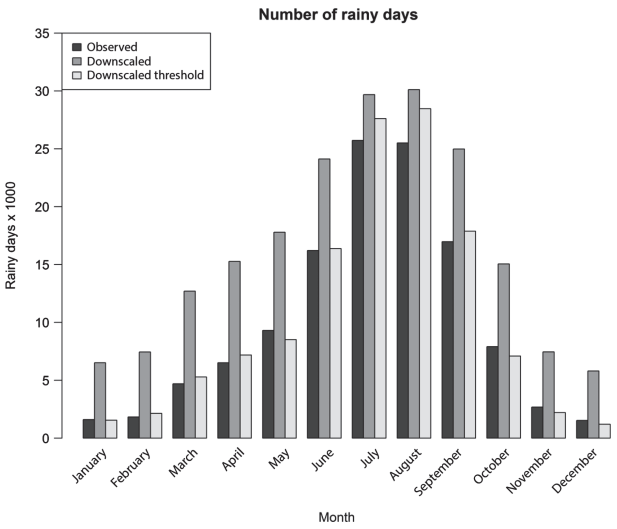

Figure 3. The total number of rainy days from 1979 to 2010 for all the 56 calibration weather stations by month. Black indicates the total number of observed rainy days; light grey indicates the total number of the downscaled rainy days; white indicates the downscaled total rainy days with a rain threshold >1 mm per day.

After applying the precipitation threshold, we compared the downscaled with the observed calibration data. Even though the downscaled data exhibited an improvement *versus* the NCEP values, a bias in the downscaled data is still evident (Figure 4).

3.2. Bias correction

The comparison was performed between the corresponding downscaled and calibration weather station data. The downscaled values for $T_{\min}$ are higher than the observed values from March to early June, which is the dry season in Ethiopia. However, the downscaled $T_{\min}$ values are lower than the observed value from July to December, in Ethiopia's typical rainy and spring seasons (Figure 4). The downscaled $T_{\min}$ improved, and the differences between predicted and observed $T_{\min}$ during the dry season converged towards zero. However, the $T_{\min}$ values diverged during the spring season. From June to August, the rainy season in the region, the downscaled $T_{\max}$ are lower than the observed $T_{\max}$ values but remained higher for the rest of the year. Values for $T_{\max}$ and $T_{\min}$ show no similar pattern. The downscaled Prcp has higher rainfall records than the observed values from June to August in the Ethiopian rainy season. The bias corrections with weather stations from calibration data were done to correct these biases in the downscaled data (Figure 4).

3.3. Validation

After applying the bias correction by using calibration weather station data, we validated each climatic variable with independent weather station data. Using ten independent weather stations for validation we obtained the

© 2016 Royal Meteorological Society

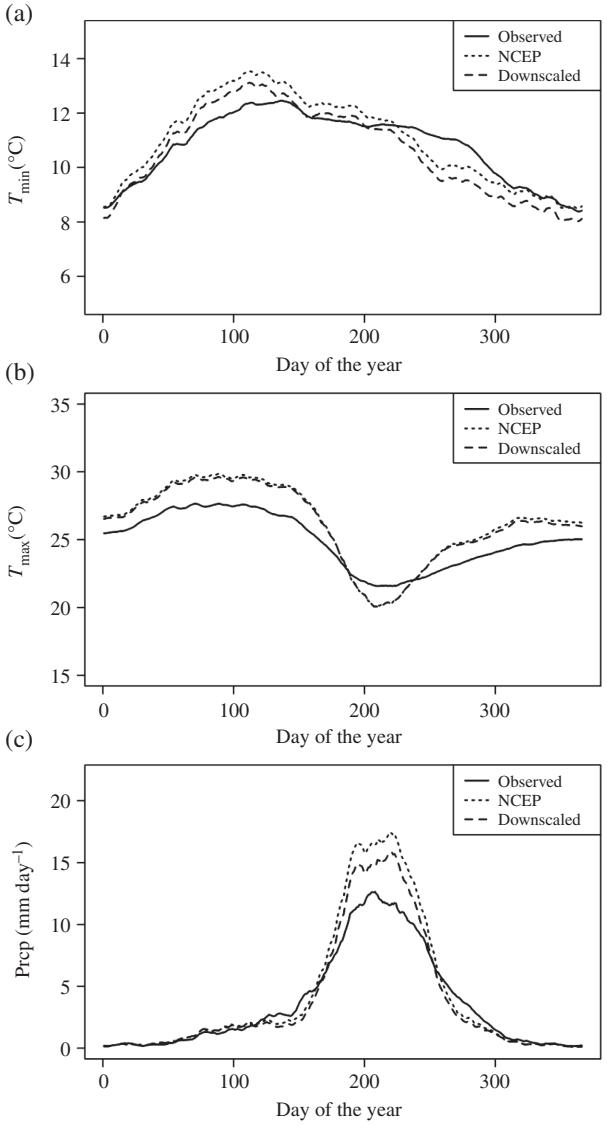

Figure 4. A 10-day moving average for observed data, NCEP and downscaled data prior to the bias correction: (a) T_{min}, (b) T_{max} and (c) Prcp.

results, summarized in Table 1. The mean values of daily precipitation for all stations improved, as shown in Table 1. Figure 5 presents the corrected values which showed considerable improvements when compared with our independent validation data sets.

The mean Prcp of NCEP is 5.8 mm. When downscaled, it is 5.6 mm and, when corrected, it is 5.3 mm. The mean daily observed precipitation is 3.8 mm. The MAE of NCEP (5.46) downscaled (5.08) and corrected (4.85) daily precipitation values decreased consistently. The R^2 value for Prcp is 0.54 in the corrected data, which is an improvement to the NCEP (0.31), and downscaled (0.52) data.

The observed mean daily minimum temperature is 11.3 °C. The mean value of daily T_{min} of all stations is 12.1 °C in the NCEP, 10.7 °C in the downscaled and 10.9 °C in the corrected values. MAE of the NCEP, downscaled and corrected daily minimum temperature values consistently decreased from 2.42 to 2.17 and to 2.07, respectively. R^2 value for T_{min} is 0.45.

Table 1. Validation results for minimum air temperature T_{min} (°C day^{-1}), maximum air temperature T_{max} (°C day^{-1}) and precipitation (mm day^{-1}).

		Mean (min, max)	Mean (min, max)	MAE	R^2	LEPS	CSI (low, high)	$\overline{D}$ (min, max)	CI	PI	TI
Var	*n*	Observed	NCEP								
T_{min}	7	11.3 (0.0, 26.0)	12.1 (0.8, 23.9)	2.42	0.24	0.1	NA (0.93, 0.20)	0.79 (−17.6, 16.5)	0.76 to 0.82	−5.18 to 6.76	−5.21 to 6.8
T_{max}	6	23.7 (0.2, 35.0)	26.8 (10.6, 42.4)	4.05	0.02	−0.02	NA (0.92, 0.14)	3.08 (−14.4, 33.1)	3.04 to 3.12	−4.98 to 11.14	−5.03 to 11.19
Prcp	10	3.8 (0.0, 107.1)	5.8 (0.0, 107.5)	5.46	0.31	NA	0.59 (1, 0.12)	2.01 (−91, 95.6)	1.92 to 2.09	−19.68 to 23.69	−19.77 to 23.78
		Observed	Downscaled								
T_{min}	7	11.3 (0.0, 26.0)	10.7 (−1.1, 21.6)	2.17	0.41	0.10	NA (0.93, 0.21)	−0.57 (−19.2, 14.4)	−0.60 to −0.55	−6.15 to 5.00	−6.18 to 5.03
T_{max}	6	23.7 (0.2, 35.0)	24.8 (8.3, 38.9)	2.28	0.87	0.34	NA (0.91, 0.26)	1.02 (−15.8, 24.6)	0.99 to 1.05	−4.49 to 6.54	−4.52 to 6.57
Prcp	10	3.8 (0.0, 107.1)	5.6 (0.0, 187.7)	5.08	0.52	NA	0.59 (1, 0.12)	1.89 (−91, 186.1)	1.81 to 1.97	−18.21 to 21.99	−18.30 to 22.08
		Observed	Corrected								
T_{min}	7	11.3 (0.0, 26.0)	10.9 (−0.7, 21.4)	2.07	0.45	0.13	NA (0.94, 0.18)	−0.4 (−19.3, 14.4)	−0.43 to 0.37	−5.83 to 5.03	−5.86 to 5.07
T_{max}	6	23.7 (0.2, 35.0)	23.6 (9.3, 37.0)	1.96	0.87	0.41	NA (0.90, 0.25)	−0.1 (−15.6, 22.7)	−0.13 to 0.08	−5.19 to 4.98	−5.22 to 5.01
Prcp	10	3.8 (0.0, 107.1)	5.3 (0.0, 168.9)	4.85	0.54	NA	0.59 (1, 0.11)	1.57 (−91, 167.3)	1.50 to 1.64	−17.39 to 20.53	−17.47 to 20.61

n: number of stations; mean (min, max): provide the mean, minimum and maximum values of the data sets; MAE provides the bias between the weather station data and predicted values; $\overline{D}$ (min, max): the mean, minimum and maximum of the differences between predicted and observed values.

© 2016 Royal Meteorological Society

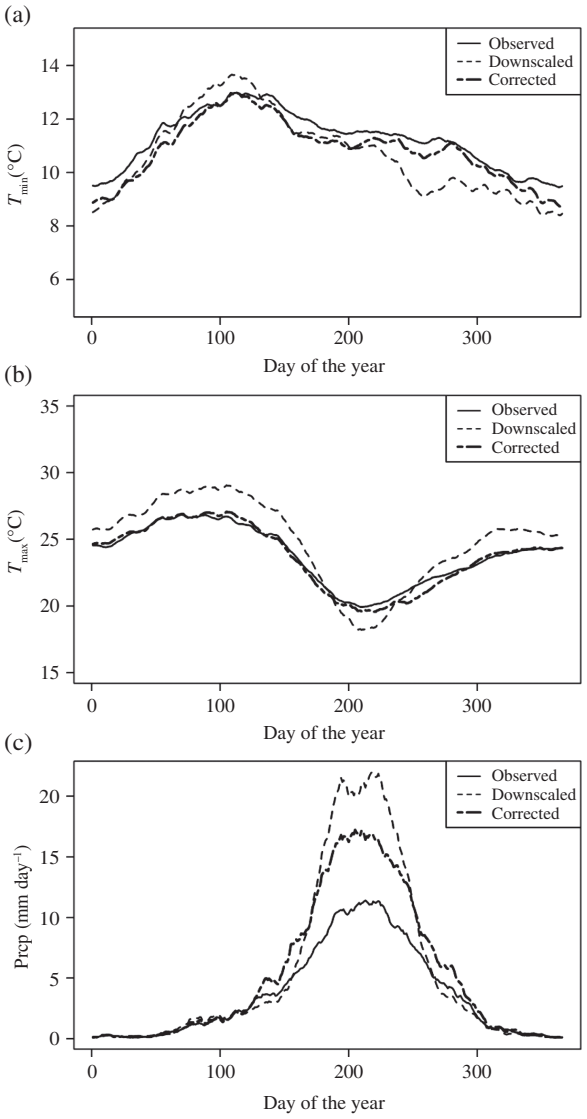

Figure 5. A 10-day moving average for observed data, downscaled and corrected data: (a) T_{min}, (b) T_{max} and (c) Prcp.

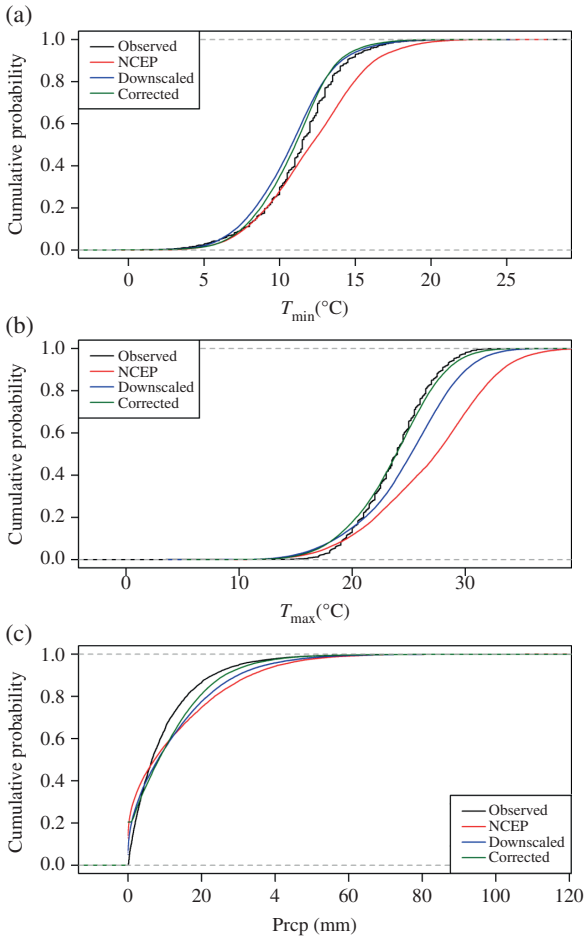

Figure 6. CDF for the observed, NCEP, downscaled and corrected data: (a) T_{min}, (b) T_{max} and (c) Prcp.

The observed mean daily maximum temperature of is 23.7 °C. The mean value of daily T_{max} of all stations is 26.8 °C in the NCEP, 24.8 °C in the downscaled and 23.6 °C in the corrected values. The MAE of T_{max} consistently improved from 4.05 (NCEP), to 2.28 (downscaled), to 1.96 (corrected). R^2 value for T_{max} is 0.87.

The LEPS value for T_{min} and T_{max} stations are 0.13 and 0.41, respectively. The Prcp CSI value is 0.59. The CSI for extreme high values for T_{min}, T_{max} and Prcp are 0.18, 0.25 and 0.11, respectively. The CSI for extreme low values for T_{min}, T_{max} and Prcp are 0.94, 0.90 and 1.0, respectively (Table 1).

We have also checked the differences between daily values of NCEP, downscaled and the corrected downscaled values with the observed values by plotting a CDF for daily T_{min}, T_{max} and Prcp (Figure 6). The CDF plots showed that the bias correction as well as downscaling of NCEP improved for all climatic variables.

The results of confidence, prediction and tolerance intervals for T_{min}, T_{max} and Prcp in the NCEP, downscaled and corrected data sets are presented in (Table 1). With a 95% probability, we are confident that the mean of residuals between corrected and observed T_{min}, T_{max} and Prcp fall between −0.43 and 0.37 °C per day, −0.13 and 0.08 °C per day and 1.50–1.64 mm per day, respectively. T_{min} and T_{max} are therefore unbiased from zero. The CI of Prcp is different from zero and biased. With the probability of 95%, we can be confident that the single future residual between corrected and observed for T_{min} will be between −5.83 and 5.03 °C, T_{max} will be between −5.19 and 4.98 °C and Prcp will be between −17.39 and 20.53 mm per day, respectively. In repeated model applications, the TI of residual between corrected and observed T_{min}, T_{max} and Prcp will be between −5.86 and 5.07 °C per day, −5.22 and 5.01 °C per day and −17.47 and 20.61 mm per day, respectively.

3.4. Daily climate data

We created a 1 × 1 km climate raster data set as the final product of our analysis containing minimum (T_{min}) and maximum (T_{max}) temperature as well as precipitation (Prcp) for the Amhara region. Figure 7 gives an example of the created raster for T_{min}, T_{max} and Prcp. The data are available for the years 1979–2010. For each year and climate variable, a GEOTIFF file was created containing

© 2016 Royal Meteorological Society

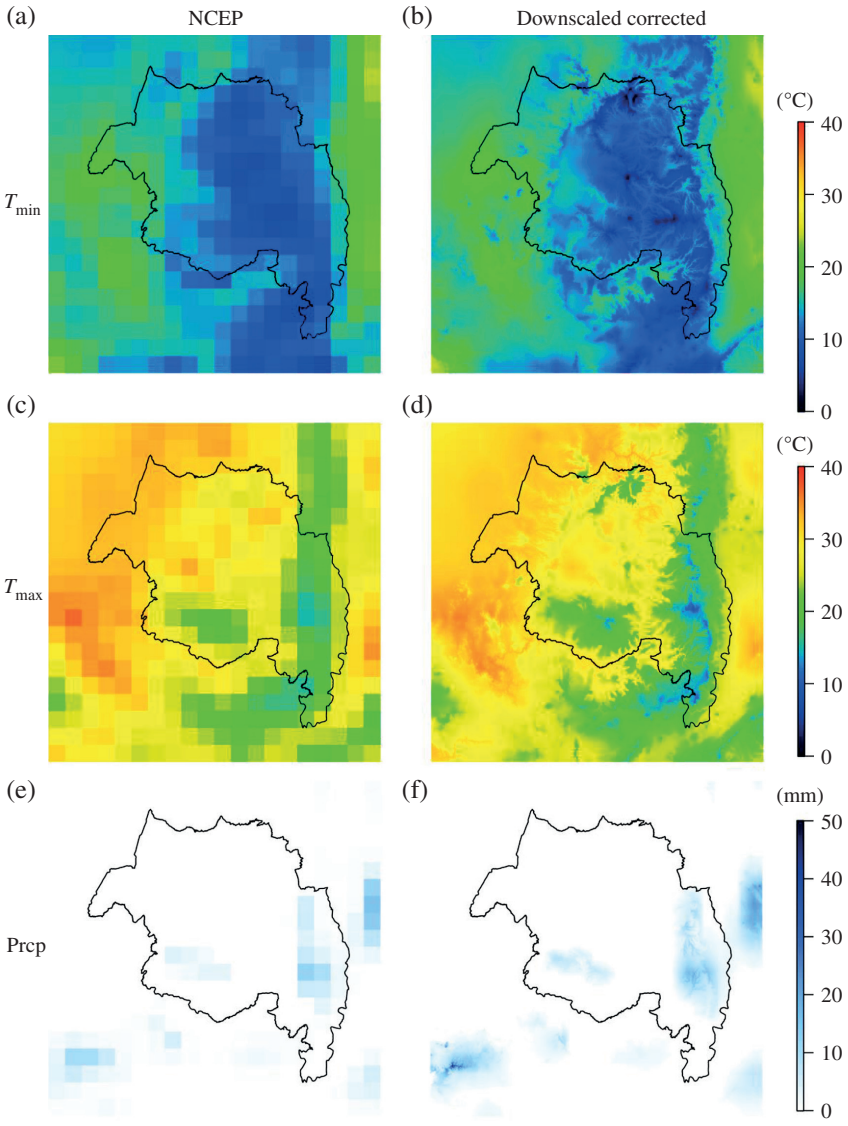

Figure 7. Daily weather data for the Amhara region: (a) NCEP T_{min}, (b) downscaled corrected T_{min}, (c) NCEP T_{max}, (d) downscaled corrected T_{max}, (e) NCEP Prcp and (f) downscaled corrected Prcp.

one rectangular raster (band) for each day. The extent of the raster has the following coordinates: top: 14.36°, left: 34.53°, right: 40.78° and bottom: 8.11°. The exact resolution is $0.008\overline{3}$ degrees, which is approximately 1 km at the Equator. Each raster file contains 750 columns and rows, in total 562 500 cells, and 96 files were created. One file has a size of 391 MB which results in about 37 GB of weather data. The data can be downloaded from: ftp://palantir.boku.ac.at/Public/ClimateDataEthiopia/

4. Discussion

We demonstrate the downscaling procedure based on the global WorldClim and NCEP climate data sets to produce daily T_{min}, T_{max} and Prcp with a 1 km^2 spatial resolution (Figure 7) for the Amhara Region in Ethiopia. The delta downscaling procedure is capable of producing fine resolution data sets. However, the downscaled global data set is associated with biases when used for regional applications (Teutschbein and Seibert, 2012). Thus, bias corrections were necessary to provide a consistent and unbiased data set for different impact applications. In our analysis, we have corrected the bias with the help of 56 regional climate stations based on a 10-day average. We then validated the corrected values with data from ten independent weather stations. The improvements resulted from downscaling and bias correction achieved are in agreement with Graham *et al.* (2007a), Lenderink *et al.* (2007) and Piani *et al.* (2010).

The methodology used here is based on global data sets. It is simple and can be applied everywhere in the world. In our study, we showed that the downscaled data (without correction) was biased as compared to regional climate stations (Figure 4). Correcting the data by observed values from regional climate stations data strongly improved the results (Figure 5). This shows the limitations of the downscaling approach if no regional climate stations are

© 2016 Royal Meteorological Society

available for a potential bias correction. Moreno and Hasenauer (2015) applied a similar downscaling algorithm on the European E-OBS data set to produce a 1×1 km climate grid across Europe. They did not apply any correction since the downscaling results were unbiased. E-OBS covers Europe and the data were produced and calibrated for Europe. In our study, we used two global data sets and downscaled them for a specific area, and this may have introduced a bias, which can be easily corrected for by obtaining local climate data as we showed in our analysis.

Availability of sufficient data at the appropriate scale is a precondition for many environmental impact studies, including climate change and ecosystem modelling applications. It is nearly impossible to get weather station coverage everywhere in the Amhara region, and so far all studies done in the region have suffered from the lack of sufficient climate data with the required coverage and information quality. For example, Ayalew *et al.* (2012) studied variability of rainfall for the whole Amhara region by using only ten meteorological stations. (Taye *et al.*, 2013) characterized the climate of Amhara region with the data of only five stations. Bewket and Conway, 2007 evaluated Amhara region's temporal and spatial variability of rainfall with 12 stations. Thus our product provides a consistent, long-term (1979–2010) and fine resolution climate data set (1×1 km) for similar studies of the whole region.

In our study, we consistently improved the bias for the $T_{\min}$, $T_{\max}$, and Prcp from NCEP to downscaled and to corrected data sets. The MAE for Prcp decreased from 5.46 (NCEP) to 5.08 by downscaling, and further declined to 4.85 after we applied bias correction. The R^2 value of precipitation improved from 0.31 to 0.54.

The LEPS values of $T_{\min}$ and $T_{\max}$ both improved with downscaling and bias correction of the NCEP data set from 0.1 to 0.13 and from -0.02 to 0.41, respectively. This increase in LEPS values along with the decrease in MAE values due to downscaling and bias correction, showed that the corrected values not only more accurately captures mean temperature values, but also captures extreme values than the NCEP values.

The CSI low score for $T_{\min}$ did change from 0.93 to 0.94 after downscaling and bias correction. The $T_{\min}$ CSI high score decreased from 0.2 to 0.18. Both CSI scores for $T_{\max}$ changed from 0.92 to 0.90 for the CSI low, and from 0.14 to 0.25 for the CSI high. The reason for the decline of the CSI values could be because of warmer temperatures at the validation stations than at the calibration stations. The CSI score for Prcp remained constant at 0.59. The Prcp CSI low score also remained constant at 1. The Prcp CSI high score decreased from 0.12 to 0.11 (Table 1). The rugged and complex topography of the Amhara region in combination with the lack of sufficient weather station data might be the reason for the small improvements in the Prcp predictions.

The CI of $T_{\min}$ and $T_{\max}$ for both NCEP and downscaled data sets are biased. The downscaling and bias correction of $T_{\min}$ and $T_{\max}$ resulted in unbiased estimates. The CI of Prcp remained biased because of the lower Prcp values evident in the validation data as compared to the calibration data, which were used for the bias correction. The PI and TI show that we can expect unbiased and consistent estimates (Table 1).

Many studies showed that a delta-change bias correction considerably improved the quality of the downscaled global data (Graham *et al.*, 2007a; Johnson and Sharma, 2011; Berg *et al.*, 2012; Rasmussen *et al.*, 2012; Teutschbein and Seibert, 2012; Hawkins *et al.*, 2013). In our study, the corrected Prcp exhibited the highest MAE (4.85) compared to $T_{\min}$ and $T_{\max}$. This makes precipitation the lowest performing climatic variable during downscaling and the bias correction processes. Downscaling of precipitation to a fine resolution of 1×1 km using a global data set is highly affected by the complex mountainous topography, which often results in unsatisfactory improvements (Hijmans *et al.*, 2005; Dinku *et al.*, 2007; Wondie *et al.*, 2011; Enyew and Steeneveld, 2014). Improved results may be achieved by better representation of complex mountainous topographies by installing more weather stations (Maraun *et al.*, 2010).

5. Conclusion

This article presents downscaled data for three climatic variables: $T_{\min}$, $T_{\max}$ and Prcp from the NCEP and WorldClim data sets, using a bias correction based on 56 local weather stations for the Amhara Region in Ethiopia. Our work has produced daily precipitation and minimum and maximum temperature data sets for the time period between 1979 and 2010 with 1×1 km spatial grid for the 156 000 km^2 Amhara region. The data set was produced to provide consistent spatial and temporal analysis and interpretation of weather data and to provide a full climate data set required for ecosystem modelling tools. Our results, in combination with soil, vegetation productivity and ecosystem modelling tools, will provide a powerful data set for climate change impact studies and carbon cycle assessments needed for the Amhara region.

Acknowledgements

This work is part of the project 'Carbon storage and soil biodiversity in forest landscapes in Ethiopia: knowledge base and participatory management'. We are grateful for the financial support provided by the Austrian Federal Ministry of Agriculture, Forestry, Environment and Water Management. The weather data were obtained from the Ethiopian Meteorological Agency without charge. We thank WorldClim and NOAA/National Centers for Environmental Prediction for freely providing the climate data used in the study. We also would like to thank the editor, Loretta Moreno, Hirut Hailu Alle and the two anonymous reviewers for their helpful comments and suggestions.

References

Abatzoglou JT. 2013. Development of gridded surface meteorological data for ecological applications and modelling. *Int. J. Climatol.* **33**: 121–131, doi: 10.1002/joc.3413.

© 2016 Royal Meteorological Society

Ayalew D. 2012. Outlook of future climate in northwestern Ethiopia. *Agric. Sci.* **3**: 608–624, doi: 10.4236/as.2012.34074.

Ayalew D, Tesfaye K, Mamo G, Birru Y, Wondimu B. 2012. Variability of rainfall and its current trend in Amhara region, Ethiopia. *Afr. J. Agric. Res.* **7**: 1475–1486, doi: 10.5897/AJAR11.698.

Bakkenes M, Alkemade JRM, Ihle F, Leemans R, Latour JB. 2002. Assessing effects of forecasted climate change on the diversity and distribution of European higher plants for 2050. *Glob. Chang. Biol.* **8**: 390–407, doi: 10.1046/j.1354-1013.2001.00467.x.

Berg P, Feldmann H, Panitz H-J. 2012. Bias correction of high resolution regional climate model data. *J. Hydrol.* **448–449**: 80–92, doi: 10.1016/j.jhydrol.2012.04.026.

Bewket W, Conway D. 2007. A note on the temporal and spatial variability of rainfall in the drought-prone Amhara region of Ethiopia. *Int. J. Climatol.* **27**: 1467–1477, doi: 10.1002/joc.1481.

Block PJ, Souza Filho FA, Sun L, Kwon HH. 2009. A streamflow forecasting framework using multiple climate and hydrological models. *J. Am. Water Resour. Assoc.* **45**: 828–843, doi: 10.1111/j.1752-1688.2009.00327.x.

Cavanaugh KC, Parker JD, Cook-Patton SC, Feller IC, Williams AP, Kellner JR. 2015. Integrating physiological threshold experiments with climate modeling to project mangrove species' range expansion. *Glob. Chang. Biol.* **21**: 1928–1938, doi: 10.1111/gcb.12843.

Charles SP, Bari MA, Kitsios A, Bates BC. 2007. Effect of GCM bias on downscaled precipitation and runoff projections for the Serpentine catchment, Western Australia. *Int. J. Climatol.* **27**: 1673–1690, doi: 10.1002/joc.1508.

Chen J, Brissette FP, Chaumont D, Braun M. 2013. Performance and uncertainty evaluation of empirical downscaling methods in quantifying the climate change impacts on hydrology over two North American river basins. *J. Hydrol.* **479**: 200–214, doi: 10.1016/j.jhydrol.2012.11.062.

Daly C, Halbleib M, Smith JI, Gibson WP, Doggett MK, Taylor GH, Curtis J, Pasteris PP. 2008. Physiographically sensitive mapping of climatological temperature and precipitation across the conterminous United States. *Int. J. Climatol.* **28**: 2031–2064, doi: 10.1002/joc.1688.

Dile YT, Srinivasan R. 2014. Evaluation of CFSR climate data for hydrologic prediction in data-scarce watersheds: an application in the Blue Nile River Basin. *J. Am. Water Resour. Assoc.* **50**: 1226–1241, doi: 10.1111/jawr.12182.

Dinku T, Ceccato P, Grover-Kopec E, Lemma M, Connor SJ, Ropelewski CF. 2007. Validation of satellite rainfall products over East Africa's complex topography. *Int. J. Remote Sens.* **28**: 1503–1526, doi: 10.1080/01431160600954688.

Enyew BD, Steeneveld GJ. 2014. Analysing the impact of topography on precipitation and flooding on the Ethiopian highlands. *J. Geol. Geosci.* **3**: 173, doi: 10.4172/2329-6755.1000173.

Feldmann H, Früh B, Schädler G, Panitz HJ, Keuler K, Jacob D, Lorenz P. 2008. Evaluation of the precipitation for South-western Germany from high resolution simulations with regional climate models. *Meteorol. Zeitschrift* **17**: 455–465, doi: 10.1127/0941-2948/2008/0295.

Fitsume D, Michael B, Lijalem K. 2015. Crop water requirement determination of chickpea in the central vertisol areas of Ethiopia using FAO CROPWAT model. *Afr. J. Agric. Res.* **10**: 685–689, doi: 10.5897/AJAR2014.9084.

Fowler HJ, Wilby RL. 2007. Beyond the downscaling comparison study. *Int. J. Climatol.* **27**: 1543–1545, doi: 10.1002/joc.1616.

Fuka DR, Walter MT, MacAlister C, Degaetano AT, Steenhuis TS, Easton ZM. 2014. Using the Climate Forecast System Reanalysis as weather input data for watershed models. *Hydrol. Process.* **28**: 5613–5623, doi: 10.1002/hyp.10073.

Gellens D, Roulin E. 1998. Streamflow response of Belgian catchments to IPCC climate change scenarios. *J. Hydrol.* **210**: 242–258, doi: 10.1016/S0022-1694(98)00192-9.

Globalweather. 2012. *Global Weather Data for SWAT*. http://globalweather.tamu.edu/ (accessed 16 March 2015).

Graham LP, Andreáasson J, Carlsson B. 2007a. Assessing climate change impacts on hydrology from an ensemble of regional climate models, model scales and linking methods – a case study on the Lule River Basin. *Clim. Change* **81**: 293–307, doi: 10.1007/s10584-006-9215-2.

Graham LP, Hagemann S, Jaun S, Beniston M. 2007b. On interpreting hydrological change from regional climate models. *Clim. Change* **81**: 97–122, doi: 10.1007/s10584-006-9217-0.

Grimm NB, Chapin FS, Bierwagen B, Gonzalez P, Groffman PM, Luo Y, Melton F, Nadelhoffer K, Pairis A, Raymond PA, Schimel J, Williamson CE. 2013. The impacts of climate change on ecosystem structure and function. *Front. Ecol. Environ.* **11**: 474–482, doi: 10.1890/120282.

Hadgu G, Tesfaye K, Mamo G, Kassa B. 2013. Trend and variability of rainfall in Tigray, Northern Ethiopia: analysis of meteorological data and farmers' perception. *Acad. J. Agric. Res.* **1**: 88–100.

Hasenauer H, Merganicova K, Petritsch R, Pietsch SA, Thornton PE. 2003. Validating daily climate interpolations over complex terrain in Austria. *Agric. For. Meteorol.* **119**: 87–107, doi: 10.1016/S0168-1923(03)00114-X.

Hasenauer H, Petritsch R, Zhao M, Boisvenue C, Running SW. 2012. Reconciling satellite with ground data to estimate forest productivity at national scales. *For. Ecol. Manage.* **276**: 196–208, doi: 10.1016/j.foreco.2012.03.022.

Hawkins E, Osborne TM, Ho CK, Challinor AJ. 2013. Calibration and bias correction of climate projections for crop modelling: an idealised case study over Europe. *Agric. For. Meteorol.* **170**: 19–31, doi: 10.1016/j.agrformet.2012.04.007.

Haylock MR, Cawley GC, Harpham C, Wilby RL, Goodess CM. 2006. Downscaling heavy precipitation over the United Kingdom: a comparison of dynamical and statistical methods and their future scenarios. *Int. J. Climatol.* **26**: 1397–1415, doi: 10.1002/joc.1318.

Haylock MR, Hofstra N, Klein Tank AMG, Klok EJ, Jones PD, New M. 2008. A European daily high-resolution gridded data set of surface temperature and precipitation for 1950–2006. *J. Geophys. Res.* **113**: D20119, doi: 10.1029/2008JD010201.

Hennemuth B, Bender S, Bülow K, Dreier N, Keup-Thiel E, Krüger O, Mudersbach C, Radermacher C, Schoetter R. 2013. Statistical methods for the analysis of simulated and observed climate data. CSC Rep. 13.

Hijmans RJ, Cameron SE, Parra JL, Jones PG, Jarvis A. 2005. Very high resolution interpolated climate surfaces for global land areas. *Int. J. Climatol.* **25**: 1965–1978, doi: 10.1002/joc.1276.

Hofstra N, Haylock M, New M, Jones P, Frei C. 2008. Comparison of six methods for the interpolation of daily, European climate data. *J. Geophys. Res. Atmos.* **113**: D21110, doi: 10.1029/2008JD010100.

Hofstra N, Haylock M, New M, Jones PD. 2009. Testing E-OBS European high-resolution gridded data set of daily precipitation and surface temperature. *J. Geophys. Res. Atmos.* **114**: D21101, doi: 10.1029/2009JD011799.

Hutchinson MF. 1995. Interpolating mean rainfall using thin plate smoothing splines. *Int. J. Geogr. Inf. Syst.* **9**: 385–403, doi: 10.1080/02693799508902045.

Ines AVM, Hansen JW. 2006. Bias correction of daily GCM rainfall for crop simulation studies. *Agric. For. Meteorol.* **138**: 44–53, doi: 10.1016/j.agrformet.2006.03.009.

Jakob Themeßl M, Gobiet A, Leuprecht A. 2011. Empirical-statistical downscaling and error correction of daily precipitation from regional climate models. *Int. J. Climatol.* **31**: 1530–1544, doi: 10.1002/joc.2168.

Johnson F, Sharma A. 2011. Accounting for interannual variability: a comparison of options for water resources climate change impact assessments. *Water Resour. Res.* **47**: W04508, doi: 10.1029/2010WR009272.

Justice CO, Townshend JRG, Vermote EF, Masuoka E, Wolfe RE, Saleous N, Roy DP, Morisette JT. 2002. An overview of MODIS land data processing and product status. *Remote Sens. Environ.* **83**: 3–15, doi: 10.1016/S0034-4257(02)00084-6.

Kebede A, Diekkrüger B, Moges SA. 2013. An assessment of temperature and precipitation change projections using a regional and a global climate model for the Baro-Akobo Basin, Nile Basin, Ethiopia. *J. Earth Sci. Clim. Change* **4**: 133, doi: 10.4172/2157-7617.1000133.

Leander R, Buishand TA, van den Hurk BJJM, de Wit MJM. 2008. Estimated changes in flood quantiles of the river Meuse from resampling of regional climate model output. *J. Hydrol.* **351**: 331–343, doi: 10.1016/j.jhydrol.2007.12.020.

Legates DR, McCabe GJ. 1999. Evaluating the use of "goodness-of-fit" measures in hydrologic and hydroclimatic model validation. *Water Resour. Res.* **35**: 233–241, doi: 10.1029/1998WR900018.

Lenderink G, Buishand A, van Deursen W. 2007. Estimates of future discharges of the river Rhine using two scenario methodologies: direct *versus* delta approach. *Hydrol. Earth Syst. Sci.* **11**: 1145–1159, doi: 10.5194/hess-11-1145-2007.

Longa CMO, Pertot I, Tosi S. 2008. Ecophysiological requirements and survival of a Trichoderma atroviride isolate with biocontrol potential. *J. Basic Microbiol.* **48**: 269–277, doi: 10.1002/jobm.200700396.

Lüttge U, Scarano FR. 2004. Ecophysiology. *Rev. Bras. Botânica* **27**: 1–10, doi: 10.1590/S0100-84042004000100001.

Manton MJ, Della-Marta PM, Haylock MR, Hennessy KJ, Nicholls N, Chambers LE, Collins DA, Daw G, Finet A, Gunawan D, Inape K, Isobe H, Kestin TS, Lefale P, Leyu CH, Lwin T, Maitrepierre L,

© 2016 Royal Meteorological Society

Ouprasitwong N, Page CM, Pahalad J, Plummer N, Salinger MJ, Suppiah R, Tran VL, Trewin B, Tibig I, Yee D. 2001. Trends in extreme daily rainfall and temperature in southeast Asia and the south Pacific: 1961–1998. *Int. J. Climatol.* **21**: 269–284, doi: 10.1002/joc.610.

Maraun D, Wetterhall F, Ireson AM, Chandler RE, Kendon EJ, Widmann M, Brienen S, Rust HW, Sauter T, Themeßl M, Venema VKC, Chun KP. 2010. Precipitation downscaling under climate change: recent developments to bridge the gap between dynamical models and the end user. *Rev. Geophys.* **48**: RG3003, doi: 10.1029/2009RG000314.

Moreno A, Hasenauer H. 2015. Spatial downscaling of European climate data. *Int. J. Climatol.* **36**: 1444–1458, doi: 10.1002/joc.4436.

Mosier TM, Hill DF, Sharp KV. 2014. 30-Arcsecond monthly climate surfaces with global land coverage. *Int. J. Climatol.* **34**: 2175–2188, doi: 10.1002/joc.3829.

Nekola JC, Brown JH. 2007. The wealth of species: ecological communities, complex systems and the legacy of Frank Preston. *Ecol. Lett.* **10**: 188–196, doi: 10.1111/j.1461-0248.2006.01003.x.

Neumann M, Zhao M, Kindermann G, Hasenauer H. 2015. Comparing MODIS net primary production estimates with Terrestrial National Forest Inventory Data in Austria. *Remote Sens.* **7**: 3878–3906, doi: 10.3390/rs70403878.

New M, Hulme M, Jones P. 1999. Representing twentieth-century space–time climate variability. Part I: development of a 1961–90 mean monthly terrestrial climatology. *J. Clim.* **12**: 829–856, doi: 10.1175/1520-0442(1999)012<0829:RTCSTC>2.0.CO;2.

Peterson TC, Vose R, Schmoyer R, Razuvaëv V. 1998. Global historical climatology network (GHCN) quality control of monthly temperature data. *Int. J. Climatol.* **18**: 1169–1179, doi: 10.1002/(SICI)1097-0088(199809)18:11<1169::AID-JOC309>3.0.CO;2-U.

Petritsch R, Hasenauer H. 2011. Climate input parameters for real-time online risk assessment. *Nat. Hazards* **70**: 1749–1762, doi: 10.1007/s11069-011-9880-y.

Piani C, Weedon GP, Best M, Gomes SM, Viterbo P, Hagemann S, Haerter JO. 2010. Statistical bias correction of global simulated daily precipitation and temperature for the application of hydrological models. *J. Hydrol.* **395**: 199–215, doi: 10.1016/j.jhydrol.2010.10.024.

Pietsch SA, Hasenauer H. 2002. Using mechanistic modeling within forest ecosystem restoration. *For. Ecol. Manage.* **159**: 111–131, doi: 10.1016/S0378-1127(01)00714-9.

Rasmussen J, Sonnenborg TO, Stisen S, Seaby LP, Christensen BSB, Hinsby K. 2012. Climate change effects on irrigation demands and minimum stream discharge: impact of bias-correction method. *Hydrol. Earth Syst. Sci.* **16**: 4675–4691, doi: 10.5194/hess-16-4675-2012.

Reynolds MR. 1984. Estimating the error in model predictions. *Forest. Sci.* **30**: 454–469.

Rose S, Apt J. 2015. What can reanalysis data tell us about wind power? *Renew. Energy* **83**: 963–969, doi: 10.1016/j.renene.2015.05.027.

Running SW, Nemani RR, Heinsch FA, Zhao M, Reeves M, Hashimoto H. 2004. A continuous satellite-derived measure of global terrestrial primary production. *Bioscience* **54**: 547–560.

Saha S, Moorthi S, Pan H-L, Wu X, Wang J, Nadiga S, Tripp P, Kistler R, Woollen J, Behringer D, Liu H, Stokes D, Grumbine R, Gayno G, Wang J, Hou Y-T, Chuang H-Y, Juang H-MH, Sela J, Iredell M, Treadon R, Kleist D, Van Delst P, Keyser D, Derber J, Ek M, Meng J, Wei H, Yang R, Lord S, Van Den Dool H, Kumar A, Wang W, Long C, Chelliah M, Xue Y, Huang B, Schemm J-K, Ebisuzaki W, Lin R, Xie P, Chen M, Zhou S, Higgins W, Zou C-Z, Liu Q, Chen Y, Han Y, Cucurull L, Reynolds RW, Rutledge G, Goldberg M. 2010. The NCEP Climate Forecast System Reanalysis. *Bull. Am. Meteorol. Soc.* **91**: 1015–1057, doi: 10.1175/2010BAMS3001.1.

Schmidli J, Frei C, Vidale PL. 2006. Downscaling from GCM precipitation: a benchmark for dynamical and statistical downscaling methods. *Int. J. Climatol.* **26**: 679–689, doi: 10.1002/joc.1287.

Seleshi Y, Zanke U. 2004. Recent changes in rainfall and rainy days in Ethiopia. *Int. J. Climatol.* **24**: 973–983, doi: 10.1002/joc.1052.

Sennikovs J, Bethers U. 2009. Statistical downscaling method of regional climate model results for hydrological modelling, 3962–3968.

Setegn SG, Srinivasan R, Dargahi B. 2008. Hydrological modelling in the Lake Tana Basin, Ethiopia using SWAT model. *Open Hydrol. J.* **2**: 49–62, doi: 10.2174/1874378100802010049.

Taye M, Zewdu F. 2012. Spatio-temporal variability and trend of rainfall and temperature in Western Amhara: Ethiopia: a GIS approach. *Glob. Adv. Res. J. Geogr. Reg. Plan.* **1**: 65–82.

Taye MT, Ntegeka V, Ogiramoi NP, Willems P. 2011. Assessment of climate change impact on hydrological extremes in two source regions of the Nile River Basin. *Hydrol. Earth Syst. Sci.* **15**: 209–222, doi: 10.5194/hess-15-209-2011.

Taye M, Zewdu F, Ayalew D. 2013. Characterizing the climate system of Western Amhara, Ethiopia: a GIS approach. *Am. J. Res. Comm.* **1**(10): 319–355.

Tesso G, Emana B, Ketema M. 2012. A time series analysis of climate variability and its impacts on food production in north Shewa zone in Ethiopia. *Afr. Crop Sci. J.* **20**: 261–274.

Teutschbein C, Seibert J. 2012. Bias correction of regional climate model simulations for hydrological climate-change impact studies: review and evaluation of different methods. *J. Hydrol.* **456–457**: 12–29, doi: 10.1016/j.jhydrol.2012.05.052.

Teutschbein C, Seibert J. 2013. Is bias correction of regional climate model (RCM) simulations possible for non-stationary conditions. *Hydrol. Earth Syst. Sci.* **17**: 5061–5077, doi: 10.5194/hess-17-5061-2013.

Thornton PE, Running SW. 1999. An improved algorithm for estimating incident daily solar radiation from measurements of temperature, humidity, and precipitation. *Agric. For. Meteorol.* **93**: 211–228, doi: 10.1016/s0168-1923(98)00126-9.

Thornton PE, Running SW, White MA. 1997. Generating surfaces of daily meteorological variables over regions of complex terrain. *J. Hydrol.* **190**: 214–251.

Van Den Besselaar EJM, Haylock MR, Van Der Schrier G, Klein Tank AMG. 2011. A European daily high-resolution observational gridded data set of sea level pressure. *J. Geophys. Res. Atmos.* **116**: D11110, doi: 10.1029/2010JD015468.

Walther G-RG-R, Post E, Convey P, Menzel A, Parmesan C, Beebee TJC, Fromentin J-MJ-M, Hoegh-Guldberg O, Bairlein F. 2002. Ecological responses to recent climate change. *Nature* **416**: 389–395, doi: 10.1038/416389a.

Willmott CJ, Matsuura K. 2006. On the use of dimensioned measures of error to evaluate the performance of spatial interpolators. *Int. J. Geogr. Inf. Sci.* **20**: 89–102, doi: 10.1080/13658810500286976.

Winkler JA, Guentchev GS, Liszewska M, Perdinan S, Tan P-N. 2011. Climate scenario development and applications for local/regional climate change impact assessments: an overview for the non-climate scientist: Part II: considerations when using climate change scenarios climate scenario development and applications II. *Geogr. Compass* **5**: 301–328.

WMO. 1996. Climatological normals (CLINO) for the period 1961–1990. World Meterological Organization, Geneva, Switzerland.

Wondie M, Schneider W, Melesse AM, Teketay D. 2011. Spatial and temporal land cover changes in the Simen Mountains National Park, a world heritage site in northwestern Ethiopia. *Remote Sens.* **3**: 752–766, doi: 10.3390/rs3040752.

WorldClim. 2005. *WorldClim – Global Climate Data*. http://www.worldclim.org/ (accessed 24 March 2015).

Zhao M, Running SW. 2010. Drought-induced reduction in global terrestrial net primary production from 2000 through 2009. *Science* **329**: 940–943, doi: 10.1126/science.1192666.

© 2016 Royal Meteorological Society